Theses and Dissertations--Civil Engineering

Civil Engineering

2016

TRANSIENT-BASED RISK ANALYSIS OF WATER DISTRIBUTION SYSTEMS

Steven Hoagland
University of Kentucky, steven.hoagland2@gmail.com
Digital Object Identifier: http://dx.doi.org/10.13023/ETD.2016.154

Right click to open a feedback form in a new tab to let us know how this document benefits you.

STUDENT AGREEMENT:

I represent that my thesis or dissertation and abstract are my original work. Proper attribution has been given to all outside sources. I understand that I am solely responsible for obtaining any needed copyright permissions. I have obtained needed written permission statement(s) from the owner(s) of each third-party copyrighted matter to be included in my work, allowing electronic distribution (if such use is not permitted by the fair use doctrine) which will be submitted to UKnowledge as Additional File.

I hereby grant to The University of Kentucky and its agents the irrevocable, non-exclusive, and royalty-free license to archive and make accessible my work in whole or in part in all forms of media, now or hereafter known. I agree that the document mentioned above may be made available immediately for worldwide access unless an embargo applies.

I retain all other ownership rights to the copyright of my work. I also retain the right to use in future works (such as articles or books) all or part of my work. I understand that I am free to register the copyright to my work.

REVIEW, APPROVAL AND ACCEPTANCE

The document mentioned above has been reviewed and accepted by the student's advisor, on behalf of the advisory committee, and by the Director of Graduate Studies (DGS), on behalf of the program; we verify that this is the final, approved version of the student's thesis including all changes required by the advisory committee. The undersigned agree to abide by the statements above.

Steven Hoagland, Student

Dr. Lindell Ormsbee, Major Professor

Dr. Y.T. Wang, Director of Graduate Studies

TRANSIENT-BASED RISK ANALYSIS OF WATER DISTRIBUTION SYSTEMS

_____

THESIS

_____

A thesis submitted in partial fulfillment of the
requirements for the degree of Master of Science
in Civil Engineering in the College of Engineering
at the University of Kentucky

By

Steven William Hoagland

Lexington, KY

Director: Dr. Lindell Ormsbee, Director Kentucky Water Resources Research Institute

Lexington, KY

2016

ABSTRACT OF THESIS

TRANSIENT-BASED RISK ANALYSIS OF WATER DISTRIBUTION SYSTEMS

Water distribution system utilities must be able to maintain a system's assets (i.e., pumps, tanks, water mains, etc.) in good working condition in order to provide adequate water quantity and quality to its customers. Various asset management approaches are employed by utilities in order to make optimal decisions regarding the renewal of system components. Part of a good asset management approach is performing a comprehensive risk analysis which consists of considering all potential ways in which the system may fail, the likelihood failure of for each scenario, and the consequences of said failure. This study investigates a water distribution system's risk of failure due to both acute transient events (e.g., pump trip) and standard pressure fluctuations due to daily system operations. Such an analysis may be useful in optimal decision making such as asset monitoring, scheduling of condition assessments or system renewal projects, policy implementation, and investment priorities in order to keep the utility's total costs at a minimum. It may also be useful as a precautionary measure to help prevent catastrophic failures such as large main blowouts for which the utility would incur substantial costs, both direct and indirect.

As part of this thesis, a database of water distribution system models is used to analyze the effects of an acute transient event for different system configurations. The database was created at the University of Kentucky and has been made available to the research community to test newly developed algorithms for various studies including optimal system operations and optimal system design.

KEYWORDS: Risk Analysis, Water Distribution System, Transient Event, Asset Management, Model Database

Steven W. Hoagland
Author

February 23, 2016
Date

TRANSIENT-BASED RISK ANALYSIS OF WATER DISTRIBUTION SYSTEMS

By

Steven William Hoagland

<u>Lindell Ormsbee</u>
Director of Thesis

<u>Y.T. Wang</u>
Director of Graduate Studies

<u>February 23, 2016</u>
Date

ACKNOWLEDGMENTS

The author would first like to acknowledge and thank his advisor Dr. Lindell Ormsbee who has guide him through his final years of school and researching efforts and who has helped the author begin his career in water resources engineering. The author also wishes to acknowledge and thank Dr. Scott Yost who taught many of his elective coursework and was always available to talk and answer questions.

The author would like to thank all of the professors at the University of Kentucky who have helped him develop a strong background in water resources engineering including Dr. Lindell Ormsbee, Dr. Scott Yost, and Dr. Jimmy Fox, each of whom served on his master's committee, and Dr. Gail Brion who stimulated the author's interest in environmental aspects of water resources. The author also wishes to broadly acknowledge and thank all of the other professors at UK who have made contributions to his education.

The author would like to acknowledge and thank the following people for the time and resources which they contributed to his research: Stacey Schal, Matthew Jolly, Tyler Mahoney, Bill Gilbert, and Dr. Srinivasa Lingireddy. The author would also like to thank Dr. Paul Boulos and the team at Innovyze for providing access to the InfoWater hydraulic modeling software which was used in this study. The author also wishes to acknowledge the members of the utility company who provided the author with the necessary data required to perform this research.

The author would like to acknowledge and thank his family for their constant love and support throughout his education. The author would like to specifically thank his parents, Jeff and Kathryn Hoagland, who have provided endless encouragement and a great opportunity to pursue a career in engineering. The author also wishes to thank his brother,

Andrew, and sister, Madeline, who have never wavered in their support and encouragement of the author's efforts. Lastly, the author would like to thank his wife Audrey, whose understanding and patience has been a great blessing these past few months. The author wishes to express his gratitude for Audrey's belief in him and her unconditional love and support throughout the author's college education.

TABLE OF CONTENTS

LIST OF TABLES

LIST OF FIGURES

CHAPTER 1 INTRODUCTION

1.1   Background

The main purpose of a water utility is to maintain and operate a water distribution system by obtaining water from a source, treating the water to an acceptable quality, and delivering the water to the consumers to meet their water needs (Mays and Tung, 1992). There are various parts to a water supply system including intakes, water treatment plants, pumps and pumping stations, and the distribution network which is defined as the underground system of interconnected pipes. "The most expensive component of a water supply system is the distribution network" (Kleiner et al., 2001). Like all other assets, distribution networks have a finite life, and pipes become more susceptible to breaking as they age (Walski and Pelliccia, 1982). "The reasons for pipe breaks are many and can be classified in several categories: 1) the quality and age of the pipe itself, 2) the type of environment in which the pipe is laid (e.g., soil corrosivity, external loading), 3) the quality of workmanship during construction, and 4) service conditions such as pressure and water hammer" (Shamir and Howard, 1979). As water mains deteriorate, breakage rates are likely to increase (Kleiner and Rajani, 2002). Due to scarce capital resources, planners and decision makers are required to seek the most cost-effective rehabilitation strategies (Kleiner and Rajani, 2002).

Since the 1980's there has been a significant amount of research dedicated to the development of pipe break prediction models and optimal strategies for the rehabilitation of water main systems. Many different approaches have been taken including statistical modeling using historical data, stochastic modeling using known probability distributions,

individual vs. group main replacement strategies, short and long term forecasting, complex evolutionary optimization algorithms, artificial intelligence, etc. Each of these approaches attempts to help manage part of the holistic problem which is the ever-increasing funds required to maintain the deteriorating underground water infrastructure. An AWWA report which was released in 2004 called "Buried No Longer" indicates that an estimated 1 trillion dollars will be required over the next 25 years in order to maintain current water service levels (Ellison et al., 2014). This projected increase in necessary funding points to a utility's immediate need for an effective asset management program.

"Asset management helps determine the need for infrastructure investments, taking into consideration customer service levels, community impacts, utility risks, and resources" (Ellison et al., 2014). When applied specifically to water supply systems, asset management programs may be used to predict future failures, assess risks, make appropriate business decisions, and prioritize mains for condition assessment or renewal (Ellison et al., 2014). Part of a comprehensive asset management program is performing risk analysis, which consists of simultaneously evaluating an asset's likelihood of failure and the potential consequences of said failure. Such an analysis may be useful in optimal decision making such as asset monitoring, scheduling of condition assessments or system renewal projects, policy implementation, and investment priorities in order to keep the utility's total costs at a minimum (Ellison et al., 2014). It may also be useful as a precautionary measure to help prevent catastrophic failures such as large main blowouts for which the utility would incur substantial costs, both direct and indirect.

1.2   Research Task Description

To date, there have not been any significant developments in comprehensive water distribution system risk analysis methodology in regard to transient events. Transient analysis is generally acknowledged to be important as it estimates the worst-case scenarios in the distribution system (Boulos et al., 2005). However, it is not given the attention it deserves in engineering curriculums and in piping system design and operation due to the complexity of the subject (Wood, 2005). With the technological advancement of powerful computing and also the development of more efficient numerical simulation models, comprehensive transient analysis is now available and practical for most utilities (Jung et al., 2007). A methodology for a transient-based risk analysis is developed and presented in this thesis.

System responses to acute transient events were analyzed for each system in a database of 15 water distribution system models which represent actual systems in Kentucky, using the hydraulic modeling software KYPIPE. The maximum pressure, minimum pressure, and pressure range were recorded for each pipe in the database and the results were displayed graphically in ArcMap. Results of the analysis were studied to observe the pressure wave propagation through the distribution networks of various system configurations (e.g., branch, loop, and grid).

In order to develop a risk analysis methodology and analyze the relationship between pressure factors and pipe failures, a real world dataset was required. A calibrated water distribution model was obtained from a utility company in the state of Kentucky. This model was created using hydraulic modeling software called InfoWater which was developed by Innovyze, Inc. This software is integrated with ArcGIS, a geographic

information system developed by ESRI, Inc., which has many useful built-in tools including the "Near" analysis and "Join" tools. InfoSurge (Innovyze's transient modeling software) utilizes the Wave Characteristic Method (WCM) algorithm (also used in KYPIPE) to analyze a system's response to transient events. For this study, pump shutdowns were modeled as the transient event of interest and resulting pressures and flows were calculated using a combination of the InfoSurge and KYPIPE software packages. Maximum pressure, minimum pressure, and pressure range were recorded as part of the analysis.

The water utility also provided the researcher with 8.5 years of pipe failure data for their system. Each pipe failure was georeferenced in shapefile format thereby making it easy to attribute failures to specific pipes. Each failure also included the date of failure which allowed for the entire dataset two be divided by year. The first 5 years of failure data (2007 – 2011) was used to score the pipes while the last 3.5 years of failure data was used to calibrate the weighting parameters.

Relationships were established between the number of breaks per length of waterline and various parameters found in the literature, which are traditionally used to predict future failures. This study further expanded on previous studies by incorporating a transient pressure factor, for which a relationship was also derived, in the prediction score. These relationships were then used to assign scores to each pipe to estimate its probability of failure relative to all other pipes in the dataset. Once pipes were scored, a global optimization algorithm was used to find the optimal combination of weighting values for each factor to best predict failures for the remaining 3.5 years of failure data. The resulting

weights were then compared to other values found in the literature as a validation of the methodology.

Impact of failure scores were assigned to each pipe based on factors taken from the utility's own proactive main replacement program. These factors incorporate many of the other factors addressed in the literature. An ultimate risk of failure score was assigned to each pipe by multiplicatively combining the probability of failure and impact of failure scores. Results were displayed graphically on the schematic of the distribution system using ArcMap's symbology classification tool for easy visual analysis.

1.3   Research Objectives

The objectives of this research are as follows:

1) Investigate system responses to transient events for various system configurations

- Complete the development of a database of 15 water distribution system models of various configurations,
- Use KYPIPE Surge analysis program to analyze the system's responses to an acute transient event,
- Compare system responses to determine if there are significant differences between configurations.

2) Determine if pressure fluctuation factors may be a significant contributor to a simple pipe failure prediction model

- Determine the relationship between pipe failures and transient pressure factors,

- Validate the assumption of a direct link between acute transient events and standard pressure fluctuations from pump operations and tank level fluctuations,

- Test the significance of pressure fluctuation factors in the pipe failure prediction model.

3) Develop and test a transient-based methodology for risk analysis

- Develop a transient-based risk analysis methodology to aid utilities in making optimal decisions regarding water main rehabilitation and replacement,

- Execute risk analysis for a calibrated water distribution system model with verifiable pipe failure data,

- Compare risk analysis results with and without transient pressure factors to verify the effectiveness of the proposed methodology.

1.4   Contents of Thesis

Chapter 1 provides background information in regard to water distribution systems and presents the need for research dedicated to infrastructure management. This chapter also provides a brief description of the various research tasks that were performed and an overview of the research objectives.

Chapter 2 provides a literature review of various approaches to asset management and optimal system rehabilitation, pipe break prediction methodologies, and risk analysis. This chapter also provides an in-depth discussion on the fundamentals of hydraulic transients, water distribution system analysis, and transient analysis.

Chapter 3 provides information about the water distribution system model database which was created at the University of Kentucky for application among the research community. This chapter discusses the creation procedure of each system and the methodology used to classify each system.

Chapter 4 explains the methodology used to analyze a water distribution system's risk in regard to transient events. This chapter discusses the simulation of acute transient events, how pressure fluctuation values were obtained, relationships between pipe failure factors and the number of pipe failures, how probability of failure and impact of failure scores were calculated, and how the overall risk of failure score was obtained.

Chapter 5 presents the results of the risk analysis, including the results of the weighting values optimization, probability of failure, impact of failure, and overall risk of failure results. The first part of this chapter discusses the transient analysis results for the model database, while the second part of this chapter discusses risk analysis results for the calibrated system.

Chapter 6 provides a discussion of the results of this study including the transient analysis performed on the model database, and the Probability, Impact, and Risk of Failure models.

Chapter 7 provides concluding remarks and recommendations from the author. This chapter also contains a discussion of the limitations and application of this research, as well as recommendations for future studies.

Appendix A provides derivations of the continuity equation, the modified Bernoulli equation, and the momentum equation, all of which are critical components of water distribution system transient analysis.

Appendix B contains the MATLAB code which was used to compare the cumulative distribution functions between the acute transient event and the small event or daily pressure fluctuations.

Appendix C contains the results of the transient analysis for the 15 system models in the database. There are 7 different figures for each system, each portraying the results of a calculated pressure metric from the transient analysis results.

CHAPTER 2 LITERATURE REVIEW

2.1 Asset Management

Asset management is an essential part of business management for water utilities (Ellison et al., 2014). While the primary business of a water utility includes capturing, treating, and delivering water, the planning, financing, design, construction, maintenance and operation of facilities and other assets are typical utility responsibilities (Ellison et al., 2014). Water distribution systems have a large number of assets to be managed including the following: pipes, tanks, pumps, treatment plants, valves, and so forth. The distribution network, which is the underground network of pipes, is generally the most expensive component (Kleiner et al., 2001). These pipes have finite lives and it has been found that pipes are more prone to breakage as they age (Walski and Pelliccia, 1982). "Breaks cause disruption in service, pose a potential danger by temporarily reducing firefighting capabilities, may cause damage to other services and to property, may cause substantial repair costs to be incurred, may cause a disruption in normal work schedules, and may create an atmosphere of public concern" (Shamir and Howard, 1979). Thus, careful consideration should be given to how these valuable assets are managed.

2.1.1 Overview

As applied directly to a water utility's most critical and costly system component (i.e., the distribution network), asset management takes into account various factors such as service levels, community impacts, risks, budgetary constraints and resources when determining appropriate infrastructure investments (Ellison et al., 2014). Asset management encompasses many things including the following: systems that record the

location, condition, and value of assets, the methods to analyze asset data, and the policies and procedures of the organization in terms of service levels, and risk management programs (Ellison et al., 2014). Sections 2.1.2 – 2.1.4 are a review of literature from 3 of the main focus areas in water distribution system asset management: 1) Predicting Pipe Failures, 2) Optimal System Rehabilitation, and 3) Risk Analysis. Many of the asset management approaches in these sections are data driven approaches. "Asset data are used to predict future failures, assess risks, set budgets, calculate financing requirements, and prioritize pipelines for detailed assessment or renewal" (Ellison et al., 2014).

2.1.2   Predicting Pipe Failures

Over the past 35 years, many researchers have focused on trying to predict pipe failures by using databases of historical data. Analysis of the historical data for many systems has shown that there are a number of statistically significant variables which are related to pipe failures including the following: material, diameter, age, soil, traffic, pipe location, pressure, joint type, freezing days, and rainfall deficit (Ellison et al., 2014). Although much effort has been directed towards developing a good prediction model, no one has been able to develop a model which works well across many datasets. One obvious obstacle in this endeavor is the fact that each has a unique combination of materials, environments, ages, and stress conditions which means that variables have different impacts for different systems (Ellison et al., 2014). Another problem with developing a universal model is inconsistency in historical data (e.g., terminology, organization, quality, etc.) (Ellison et al., 2014).

There are two main types of pipe failure prediction models: 1) grouped failure prediction models, and 2) individual failure prediction models. Grouped failure prediction

models try to predict the number of pipe breaks over a given time frame (usually a year) for a group of pipes. This group of pipes can be as big as the entire distribution network, or it can be a small group of pipes with like characteristics (i.e., cohort of pipes). On the other hand, individual failure prediction models attempt to predict when an individual pipe is going to fail, resulting in an estimated remaining useful life (RUL) for each pipe.

A number of studies have been performed which focus on identifying the relationship between pipe failures and various factors which may cause them to fail. Shamir and Howard (1979) initiated this field of study by establishing an exponential deterioration model which was applicable to pipe groups; this study established that pipes are more likely to break with age. Walski and Pelliccia (1982) furthered this study by including pipe age, diameter, and the number of previous breaks as variables in their model. Kettler and Goulter (1985) found an inverse relationship between pipe failures and diameter in cast-iron pipes. Goulter and Kazemi (1988) determined the probability of subsequent pipe breaks after an initial break. Malandain (1999) used structural and environmental factors to establish cohorts for their pipe failure prediction model. Kleiner and Rajani (2002) used time-dependent variables such as freezing index and rain deficit to predict pipe failures. Boxall et al. (2007) analyzed the effects of soils conditions on various pipe materials in the United Kingdom. Harvey et al. (2014) studied the effects of cement mortar lining and cathodic protection on cast iron and ductile iron mains in Scarborough, Canada. Results for many of these studies may be directly incorporated into asset management programs for water utilities. Partnering with a water utility provides a large real-world data source and a place to test the researcher's methodology in some cases. Not all of the results of the studies completely agree with each other. However, there are three main areas of general

agreement among nearly all statistical studies of main breaks: 1) once a failure has occurred on a particular pipe, a model can predict future failures much more accurately, 2) smaller diameter pipes break at an earlier age than large diameter pipes, and 3) pipes break at an earlier age when they are placed in corrosive soils (Ellison et al., 2014).

There are a number of other studies that have been performed which focus on identifying the best models and methods to predict pipe failures based on significant variables related to the physical nature of the pipe and the pipe's environment. These methods can be broadly classified into deterministic, probabilistic multi-variate, and probabilistic single-variate models. Kleiner and Rajani (2001) have published a thorough literature review on statistical models which have been used to predict pipe failures. Deterministic models included time-exponential models and time-linear models where pipes failures are exponentially modeled and linearly modeled with time, respectively (Kleiner and Rajani, 2001). Probabilistic multi-variate models include proportional hazards models, accelerated lifetime models, and time-dependent Poisson models. Proportional hazards models have a group of variables which act in a multiplicative manner on the baseline hazard function, accelerated lifetime models suggest that the time to failure relationship expands or contracts relative to a vector of predictive variables, and time-dependent Poisson models suggest that the mean breakage rate depends on pipe age but breakage follows a Poisson process (Kleiner and Rajani, 2001). Probabilistic single-variate models consist of cohort survival models which use a probability density function based on variables taken from groups of like pipes, Bayesian diagnostic models which predict the probability of failure using Bayes theorem, semi-Markov processes which thinks of breaks

12

as states of the asset, and break clustering which uses spatial and temporal clustering of historical main breaks to predict future breaks (Kleiner and Rajani, 2001).

2.1.3 Optimal System Rehabilitation

Water distribution network components have a finite useful life and there comes a time over the useful life of a water main when it becomes more economical to replace the main than to continue maintenance (Walski and Pelliccia, 1982). There are a number of studies that have been performed which focus on determining the appropriate timing of pipe rehabilitation. In this context, the term rehabilitation means improvement and is not distinguishing between the act of pipe replacement or pipe rehabilitation (relining, pigging, etc.).

Shamir and Howard (1979) developed a model to optimally replace a pipe once the projected maintenance costs exceeded the capital cost per year. Thus, total cost is minimized for the life cycle of the pipe which optimizes the owner's return on investment (ROI). Woodburn et al. (1987) optimized pipe replacement by minimizing total cost while using hydraulic factors as constraints. Lansey et al. (1992) included a budgetary constraint in their optimal scheduling program. Arulraj and Suresh (1995) introduced a concept called significance indexing to optimize the rehabilitation timing of water mains. Halhal et al. (1997) used multiple objective genetic algorithm programming to maximize quantifiable benefits while minimizing total cost of pipe replacement. Kleiner et al. (2001) considered both network economics and hydraulic capacity over a predefined period of analysis for optimal scheduling. Burn et al. (2003) prioritized the replacement of pipe cohorts using risk management. Renaud et al. (2007) considered cutting costs by coordination with other public construction works in optimal scheduling water main rehabilitation. Nafi and

Kleiner (2010) proposed incorporating cost discounts for economies of scale. Creaco et al. (2013) optimized replacement based on the scheduling of water main upgrades to account for future increases in consumer demands. Achim et al. (2007) and Harvey et al. (2014) used artificial neural networks to predict the remaining useful life for each pipe and also to identify significant variables.

2.1.4   Risk Analysis

"The decision of whether to replace a main or not is often an economic one, comparing the costs of replacement with expected costs of future break damage and repair" (Male et al., 1990). The break of a 6 inch distribution main in a rural part of the network is likely to have the exact same effect as the break of another 6 inch main in a different rural part of the network. However, a break in a highly urbanized, downtown area is likely to have different consequences of failure than breaks in a rural district and would be a higher risk to the utility and community. Thus, the risk of a break is associated with both its likelihood and consequences (Ellison et al., 2014).

The concept of risk for pipeline failure has two dimensions: 1) the probability that the pipeline will fail, and 2) the impact of said failure. In order to determine the degree of risk, both dimensions need to be accounted for (Ellison et al., 2014). Risk associated with a water distribution main failure is expressed in Equation 1.

$$Risk\ of\ Failure = Probability\ of\ Failure \times Impact\ of\ Failure \qquad (1)$$

Probability of failure is expressed as a number between 0 and 1, and is therefore non-dimensional. This term may be calculated over a finite period of time (i.e., probability of failure within the next 10 years), or it may be calculated relatively (i.e., probability of

14

failure relative to all other pipes in the system). For this study, all probability of failure values were calculated relative to other pipes in the system.

Impact of failure may be represented in multiple ways also. The impact of failure may be quantified in terms of dollars and can include cost of repair, replacement, damage, lost service, etc. Impact of failure may also be calculated relative to other pipes in the system (e.g., larger pipes will have a greater impact of failure than small pipes), as was done in this study. Since probability of failure is non-dimensional, the units of failure risk are the same as those of impact of failure.

Ellison et al. (2014) showed that can be very helpful to depict failure risk as a matrix with probability of failure as one dimension and impact of failure as another. A relative failure risk matrix where the risk of failure is lowest for any given pipe if it is classified in the bottom left part of the matrix and is highest for pipes classified in the top right part of the matrix. As pipelines age, their likelihood of failure increases, as can their consequence of failure in developing areas; therefore, these pipes move from the bottom left corner to upper right corner of the risk matrix.

Risk analysis is a useful tool in water distribution system asset management as a means of prioritizing assets for the next appropriate course of action. If an asset is classified as high risk, a decision may be made to schedule the replacement of the asset. A less severe course of action may be to schedule a condition assessment of the asset to validate the high risk classification prior to replacement. Risk classifications can be updated and made more accurate after condition assessments have been completed.

One risk classification method is the weighted-score method (Ellison et al., 2014). This method assigns weights to the probability of failure factors and the impact of failure factors based on their total contribution or relative contribution to the overall risk. The scores are then summed for each pipe, resulting in a combined probability of failure score and combined impact of failure score. These scores can be scaled as desired (e.g., probability of failure score can be scaled to values between 0 and 1 by dividing by the maximum possible score for each pipe). This method is straightforward and easy to apply.

This study introduces a transient-based risk analysis, meaning that transient pressures (maximum and minimum) are included as variables in the probability of failure factor. This study follows initial work performed by Wang et al. (2014) in which risk was calculated for each pipe and node using the weighted-score method. Individual risk factors included maximum transient pressure, minimum transient pressure, maximum vapor volume, and maximum transient force. A cumulative risk factor was then calculated and color coded onto a schematic of the system. This was performed for a small synthesized water distribution system and also for a large real distribution system in China. The authors found that water hammer hazard assessment can determine the areas where the water supplier can implement actions to minimize the effects of water hammer or prevent it from occurring (Wang et al., 2014).

2.2   Water Distribution System Modeling

Modern day analysis of water distribution system covers a wide range of subjects including network optimization, asset management, real time monitoring, water security, leakage, and energy management. A very important component that is included in many of these subjects is water distribution system modeling. Present day modeling consists of

using a software program to run numerical simulations. These simulations replicate the dynamics of a real or proposed system mathematically and can be used to predict the system's response to various boundary conditions without disturbing the real infrastructure (Walski et al., 2007). These mathematical models are based on fundamental equations and principles which have been discovered and developed over time to describe water system dynamics. These fundamentals are then applied to numerical models in order to gain insight into system dynamics at a specific point in time (i.e., steady-state), or over a predefined period of time (i.e., extended-period simulation). Numerical models have also been developed to analyze the effects of transient events. As technology has advanced, graphical user interfaces (GUIs) have been applied to the numerical models in order to make them user friendly. The fundamental equations and specific simulation types as applied to water distribution systems are discussed in Sections 2.2.1 – 2.2.4.

2.2.1   Conservation Principles

"To effectively utilize the capabilities of water distribution system modeling software and interpret the results produced, the engineer or modeler must first understand the mathematical principles and equations involved" (Walski et al., 2007). In a general sense, water distribution networks can be analyzed and solved using the three conservation laws: mass, energy, and momentum. Steady-state and extended-period simulations can be solved using mass and energy conservation laws, while transient analysis also requires the conservation of momentum principle.

Conservation of Mass:

The principle of conservation of mass states that the quantity of mass in a closed system must remain the same over time. Unless mass is added or removed from the closed system, the quantity of mass must remain the same. As water distribution systems convey water, a constant fluid density is assumed. Therefore, the mass flow rate into the system must equal the mass flow rate out of the system (assuming no internal storage). The principle of conservation of mass based on volumetric flowrate can be summarized by Equation 2, which is a simplified form of the continuity equation. For the full derivation of the continuity equation, see Appendix A.

$$\sum Q_{in} = \sum Q_{out} \tag{2}$$

In Equation 2, $\sum Q_{in}$ is the volumetric flow rate entering the system, and $\sum Q_{out}$ is the volumetric flow rate exiting the system. The volumetric flow rate is equal to the average velocity of the fluid entering a pipe multiplied by the cross sectional area of the pipe. This is summarized by Equation 3

$$Q = VA \tag{3}$$

where Q represents the volumetric flow rate, V represents the cross sectional averaged velocity, and A represents the cross sectional area of the pipe (assuming the pipe flows full). Therefore, by multiplying the velocity of a fluid traveling through a pipe by the cross-sectional area of the inside of the pipe (assuming closed conduit flow), the flow rate of the fluid can be calculated.

Conservation of Energy:

The principle of conservation of energy states that the total energy at a specified point in a system equals the energy at a downstream point, plus the energy losses (e.g., friction, minor) or gains (e.g., head gain from pump). This principle is derived from the first law of thermodynamics. Reworded, the conservation of energy principle states that energy can neither be created nor destroyed, but that it transfers from one form to another. In water distribution systems, the conservation of energy between two points can be written using a modified Bernoulli's equation

$$\frac{P_1}{\gamma} + z_1 + \frac{V_1^2}{2g} + H_G = \frac{P_2}{\gamma} + z_2 + \frac{V_2^2}{2g} + H_L \tag{4}$$

where $\frac{P}{\gamma}$ is equal to the pressure head, z is equal to the elevation head, $\frac{V^2}{2g}$ is equal to the velocity head, H_G is equal to head gains from pumps, and H_L is equal to head losses. Specifically, P is pressure, γ is the specific weight of the fluid, z is elevation, V is the velocity of the fluid, and g is acceleration due to gravity. For full derivation of the modified Bernoulli's equation, see Appendix A. Note that all of the units are in length terms (i.e., feet or meters), and the subscripts 1 and 2 denote position 1 and 2, respectively. Terms without a subscript (i.e., H_G and H_L) refer to gains and losses between position 1 and 2. In water distribution systems, there are several simplifying assumptions that are made pertaining to the energy equation at specific points in a network that help in the analysis. For example, water is exposed to atmospheric pressure (i.e., zero gauge pressure) at storage tanks. Additionally, the velocity at the surface of storage tanks and reservoirs is assumed to be zero due to the relatively large cross sectional area. The terms in the modified

Bernoulli Equation are grouped to make up the energy grade line (EGL) and the hydraulic grade line (HGL), of which the formulas are shown in Equations 5 and 6, respectively.

$$EGL = \frac{P}{\gamma} + z + \frac{V^2}{2g} \tag{5}$$

$$HGL = \frac{P}{\gamma} + z \tag{6}$$

Energy gains in the system are represented by head gains from pumps. Head gains from pumps are a function of the flow rate through the device. This relationship is best presented in the form of a head discharge curve, also called a pump head characteristic curve.

Energy losses in the system are represented as head losses. Head losses are comprised of two components: 1) frictional head loss and 2) minor head loss. Frictional losses are created due to the fluid's contact with the pipe wall, while minor losses are created due to turbulent flow through various network components such as valves, bends, and fittings. Note that both frictional and minor losses are dependent on the velocity of the fluid in the pipe. The equation for total head is

$$H_{L_T} = H_{L_f} + H_{L_M} \tag{7}$$

where H_{L_T} is the total head loss, H_{L_f} is the frictional head loss, and H_{L_M} is the minor head loss. Note that all terms in the equation are in units of length.

Conservation of Momentum:

Newton's second law of motion for a system states that the time rate of change of the linear momentum of the system is equal to the sum of external forces acting on the

20

system. To simplify this statement, the resultant force acting on a fluid element is equal to the rate of change in momentum. A simplified version of the momentum equation for one dimensional pipe flow is shown in Equation 8

$$\frac{\partial H}{\partial x} = -\frac{1}{gA_L}\frac{\partial Q}{\partial t} + f(Q) \tag{8}$$

where H is the pressure head, Q is the volumetric flow rate, g is the gravitational acceleration, A_L is the pipe cross sectional area, and $f(Q)$ is a pipe resistance term. Flow conditions in Equation 8 are expressed relative to spatial (∂x) and time (∂t) variations. A complete derivation of the momentum equation is presented in Appendix A.

2.2.2   *Fundamental Equations*

There are a number of fundamental equations used in water distribution system modeling that are used almost universally to quantify energy losses within a system. Two widely accepted equations for quantifying frictional head loss are the Darcy-Weisbach equation and the Hazen Williams equation. A third equation to calculate frictional head loss which is less commonly used for analyzing pipe flow is the Manning equation. Each of these equations will be discussed, as well as the method for quantifying minor losses.

Darcy-Weisbach Equation:

Henry Darcy and Julius Weisbach expanded on previous work by Gotthilf Hagen, Jean Louis Poiseuille, and Antoine Chezy to establish an equation for predicting head loss around 1845 (Rouse and Ince, 1980). Equation 9 became famously known as the Darcy-Weisbach equation, which predicts frictional head loss (h_{L_f}) based on conduit length (L)

21

and diameter (D), gravitational acceleration (g), the velocity of the fluid (V), and a roughness factor (f).

$$h_{L_f} = f\frac{LV^2}{D2g} = \frac{8fLQ^2}{gD^5\pi^2} \qquad (9)$$

The roughness factor, f, is called the Darcy-Weisbach friction factor. The friction factor is dependent upon the Reynolds number, which takes velocity, density, viscosity, and diameter into account, and the conduit's relative roughness, which takes into account the internal roughness of the pipe wall. Friction factors were experimentally determined for various relative roughness values. One of the most popular formulas developed for predicting the friction factor is the Colebrook-White equation shown in Equation 10.

$$\frac{1}{\sqrt{f}} = -0.86\ln\left(\frac{\epsilon}{3.7D} + \frac{2.51}{Re\sqrt{f}}\right) \qquad (10)$$

In Equation 10, ϵ is the internal pipe roughness, D is the conduit diameter, and Re is the Reynolds number. A notable challenge with using the Colebrook-White equation is the fact that f is present on both sides of the equation. This requires an iterative solution procedure to solve for f. Another popular method of solving for f is to use the Moody Diagram, which plots the friction factor versus the Reynolds number for varying relative roughness values.

However, due to the computational burden of solving for the f factor implicitly, a number of explicit equations were developed to decrease the time required to solve a network. One of the most popular explicit equations which is used in most water

distribution modeling software is the Swamee-Jain formula, shown in Equation 11, where the variables are identical to the Colebrook-White equation.

$$f = \frac{1.325}{\left[\ln\left(\frac{\epsilon}{3.7D} + \frac{5.74}{Re^{0.9}}\right)\right]^2} \tag{11}$$

Hazen-Williams Equation:

One of the most widely used equations for predicting frictional head loss in pipe flow is the Hazen-Williams equation, shown in Equation 12, where C_f is a unit conversion factor, and C is the empirically derived Hazen-Williams "C-factor".

$$h_{L_f} = \frac{C_f L}{C^{1.852} D^{4.87}} Q^{1.852} \tag{12}$$

The Hazen-Williams C-factor represents the internal roughness of the pipe, similar to the friction factor in the Darcy-Weisbach equation. If a pipe is assigned a high C-factor, this means that the pipe is smooth. Oppositely, lower C-factors are assigned to rougher pipes. Pipes that are subject to internal corrosion, such as cast iron mains, generally get rougher with age, thus some C-factors may need to be regularly updated. It is theorized that C-factors should vary with velocity under turbulent conditions (Walski et al., 2007). Thus, the purpose of Equation 13, where C is the velocity-adjusted C-factor, C_o is the original C-factor, V_o is the velocity reference value, and V is velocity, is to adjust the C-factor based on flow velocity.

$$C = C_o \left(\frac{V_o}{V}\right)^{0.081} \tag{13}$$

However, the C-factor corrections are typically very small. "A two-fold increase in the flow velocity correlates to an apparent five percent decrease in the roughness factor, which is typically within the error range for initial C-factor estimates" (Walski, 1984). Therefore, most modelers assume a constant C-factor for varying flow velocities. This method has gained much popularity due to the ease of using a constant C-factor in modeling.

Manning Equation:

Although it is rarely applied to closed conduit analysis, the Manning equation, shown in Equation 14, is another equation that can be used to predict frictional head loss in pipe flow.

$$h_{L_f} = \frac{C_f L (nQ)^2}{D^{5.33}} \tag{14}$$

In Equation 14 n is the Manning roughness coefficient (often called "Manning's n") which is experimentally derived for various pipe materials.

Minor Losses:

The predominant loss of energy in closed conduit flow is frictional head loss. However, head loss also occurs at various system components such as valves, intersections, and bends. These losses are called minor losses, due to the relatively small amount of energy that is lost compared to frictional losses. These minor losses are due to turbulent eddies that are developed as the flow moves through the various appurtenances and bends. The minor loss equation is

$$h_{L_M} = K_L \frac{V^2}{2g} \tag{15}$$

where the minor loss coefficient, K_L, is experimentally determined for each of the various appurtenances (i.e., valves, bends, etc.). However, due to the often insignificant proportion of energy loss, minor losses are typically ignored in water distribution system models. Minor losses may play a more significant role in other parts of the system such as pump stations, where there may be more fittings and higher velocities (Walski et al., 2007).

General Form Head Loss Equation:

Equations 9, 12, 14, and 15, listed previously in this section, are all equations for predicting head loss in closed conduit flow. However, Equation 7 for total head loss can be written in general form as shown in Equation 16

$$h_{L_T} = h_{L_f} + h_{L_M} = K_P Q^s + K_M Q^2 \tag{16}$$

where the frictional head loss term is represented by $K_P Q^s$, where K_P is the pipe resistance coefficient, and s is the exponent for the flow rate which varies depending on the loss equation that is used; the minor loss term is represented by $K_M Q^2$, where K_M is the minor loss resistance coefficient. This general form of the head loss equation is advantageous for modeling head loss since it allows for virtually any head loss prediction equation (i.e., Darcy-Weisbach, Hazen-Williams, Manning) to be used. The head loss prediction equations are embedded in the K_P term for frictional head loss. The various K_P terms with their respective prediction equations are shown in Equations 17 – 19. Note that the terms

in Equations 17 – 19 represent the same parameters as shown in the original head loss

prediction equations (i.e., Equations 9, 12 and 14).

Darcy-Weisbach K_P Term:

$$K_P = f \frac{L}{2gA^s D} \tag{17}$$

Hazen-Williams K_P Term:

$$K_P = \frac{C_f L}{C^s D^{4.87}} \tag{18}$$

Manning K_P Term:

$$K_P = \frac{C_f L n^s}{D^{5.33}} \tag{19}$$

The minor loss resistance coefficient, K_M, is calculated by summing the individual minor

loss coefficients (K_L) and dividing by the gravitational acceleration term (g) and the area

of the conduit (A) squared as shown in Equation 20.

$$K_M = \frac{\sum K_L}{2gA^2} \tag{20}$$

Energy Gains:

Pumps represent energy gains in water distribution system analysis. The energy gain from

a constant power pump (E_P) may be calculated from Equation 21 which includes the

pump's horsepower (HP), and the flowrate (Q).

$$E_P = \frac{550 \times HP}{62.4 \times Q} \tag{21}$$

2.2.3 Steady-State Modeling

The purpose of steady-state modeling is to calculate pressure and flow rates throughout a distribution system at a specific instant in time. With respect to transient analysis, steady-state analysis must be performed prior to analyzing the effects of a transient event. For steady-state analysis, boundary conditions (i.e., tank and reservoir levels) are set and remain constant as the simulation solves for pressure and flow. Real water distribution systems cannot be described by a single set of equations but rather a continuity equation for each node in the system and an energy equation for each loop or path (Walski et al., 2007). Many methods for solving networks have been developed over the years, and the most efficient algorithms have been incorporated into hydraulic modeling software. Each of these methods set up systems of equations in matrix form and solves them iteratively to obtain a steady-state solution of pressure and flowrate. A simple example of the Simultaneous Pipe Method, a solution method for solving steady-state networks developed by Wood and Charles (1972) which is employed in hydraulic modeling software KYPIPE, is shown.

Simultaneous Pipe Method:

A schematic of a simple water distribution system from Wood (1981) is shown in Figure 2.1, where the nodes are labeled in circles and the pipes are labeled in brackets. Tables 2.1 and 2.2 present pipe information and node information, respectively, which were also taken

from Wood (1981). Note that the Hazen-Williams equation is used to predict head loss in this example.
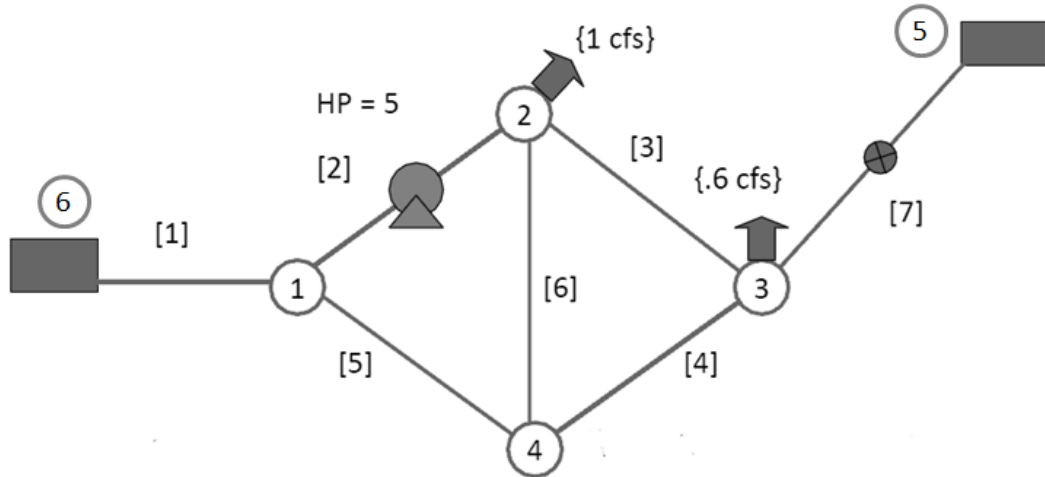
Figure 2.1: Example Schematic.

Table 2.1: Pipe Information.

Pipe No.	Kp	Km	Z	Qi (cfs)
1	3.36	0	0	2
2	18.18	0	44.1	1.5
3	73.78	0	0	0.6
4	76.24	0	0	0.4
5	2.69	0	0	0.5
6	24.23	0	0	0.1
7	122.97	64.44	0	0.4

Table 2.2: Node Information.

Node No.	Head (ft)	Elevation (ft)	Demand (cfs)
1		90	
2		100	1
3		90	0.6
4		80	
5	190	190	
6	215	100	

In Table 2.1, the Kp term is the pipe resistance coefficient as described in Equations 17 – 19, the Km term is the minor loss resistance coefficient as described in Equation 20, the Qi term is the estimated initial flowrate through the pipes, and the Z term represents the energy of the pump and is calculated using Equation 21, where HP is the pump horsepower.

$$Z = \frac{550 \times HP}{62.4}$$ (22)

The number of energy equations (EE) that must be written for the entire system to be solved is the number of loops plus the number of paths as shown in Equation 23. For this example, 3 energy equations are required.

$$EE = L + Pa$$ (23)

By analyzing the pipe and node information in Tables 2.1 and 2.2, the number of loops in the system is calculated to be 2 using Equation 24, where P is the number of pipes, J is the number of nodes (junctions), F is the number of fixed grade nodes (i.e., tanks or reservoirs), and L is the number of loops. The 2 loops can be identified in the simple schematic in Figure 2.5, however for more complex systems it very tedious to count the large number of loops.

$$L = P - J - F + 1$$ (24)

Additionally, the number of paths (Pa) in the system may be calculated using Equation 25, where F is the number of fixed grade nodes. For this example, there is 1 path.

$$Pa = F - 1$$ (25)

Before writing the energy equations, the gradient (G) and head change (H) terms

must be calculated for each pipe. The head change is presented in Equation 26, and is the

same as head loss equation shown in Equation 15 with the addition of a pump term $(-\frac{Z}{Q_i})$,

where the s term is equal to 1.852 (due to use of the Hazen-Williams equation). The

gradient term is the derivative of the head change term, and is shown in Equation 27.

$$H = K_P Q^s + K_M Q^2 - \frac{Z}{Q_i} \tag{26}$$

$$G = s K_P Q^{s-1} + 2 K_M Q + \frac{Z}{Q_i^2} \tag{27}$$

The general energy conservation equation is shown in Equation 28 in terms of G, H, Q,

and the elevation difference between the start and end points (ΔE) of the loop or path.

$$\sum GQ = \sum (GQ - H) + \Delta E \tag{28}$$

The energy equations for each loop and path in the example problem are shown in

Equations 29, 30, and 31.

($Loop$ 1) $G_2 Q_2 - G_5 Q_5 - G_6 Q_6 = (G_2 Q_2 - H_2) + (G_5 Q_5 - H_5) + (G_6 Q_6 - H_6)$ (29)

($Loop$ 2) $G_3 Q_3 - G_4 Q_4 + G_6 Q_6 = (G_3 Q_3 - H_3) + (G_4 Q_4 - H_4) + (G_6 Q_6 - H_6)$ (30)

($Path$ 1)

$$G_1 Q_1 + G_2 Q_2 + G_3 Q_3 + G_7 Q_7 =$$
$$(G_1 Q_1 - H_1) + (G_2 Q_2 - H_2) + (G_3 Q_3 - H_3) + (G_7 Q_7 - H_7) + 25 \tag{31}$$

Along with the energy equations, continuity equations must also be written for each

node in the system. These equations satisfy the conservation of mass law and are simply

an accounting of all of the flow into and out of each node. Note that continuity equations are only written for junction nodes; tanks, pumps and reservoirs are not included. The continuity equations for this example are shown in Equations 32 – 35. The right hand side of each equation is equal to the demand at that node.

$(Node\ 1)$ $\qquad\qquad\qquad Q_1 - Q_2 - Q_5 = 0 \qquad\qquad\qquad$ (32)

$(Node\ 2)$ $\qquad\qquad\qquad Q_2 - Q_3 + Q_6 = 1 \qquad\qquad\qquad$ (33)

$(Node\ 3)$ $\qquad\qquad\qquad Q_3 + Q_4 - Q_7 = 0.6 \qquad\qquad\qquad$ (34)

$(Node\ 4)$ $\qquad\qquad\qquad -Q_4 + Q_5 - Q_6 = 0 \qquad\qquad\qquad$ (35)

The energy equations and the continuity equations can be represented using a coefficient matrix, where flow (Q) is the variable that is being solved for. The first four rows of the coefficient matrix are comprised of the continuity equations, while the last three rows are comprised of the energy equations. This coefficient matrix is called the "A" Matrix and is shown in Figure 2.2.

A Matrix:

Node 1	1	-1			-1			
Node 2		1	-1			1		
Node 3			1	1				-1
Node 4				-1	1	-1		
Path 1	G_1	G_2	G_3					G_7
Loop 1		G_2			$-G_5$	$-G_6$		
Loop 2			G_3	$-G_4$		G_6		

Figure 2.2: "A" Matrix.

The values from the right hand side (i.e. known quantities) of the continuity and energy equations are thrown into another matrix called the "B" Matrix. The "B" Matrix is shown in Figure 2.3.

$$
\begin{array}{c|c|}
Node\ 1 & Demand\ @\ Node\ 1 \\[1em]
Node\ 2 & Demand\ @\ Node\ 2 \\[1em]
Node\ 3 & Demand\ @\ Node\ 3 \\[1em]
Node\ 4 & Demand\ @\ Node\ 4 \\[1em]
Path\ 1 & \begin{aligned}(G_1Q_1 - H_1) + (G_2Q_2 - H_2) + (G_3Q_3 - H_3)\\ +(G_7Q_7 - H_7) + 25\end{aligned} \\[1em]
Loop\ 1 & (G_2Q_2 - H_2) + (G_5Q_5 - H_5) + (G_6Q_6 - H_6) \\[1em]
Loop\ 2 & (G_3Q_3 - H_3) + (G_4Q_4 - H_4) + (G_6Q_6 - H_6) \\
\end{array}
$$

Figure 2.3: "B" Matrix.

The "A" and "B" Matrices can then be used to solve for the "Q" Matrix, which consists of all of the flows that are being calculated. The "Q" Matrix is shown in Figure 2.4. Equation 36 used to calculate the values in the "Q" Matrix.

$$\begin{vmatrix} Q_1 \\ Q_2 \\ Q_3 \\ Q_4 \\ Q_5 \\ Q_6 \\ Q_7 \end{vmatrix}$$

Figure 2.4: "Q" Matrix.

$$[Q] = [A]^{-1} \times [B] \tag{36}$$

The values calculated in the "Q" Matrix are then dumped back into the estimated flow values (Q_i in Table 2.1), and then entire process is repeated until the flow values converge to within a specific error tolerance. In practice, Equation 36 is normally solved using a more computationally efficient (e.g., LU Decomposition) that does not require the full solution of $[A]^{-1}$.

2.2.4 Extended-Period Simulations

Each of the database models, mentioned in Chapter 1 and further discussed in Chapter 3, is set up for the user to run an extended-period simulation. Although not required for transient analysis, extended-period simulations can offer further insight into the hydraulic dynamics of a particular system. The purpose of an extended-period simulation is to analyze a system's response (i.e., pressure and flow changes) to external demands over a predefined period of time. Throughout the simulation, various boundary conditions may change such as nodal demands and tank levels. Operational conditions may also change as pumps are switched off and on and valves are opened or closed. Extended period

simulations are often used to observe tank level fluctuations over a 24 hour period, and also in water quality simulations to keep track of water age or chlorine residual.

The analysis of an extended-period simulation is relatively straightforward. It consists of running multiple steady-state simulations at specified moments in the simulation time which are called computational intervals. A computational interval is typically on the order of minutes or hours, and is dependent upon what time scale the user wishes to observe the system's response. For each computational interval, a single steady-state simulation is performed. However, the volume of water that enters or exits the closed system is calculated based on Equation 37, where V_w is the volume of water, Q is volumetric flow rate, and t_c is the computational time interval.

$$V_w = Q \times t_c \qquad (37)$$

Demand nodes are considered as volume sinks while reservoirs and tanks are considered as volume sources. Thus, the amount of water entering and exiting tanks is closely monitored and the resulting tank levels are calculated based on tank geometry. Note that reservoirs are modeled as infinite sources of water which remain at a constant elevation.

2.3   Hydraulic Transients

"A hydraulic transient is the flow and pressure condition that occurs in a hydraulic system between an initial steady-state condition and a final steady-state condition" (Walski et al., 2007). These conditions are often referred to as "events" due to the relatively short time frame over which transients are analyzed. Transient events are initiated by changes in hydraulic devices (i.e., pumps or valves) or boundary conditions (i.e., tanks, reservoirs, or

demands). These events can create serious consequences for water utilities if not considered in design and operation (Wood, 2005). Wood (2005) suggests that transient analysis is often more critical than the analysis of the steady-state operating conditions which engineers normally use as the basis for design. Understanding the cause and effects of hydraulic transients is critically important to be able to perform the type of risk analysis proposed in this study.

2.3.1   Fundamentals of Hydraulic Transients

As mentioned in Section 2.1, hydraulic transients are conditions which occur between steady-state conditions. Steady-state conditions are defined as those in which hydraulic demands and boundary conditions do not change with respect to time (Walski et al., 2007). Under these conditions, steady flow is assumed. Steady flow is defined as flow in which the velocity at a given point in the given space or system does not vary with time (Munson et al., 2009). The definition of hydraulic transients implies that there is a change in the system as it goes from one steady-state to another. The flow during this transition period is called unsteady flow, which means it varies with time at a given location. Note that flow and velocity may be used interchangeably here since the definition states that these quantities change at a given location. At a single point in a distribution system, the diameter of the pipe is held (i.e., assumed) constant. In this case, flow and velocity are directly related and thus may be used interchangeably. Hydraulic transients occur when there are changes in flow; however, this study will only focus on large transient events which are initiated under rapid flow changes within a system.

Along with rapid changes in flow, hydraulic transients are responsible for inducing pressure waves. These pressure waves travel at acoustic or sonic velocity; however, they

are also dependent on the elasticity of the pipe walls (Wood, 2005). These pressure waves can bring dramatic increases or decreases in pressure depending on the initiation of the transient. Friction losses in the pipe cause energy losses which reduce the wave's amplitude over time and eventually bring the system to a new steady-state.

2.3.2   Potential Impacts

Transient events are unavoidable and will be most frequently and severely experienced in areas of the system such as pump stations, valves, elevated areas, and distant areas from storage tanks (Friedman, 2003). Since transient events cannot entirely be prevented, it is the responsibility of the engineer or the operator to ensure that the system is adequately protected. The engineer should be most concerned with dangerous transient situations that may endanger the plant, the equipment, personnel at the plant and the community (Wood, 2005).

Transient conditions can result in excessively high or low pressures within the system. These pressures can cause problems when the high pressures are superimposed on the existing steady-state conditions the pipe (Wood, 2005). A general rule of thumb in transient analysis states that for every 1 ft/s sudden drop in velocity, the water pressure increases 50 to 60 psi (depending on the pipe material, pipe characteristics, etc.). Sudden increases in velocity will cause pressure decreases on a similar scale (Kirmeyer et al., 2001). High transient pressures may cause the pipe to break if the pressure rating is exceeded or if a week joint is exposed. Negative pressures within a pipeline can cause it to collapse inward on itself or contaminate the water by pulling in pollutants through the groundwater (Walski et al., 2007).

In addition to extreme pressure conditions, transient events may also cause a phenomenon called column separation. When a negative pressure wave is traveling along a pipe, it is changing the velocity of the fluid from a steady-state velocity to zero. However, the fluid ahead of the wave is still traveling at steady velocity. The velocity difference between the fluid particles in the same pipe induces tension into the water column. Once the pressure in the pipe reaches the vapor pressure of water, a vapor cavity is formed. This phenomenon is called column separation and it typically occurs in areas of high elevation in the system. The two separated columns of water will eventually collapse, resulting in a pressure wave wiith an amplitude that is proportional to the fluid's change in velocity (Wylie and Streeter, 1978).

As a result of negative pressures, transient events may also have serious effects on water quality. During events which induce negative pressures, pipe breaks and leaks provide a potential entry portal of groundwater into the system. Fecal material and viruses have been found in the soil matrix surrounding water mains (LeChevallier et al., 2003).

2.3.3 Mitigation Devices

Ideally, a system will be designed to minimize transient events; however, methods for controlling transients are necessary since they cannot be entirely prevented (Walski et al., 2007). Transient control devices can be broadly categorized in two classes: 1) Active Devices, and 2) Passive Devices. Active Devices attempt to prevent pressure waves by provided water to the system from an outside source or allowing water to escape the closed system. Oppositely, passive devices attempt to limit the negative effects of the pressure waves once a transient has been initiated (Wood et al., 2005).

Various types of transient control devices are subsequently discussed. The first device is called a surge tank. Surge tanks are active transient control devices and can either be closed or open tanks (i.e., pressurized or open to the atmosphere and are designed to serve 2 purposes in a distribution system: 1) to receive water from the pipe during high pressure transients and 2) to provide water to the system during low pressure transients. There are many variations of the surge tank and each variation has a different name associated with it (e.g., bladder tank, hybrid tank, feed tank, etc.). However, these tanks generally serve the same purposes as described previously (Wood et al., 2005).

Another surge control device is a pressure relief valve. These valves eject liquid from the main pipeline in order to prevent high pressure transients. Telemetry is required for these valves to operate as they open once the pressure in the line reaches a certain threshold and close once it falls beneath another. More common devices are air release valves which draw air into the system during low pressure situations and expel air once pressure is restored. These valves are commonly placed at high elevation points within the system which are vulnerable to low pressures (Wood et al., 2005).

Valve stroking, although not a device, is a common mitigation strategy. It refers to the intentional slow closure of a valve in order to prevent maximum transient pressures. Valve stroking should be used when valves are closed, especially for those on lines with high fluid velocity. Other mitigation devices include flywheels, which contributes to the inertia of the pump impeller, and allows it to continue to rotate in the case of a sudden pump shutdown. Variable frequency drives are also helpful in mitigating transient events. These drives allow pumps to start and stop over a pre-defined period of time, adjusting the speed ratio incrementally in order to reduce transient effects (Wood et al., 2005).

2.3.4   Transient Analysis

Transient analysis has traditionally not received the attention it deserves in engineering curriculums and system design. The principal reason for this situation is that transient analysis has been presented to engineers as a complex phenomenon to analyze (Wood, 2005). Two different methods have normally been used for transient analysis: the Method of Characteristics (MOC), and the Wave Plan Method (WPM) which was developed by Wood et al. (1966). The original WPM has been improved and is now called the Wave Characteristic Method (WCM) and is employed in various hydraulic modeling software packages (i.e., KYPIPE, Innoyvze). Both the MOC and the WCM are discussed in this section, with additional emphasis on the WCM as this was the method used to perform transient analysis for this study.

Method of Characteristics:

The Method of Characteristics (MOC) is an Eulerian approach to solving transient problems. In an Eulerian approach, fluid motion is given by completely defining properties (i.e., pressure, density, velocity, etc.) as functions of space and time. Information about the flow is obtained at fixed points in space as the fluid flows through those points (Munson et al., 2009). The MOC expresses partial differential equations of motion and continuity as four total differential equations in finite difference form (Wylie and Streeter, 1978). The two partial differential equations of motion and continuity are shown in Equations 38 and 39, respectively.

$$\frac{\partial Q}{\partial t} + gA\frac{\partial H}{\partial x} + \frac{fQ|Q|}{2DA} = 0 \tag{38}$$

$$\frac{\partial H}{\partial t} + \frac{a^2}{gA}\frac{\partial Q}{\partial x} = 0 \tag{39}$$

These equations are one-dimensional unsteady flow equations which are simplified and broken down into the four total differential equations shown in Equations 40 – 43.

$$\frac{g}{a}\frac{dH}{dt} + \frac{dV}{dt} + \frac{fV|V|}{2D} = 0 \tag{40}$$

$$\frac{dx}{dt} = +a \tag{41}$$

$$-\frac{g}{A}\frac{dH}{dt} + \frac{dV}{dt} + \frac{fV|V|}{2D} = 0 \tag{42}$$

$$\frac{dx}{dt} = -a \tag{43}$$

These equations are solved simultaneously in order to obtain a solution for each predefined spatial increment over a specific time period. There are often many spatial increments per pipe when analyzing water distribution system transients using the MOC. The solution methodology is quite stable; however, it requires a very large number of calculations for networks with many pipes.

Wave Characteristic Method:

The Wave Characteristic Method (WCM) follows a Lagrangian approach to analyzing transient events. The Lagrangian approach involves following individual fluid particles as they move and determining how the fluid particle's properties change as a function of time (Munson et al., 2009). The WCM incorporates the same partial differential

equations as the MOC (Equations 38 and 39) into the solution methodology. However, the WCM does not require calculations for a fixed spatial grid for each time interval. Rather, the WCM only makes calculations when change is occurring in the system. "For complex water distribution systems, the WCM typically requires orders of magnitude fewer calculations which allows for a much faster simulation time" (Wood et al., 2005).

CHAPTER 3 MODEL DATABASE

3.1   Development of Models

As part of this research effort, a database of water distribution system models was developed for application and use among the research community. The database consists of 15 models representing small to medium sized water distribution systems. Each model is spatially representative of an existing water distribution system in Kentucky and contains accurate information on pipe characteristics (i.e., diameter, length) and tank characteristics (i.e., volume), including georeferenced locations. "These models may be quite valuable to the research community as a robust database for testing and evaluating new algorithms for a wide range of network issues such as sensor placement, optimal design, and optimal operation of systems" (Jolly et al. 2014).

Jolly et al. (2014) made the first contributions to this database, followed by Schal (2013). Hoagland and Ormsbee (2015) edited and expanded the database in order to investigate a new classification methodology for water distribution systems. Various system parameters (e.g., average pipe length, number of loops, etc.) were compared between configurations in order to identify statistically significant differences. Currently, this database is being managed by faculty at the University of Kentucky and is available to researchers upon request.

3.1.1   Procedure for Model Creation

Water distribution system data was obtained for each of the 15 models from the Water Resources Information System (WRIS). This information system is hosted online by the Kentucky Infrastructure Authority (KIA), which also compiles data on other

infrastructure systems in the state (e.g., sanitary sewer system). Water distribution system infrastructure data including water mains, storage tanks, pumps, and reservoirs are available for download in Geographic Information System (GIS) shapefile format. Pipe, tank, pump, and reservoir data for the entire state of Kentucky was downloaded and imported into ArcGIS. Systems which have a total daily demand between 1 and 3 million gallons per day (MGD) were selected to be included in the database. These systems were selected individually using the "Select by Attributes" tool which is built into ArcGIS. Each system was selected via the "owner" attribute and exported to a hydraulic modeling software program (i.e., KYPIPE).

Importing the shapefiles to the modeling software involved using a built-in conversion tool which translates shapefiles to their respective elements (i.e., pipes, tanks, pumps, reservoirs). Attribute data for each shapefile must be manually defined in the conversion tool such that the modeling software is able to accurately translate the shapefiles to the correct modeling element, along with their attribute information. For example, the waterlines shapefile was chosen to be converted first. The shapefile attribute for diameter was matched up with the hydraulic model's attribute code for pipe diameter. This meant that for every waterline feature in the shapefile, the diameter would also be converted and assigned to the pipe element created in the model. This attribute matching step was also performed for tanks, pumps, and reservoirs. A successful import allows for the creation of a basic hydraulic model.

At this point in the process, junction nodes have been created at the intersection of two or more pipes, which are critical elements in hydraulic modeling of water distribution systems. Junctions play a crucial role in modeling by providing specific points in the

43

network to attribute continuity, demand, and elevation information. However, the newly created junctions are missing demand and elevation information which must be accounted for. The newly created junctions (along with tanks, pumps, and reservoirs) must be exported back to ArcGIS in order to obtain elevation data. An export tool, which is also built into the hydraulic modeling software, is used to export the junction nodes back to ArcGIS. Once imported back to ArcGIS, the nodes are seen directly overlaying the original shapefiles as shown in Figure 3.1.
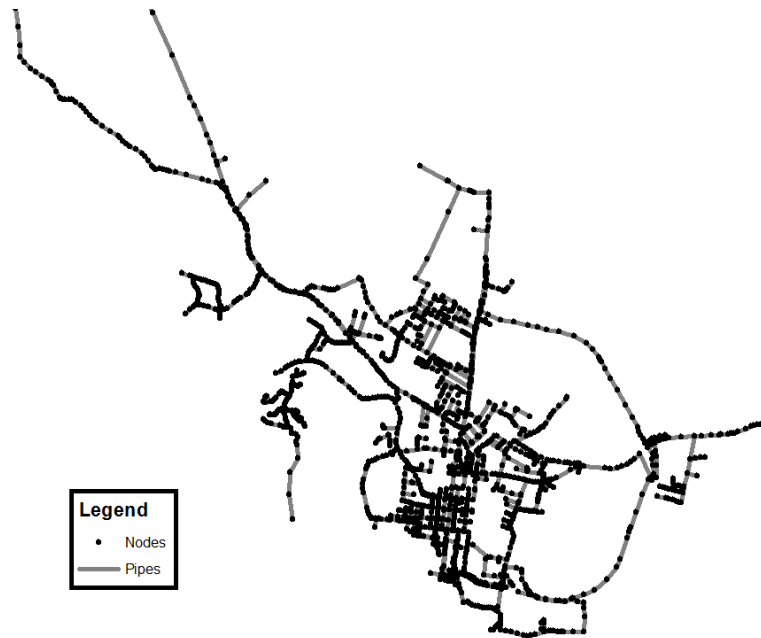
Figure 3.1: Shapefile with Overlain Nodes.

Once the nodes have been successfully imported into ArcGIS, ground elevation data must be added to the map. This data is available in the form of Digital Elevation Models (DEMs) which are downloadable from the Geospatial Data Gateway hosted by the National Resources Conservation Service (NRCS). The area on the ground represented by a cell or pixel, also known as the spatial resolution, is 10 meters by 10 meters. Each pixel

has a specific elevation associated with it. The higher resolution DEMs will provide greater elevation accuracy, however the amount of data collected is much greater, resulting in smaller areas for each DEM. The 10 meter by 10 meter DEMs were chosen as a good balance of accuracy and spatial extent. The DEMs may be imported into ArcGIS and set to appear behind the current shapefile and node layers as shown in Figure 3.2.
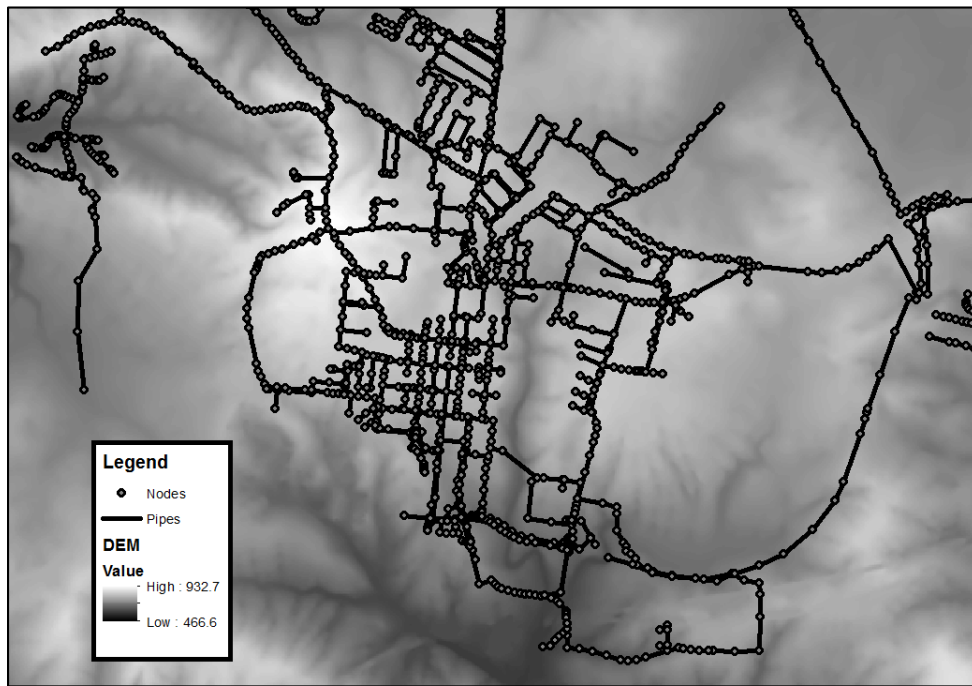
Figure 3.2: Digital Elevation Model.

For distribution systems that cover a large spatial extent, it may be required to combine multiple DEMs in order to cover all of the nodes in the system. Once the entire system has been covered with a DEM, the "Extract Value to Points" tool, which is built into ArcGIS, may be used to extract ground elevations to all of the junctions, tanks, pumps, and reservoirs. It should be noted that the ground elevation is an approximation for the elevation of the pipes since it is known that pipes are generally buried 3 to 6 feet below the ground. However, this approximation should not affect the hydraulics of the system since

the estimate is applied to the entire system. This consistency should maintain the relative

accuracy of the system's grades and pressures. Once elevations have been extracted to the

nodes, a simple copy and paste function of the values into the hydraulic model's data tables

will complete the process of assigning elevation data to the system.

This process has resulted in a hydraulic model with all of the main system elements

such as reservoirs, tanks, pumps, pipes, and junctions. Elevation data was also added to the

model through DEMs and ArcGIS tools. Additional modifications must be made to each

of the models prior to analyzing the system's hydraulics. These modifications are covered

in Section 3.2. The procedure up to this point is nicely summarized in Figure 3.3 from Jolly

et al. (2014).
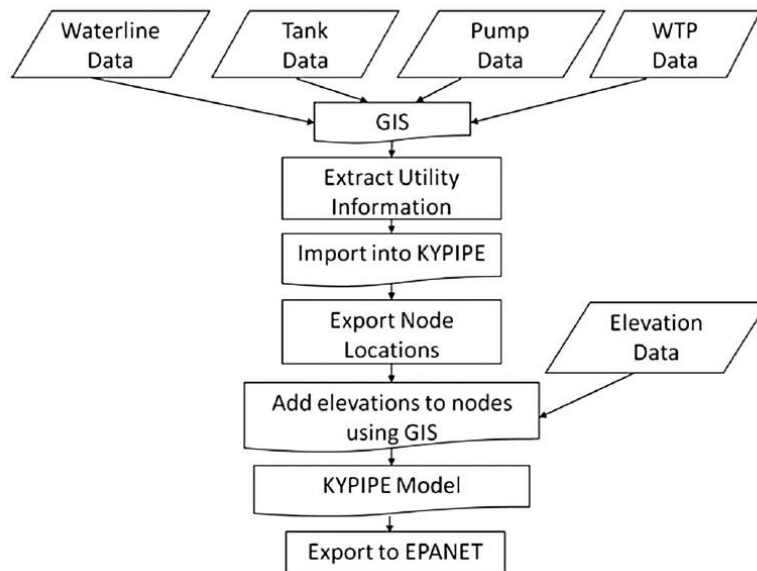
Figure 3.3: Model Development Flowchart (Jolly et al. 2014).

Figure 3.3 also includes an additional step not mentioned previously, which

consists of exporting the hydraulic model to EPANET format. Most researchers use

EPANET hydraulic modeling software due to the fact that it is freely available for

download. Thus, this last step is extremely important to include so the database is freely available to the research community.

3.1.2   Additional Modifications

Before these water distribution system models are ready for hydraulic analysis, some additional modifications are required. The first necessary modification consists of checking for connectivity errors. Connectivity errors are mistakes in the conversion process from the waterline shapefiles to the pipe and junction elements in the hydraulic model. These errors result in certain pipes being entirely disconnected from the rest of the distribution system. Almost all of these errors are unnoticeable just by looking at the system from a normal level of zoom. However, when the pipe intersection is magnified, the missing junction node becomes apparent. An example of a connectivity error is shown in Figure 3.4, where the image on the left of the figure is a normal zoom level and the image on the right is the magnified intersection of the two pipes.
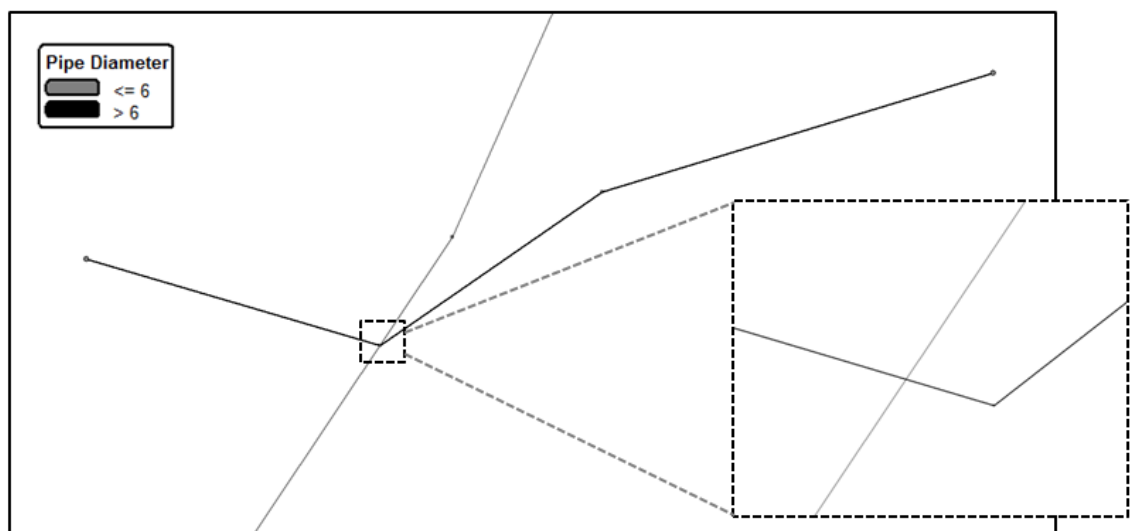
Figure 3.4: Connectivity Error.

These errors are virtually undetectable at the normal zoom level. Note that it would take a great deal of time to check each pipe manually for connectivity. A tool in KYPIPE was used to check for these errors called the "Connectivity Check" tool. This tool highlighted all pipes in the system which were completely disconnected. The amount of connectivity errors in a created model tends to vary quite a bit. These errors are created by the end coordinates of all of the shapefile waterlines being further away from each other than a specified threshold in the conversion tool. When the ends of the pipe segments are too far from one another (i.e., further than threshold distance), then the conversion tool creates a new pipe segment that is disconnected from the rest of the system. In this instance, and in almost all instances, it is extremely obvious where the intersection of the two pipes should be. Thus, a manual correction of these errors is required.

Another necessary modification to the hydraulic model is the addition of pipe roughness coefficients. Pipe roughness coefficients are assigned in each model as Hazen-Williams C-factors to account for the frictional energy loss in pipe flow. The higher the C-factor the smoother the pipe, which means less energy losses. Since these models are uncalibrated, the C-factors are assigned to each pipe based on typical C-factors associated with certain pipe parameters such as those developed by AWWA (2012) based on pipe material and age.

The next step of creating a working hydraulic model is assigning demand data to various junction nodes in the system. Estimating the demand, or the amount of water exiting the system, at various points in the system can be done quite accurately with the use of flow meters. Utilities attach flow meters to service connections so that they can measure the amount of water a specific customer uses per month and bill them for their

usage. This meter data can also be grouped, edited, and assigned to a specific junction node to provide accurate demand estimates in a hydraulic model. However, this data was not provided by the utility; therefore, the average daily demand for each system (obtained from the KIA) was distributed to all junction nodes in the respective system based on the diameters of the pipes leading to each junction node. Higher fractions of the demand were assigned to junctions which had larger pipes leading to it and lower fractions of the demand were assigned to junctions which had smaller pipes leading to it. This was done using a tool called the "Automatic Demand Distribution" tool in KYPIPE. This method is fairly representative of how water utilities design and operate their systems and was deemed appropriate for this study. Utilities design their systems as such to prevent excessive energy losses or water quality issues from pipes being designed too small or too large, respectively.

Much water distribution system research involves running both steady-state simulations and extended-period simulations. In order to ensure the model was set up to also run an extended-period simulation, some additional steps needed to be taken. The following steps were performed to ensure the model would be representative of the real system's flow dynamics over an extended-period of time. First and foremost, a demand curve was applied to the model to represent average demand fluctuations throughout a typical day. For a typical community, there is a low water demand throughout the night while most people are sleeping. There is a spike in demand around 7 am when many people are waking up to shower and get ready for their work day. Demand may level off or even drop slightly during most of the day. Another spike is observed around 8 pm when people are home from work and using water for various household tasks (i.e., washing dishes, doing laundry, taking showers, etc.). The demand then drops considerably over the course

49

of the night. This typical demand curve is implemented in a hydraulic model by using "demand factors" which were developed by the American Water Works Association (AWWA, 2012). The demand factors are multiplied by the average demand at that junction to either decrease (factors < 1), increase (factor > 1), or keep the same demand (factor = 1).

Initial grades at the reservoirs, minimum, initial, and maximum elevations for storage tanks, and pump horsepower values are also required for each of the respective elements prior to running the model. Pump horsepower was tweaked in a guess-and-check fashion in order to get water to flow into the storage tanks during extended-period simulations, while ensuring that pressures remained within acceptable ranges (40 − 150 psi). Clearwells, reservoirs, and storage tanks must have an initial grade defined in order for the model to properly run. For this study, estimates were made for each initial grade. Grades were assumed and then pressures were subsequently checked to make sure that reasonable pressures (40 − 150 psi) were being calculated in the system. More accurate elevations of the grades can be obtained by observing aerial imagery of the site of interest. Elevated storage tanks and ground storage tanks are discernable via relief displacement in the photograph. Many of the tanks are also viewable using street view images, which provides another viewing angle of the storage tank from a nearby road. Other elements in the picture may help to discern the tank's relative height. Figure 3.5 shows an aerial image and street view image of a storage tank.

Figure 3.5: Aerial and Street View Images of Storage Tanks.

Ultimately, this process resulted in a working hydraulic model for each of the 15 water distribution systems. Certain assumptions were made in the creation of these models which allow for the models to be generated in a timely manner. Among these assumptions were the distribution of demand, elevation of nodes from remote sensed data, and various element characteristics such as tank elevations and pump horsepower. Although these models are uncalibrated, it is reasonable to assume that they are fairly representative of the flow dynamics in the actual systems. That being said, these models may prove to be extremely valuable to the research community in developing and validating new algorithms.

3.1.3 Models Used in this Study

A database of 15 synthesized models is used as a robust dataset in analyzing the distribution of risk due to the occurrence of a large transient event caused by a pump shutdown. Each of these models was created by following the procedure described in Sections 3.1.1 and 3.1.2. Therefore all of the assumptions and limitations listed in those sections apply to these 15 systems. To protect the identity of the water distribution system of which each model is representative, the models were given standardized names in the form "KY #". Additionally, all other system identifying information was removed such as

the names of storage tanks and pump stations. Each of the systems was also classified into one of three general configurations of water distribution systems. The method used to classify the systems is covered in Section 3.2 along with the classification results. All of the systems in the database are listed in Table 3.1, along with some information regarding their assets and operation.

Table 3.1: Database Characteristics

System Name	Config-uration	# of Tanks	# of Pumps	# of Pipes	# of Nodes	Total Length of Pipes (mi)	Avg Pipe Length (ft)	# Pipes/ # Nodes	Avg Pipe Diameter (in)	Avg Pipes/ Node	Demand (MGD)	Range in Elevation (ft)
KY 1	Grid	2	1	984	858	40.8	218.8	1.15	7.86	2.29	2.00	122.0
KY 2	Grid	3	1	1124	814	94.6	444.4	1.38	5.41	2.76	2.09	96.0
KY 3	Grid	3	5	366	270	56.7	818.3	1.36	7.92	2.66	2.02	144.6
KY 4	Loop	4	2	1156	962	161.7	738.6	1.20	7.08	2.38	1.51	249.4
KY 5	Loop	3	9	496	418	60.0	638.8	1.19	7.18	2.32	2.28	292.4
KY 6	Loop	3	2	644	545	76.6	627.6	1.18	6.10	2.34	1.56	333.7
KY 7	Grid	3	1	603	484	85.2	745.7	1.25	6.24	2.49	1.53	270.9
KY 8	Loop	5	4	1614	1319	153.7	502.8	1.22	7.58	2.42	2.47	468.8
KY 9	Branch	15	15	1270	1096	597.7	2484.9	1.16	4.57	2.01	1.38	459.0
KY 10	Branch	13	13	1043	917	267.2	1352.7	1.14	6.12	2.23	2.26	359.0
KY 11	Branch	28	21	846	795	285.4	1781.0	1.06	5.50	2.04	1.93	892.6
KY 12	Branch	7	15	2426	2318	403.0	877.2	1.05	4.66	2.06	1.38	470.0
KY 13	Loop	5	4	940	780	95.3	535.0	1.21	7.51	2.40	2.36	306.9
KY 14	Grid	3	6	548	378	64.5	621.2	1.45	8.14	2.85	1.04	212.1
KY 15	Branch	8	13	671	633	299.5	2356.6	1.06	5.41	1.99	1.52	929.6

As mentioned previously, a pressure zone model of a distribution system in Kentucky was also obtained from a water utility in order to study possible transient scenarios in their system. This model was developed and calibrated by the utility company, thereby providing more accurate insights into the system's flow dynamics. This model, named System 1, will be used as a real-world calibration and validation of the risk analysis presented in this study. Characteristics of the pressure zone will not be presented in order to protect the water utility's information.

3.2   Classification of Water Distribution Systems

Historically, water distribution systems have been classified as one of three basic configurations: branch, loop, or grid (Hoagland et al., 2015). Examples of these configurations are shown in Figures 3.6, 3.7, and 3.8. These configurations can significantly differ in the way systems are designed and operated. In practice, no water distribution system is designed as a specific configuration. However, the understanding of a system's configuration may provide useful insights as to how to better operate and upgrade the network.

3.2.1   Traditional Configurations

Branch configurations are named after the schematic's visual similarities to a tree or a tree branch. The idea is that smaller pipes will branch off of a larger main, similar to the structure of a tree (National Research Council, 2006). Branch systems are common in rural areas, where demands are often spaced out over a large area. High flows are present near the source or the water treatment plant, and flows generally decrease as pipes reach further away from source. Branch systems typically have a higher number of assets due to the large spatial extent; however, it should be noted that the average pipe diameter is typically smaller than in grid and loop systems (Schal, 2013). Reliability may also be of concern in branch systems due to the linear nature of service. If a pipe breaks at the start of a branch line, that break will often require the line to be closed while the break is repaired. This can result in many customers losing service. An example of a branch system is shown in Figure 3.6.
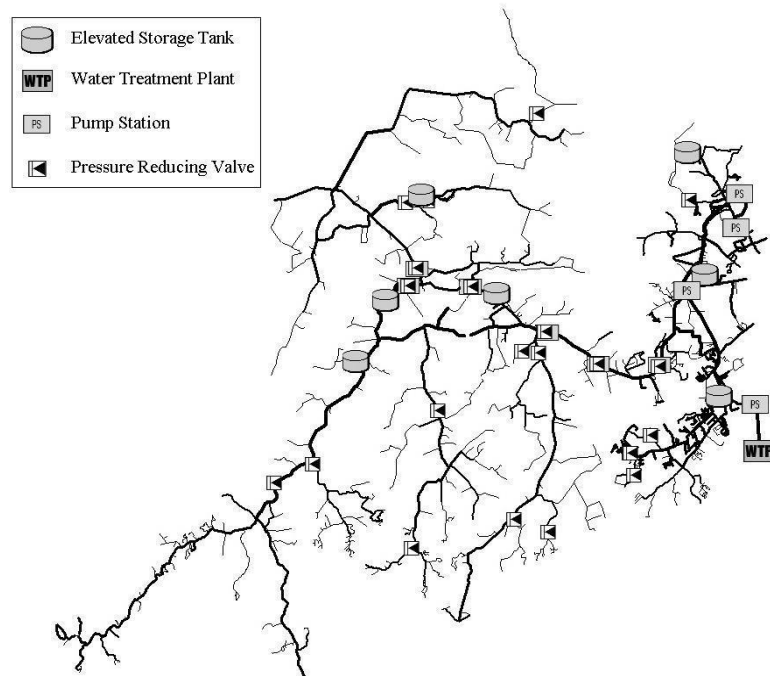
Figure 3.6: Example of a Branch Configuration (Hoagland et al., 2015).

Loop configurations are much harder to distinguish than a branch system just by looking at the system schematic. Loop systems are characterized by having multiple redundancies, or multiple paths for the water to reach a customer. These systems are more common in urbanized areas where loops are designed to maximize the reliability of a system, assuming that valves are appropriately placed. In a traditional loop system, there is a transmission main that runs through the middle of the system which feeds smaller distribution lines that ultimately deliver water from the central area of the system to the consumers in the outer areas (Von Huben, 2005). Loop systems typically have less total length of pipe in service due to a more concentrated spatial extent; however, the average pipe diameter is greater than a branch system due to higher demands (Schal, 2013). An example of a loop configuration is shown in Figure 3.7.
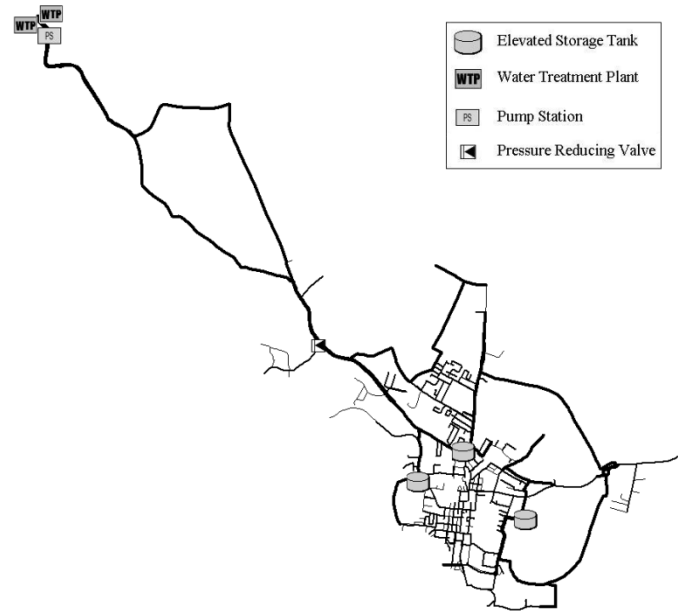
Figure 3.7: Example of a Loop Configuration (Hoagland et al., 2015).

Grid configurations are also much harder to distinguish than a branch configuration, although they are easier to identify than loop systems. Grid systems are named after their schematic's similarity to a checkerboard. The transmission mains travel around the outside of the network and connect to smaller mains which populate the interior of the system (Von Huben, 2005). The distribution mains then form the grid pattern, almost always following the gridded pattern of roads in a city's downtown area. Grid systems are also typical of urbanized areas since they provide more reliability than a branch system, assuming appropriate valve placement. Asset and operational characteristics of grid systems are very similar to loop systems (Schal, 2013). An example of a grid configuration is shown in Figure 3.8.
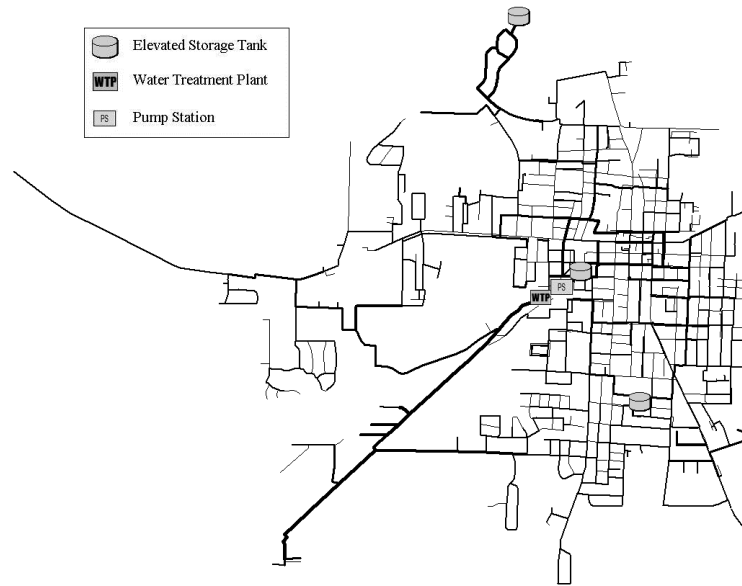
Figure 3.8: Example of a Grid Configuration (Hoagland et al., 2015).

Traditionally, water distribution systems have been classified based on a subjective analysis of the configuration of the system as viewed from a graphical representation of the network (Von Huben, 2005). Specifically, the location of transmission mains in relation to the rest of the network have been used to classify systems. Branch systems are often easily identifiable by looking at the network schematic. However, grid and loop systems look very alike and are generally undistinguishable from one another just by looking at the schematics. Additionally, many systems have characteristics of multiple configurations which adds confusion to a subjective classification process. Therefore, a new objective classification methodology proposed by Hoagland and Ormsbee (Hoagland et al., 2015) is presented in Section 3.2.2.

3.2.2 Classification Methodology

A traditional method for classifying water distribution systems was presented in Section 3.2.1. This method involved subjectively analyzing the schematic of the system,

specifically the location of transmission mains (i.e., large diameter pipes). In the early years of a newly designed water distribution system, this method of classification may be appropriate. However, a water distribution system will often grow more complex the longer it is in service due to population increase and new developments. New subdivisions may be developed, a large apartment complex may be added to the downtown area, or a stadium for a new sports team may be built during the life of the distribution system. Water distribution system operators will constantly be approving new projects to change and improve their system. Many years down the road, the water distribution system which used to look like a well-designed grid system now looks like a mixture of grid, loop, and branch systems as shown in Figure 3.9.
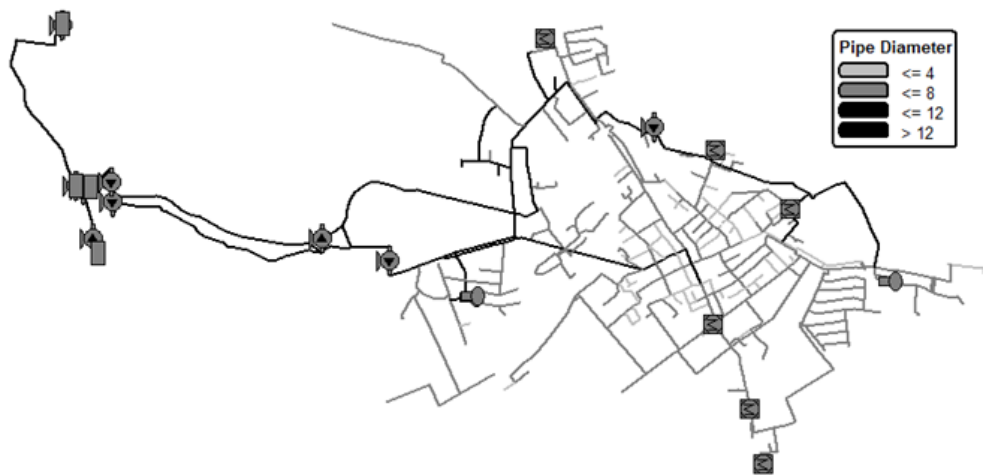
Figure 3.9: Distribution of Pipe Diameters.

As shown in Figure 3.9, the distribution of pipe diameters in present day water distribution systems may appear to be randomly distributed. Water distribution systems such as the one in Figure 3.9 would make the subjective classification process extremely difficult, if not impossible. Therefore, an objective classification methodology is proposed

which assigns a configuration based on the frequency of specific loops in the system. This method was developed by Hoagland and Ormsbee (Hoagland et al., 2015).

A group of 15 water distribution systems was subjectively classified into 3 configurations (i.e., branch, loop, and grid) based on the layout of the system's loops, or lack thereof. Each configuration group contained 5 water distribution systems. Quantitative parameters were regressed from each configuration set and compared. Five parameters were found to be of significant interest which are: the number of branch pipes (i.e., # of pipes not in a loop), the number of 3-pipe loops (i.e., the number of loops which contain 3 pipes), the number of 4-pipe loops, the number of 5-pipe loops, and the number of total pipes. It was found that branch configurations were discernable by the ratio of branch pipes to total pipes, and the loop and grid configurations were distinguishable by analyzing the number of 3, 4, and 5-pipe loops. The algorithm shown in Figure 3.10 is proposed for the classification of water distribution systems.
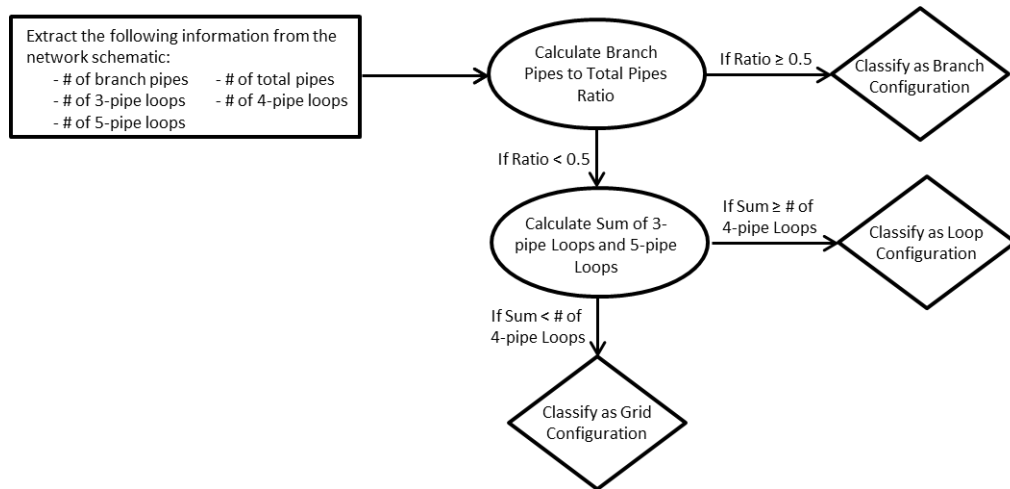
Figure 3.10: Classification Algorithm (Hoagland et al., 2015).

Counting loops or pipes in a distribution system can be very time consuming if performed manually. "To automate the classification process, a visual basic code was

58

developed that is able to read in a KYPIPE or EPANET input data file and then generate a histogram of pipe loop densities which can then be used in applying the classification algorithm" (Hoagland et al., 2015). An example of a pipe loop density histogram for a grid system is shown in Figure 3.11.
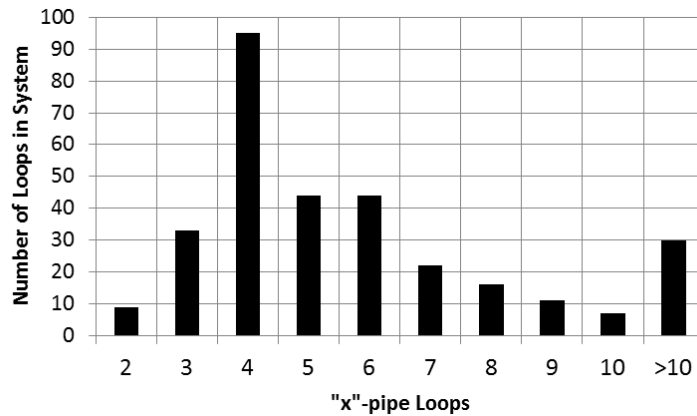
Figure 3.11: Pipe Loop Density Histogram (Hoagland et al., 2015).

As evidenced by Figure 3.11, the number of 4-pipe loops exceeds the sum of the number of 3-pipe and 5-pipe loops. Therefore the system would be classified as a grid system. This assumes that the ratio of number of branch pipes to total pipes had already been determined to be less than 0.5. The Pipe Loop Density Tool is currently employed in KYPIPE but can easily be expanded to work in other hydraulic modeling software programs such as EPANET.

3.2.3   Classification of Models in Study

Each of the database models was classified using the proposed methodology presented in Section 3.2.2. The classification resulted in 5 branch systems, 5 loop systems, and 5 grid systems. Each of the groups of systems are shown below in Figures 3.12 – 3.14.
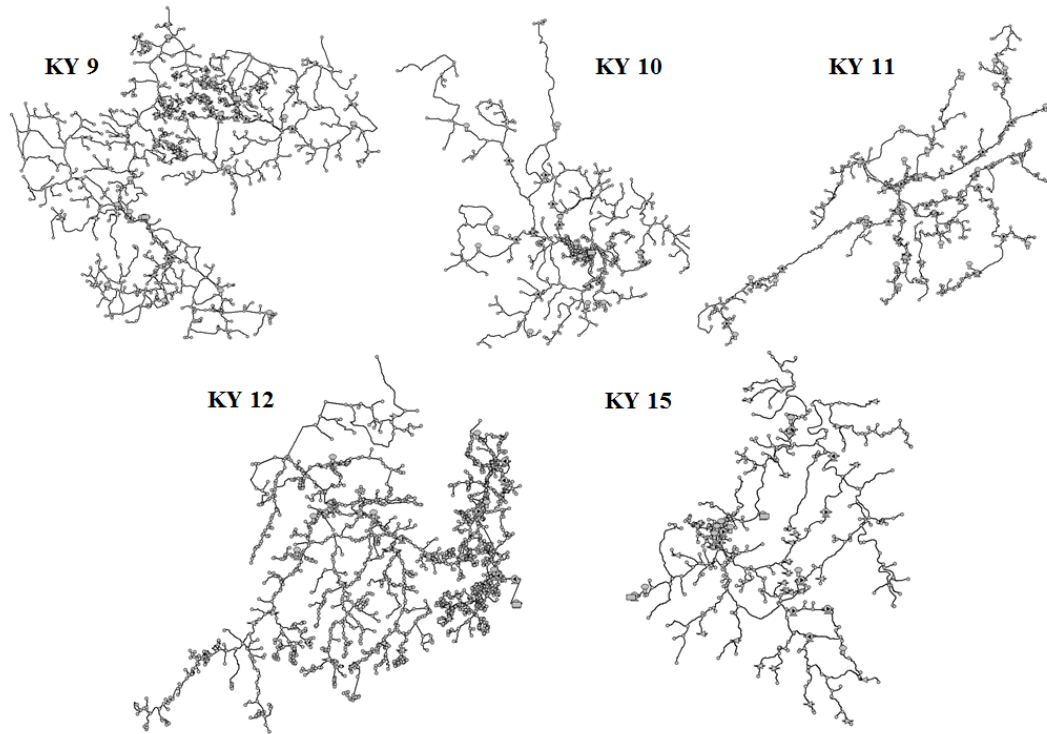
Figure 3.12: Branch Systems (KY 9, 10, 11, 12, and 15).
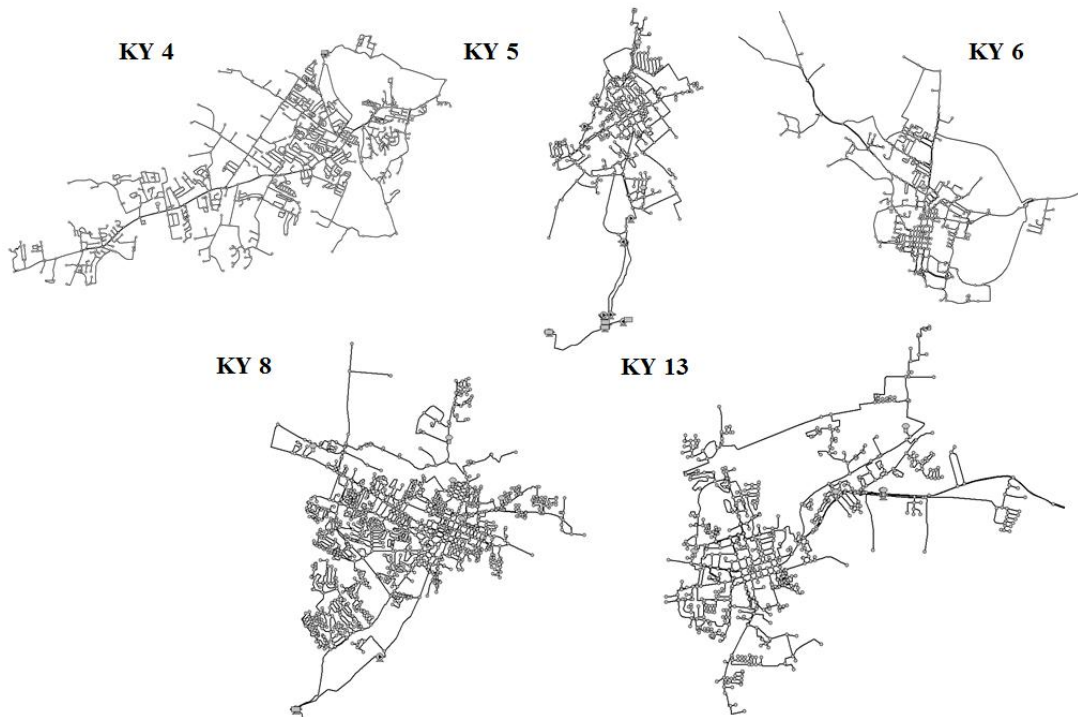
Figure 3.13: Loop Systems (KY 4, 5, 6, 8, and 13).
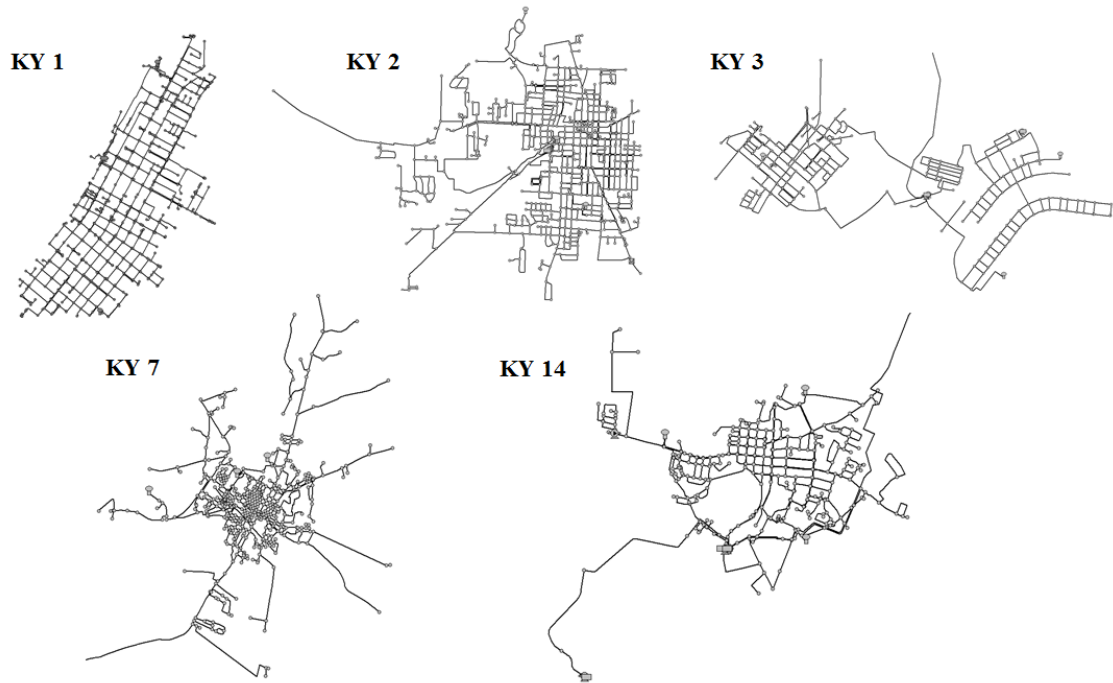
Figure 3.14: Grid Systems (KY 1, 2, 3, 7, and 14).

The 16th and final model, which is a calibrated pressure zone from a utility in Kentucky, is shown in Figure 3.15. Note that this system was used for calibration of parameter scoring and validation of the general relationships between pipe failures and the factors described in Section 4.3.1. Therefore, this system was not classified with the other database systems. This system will be referred to as System 1 throughout the remainder of this study.
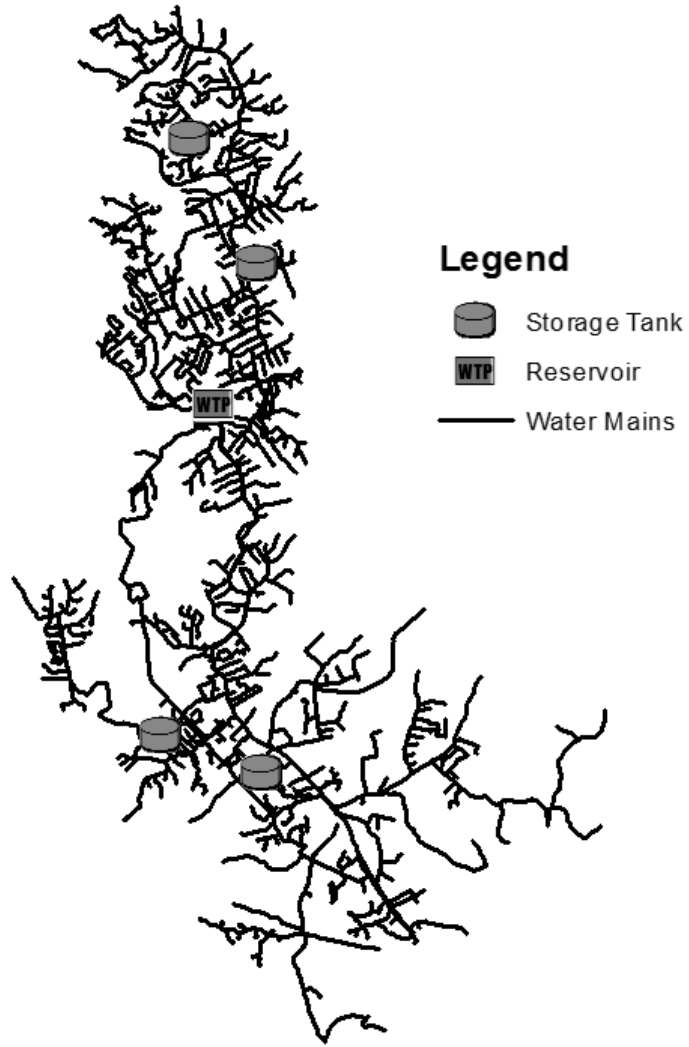
Figure 3.15: System 1 (Calibration/Validation System).

CHAPTER 4 METHODOLOGY

4.1   Initiation of Transient Event

In order for a water distribution system to be analyzed for its risk pertaining to transient events, a transient event must first be modeled. Since a hydraulic transient is defined as a flow and pressure condition that occurs between an initial steady-state condition and a final steady-state condition (Walski et al., 2007), it can be said that there are many different transient events occurring in the system at any given time. Small transient events are almost constantly occurring due to demand changes at service connections (i.e., residential water usage). However, the effects of these transients are assumed to be negligible due to the relatively small pressure change (i.e., small relative to the normal operating pressure). Pump and valve operations cause many of the important transient events (Wylie and Streeter, 1978). These are the most commonly modeled transient events due to their noteworthy effects on a system, although large demand changes may also have significant effects.

4.1.1   Pump Operations

The pump motor conveys energy to the impeller by exerting a torque on the rotating shaft. This causes flow through the pump which develops a total dynamic head (TDH) increase from the suction side of the pump to the discharge side. The total dynamic head (TDH) is defined as the energy increase per unit weight of liquid pumped. "In the event of a quick pump shutdown, the reactive torque of the liquid on the impeller causes it to reduce its rotational speed, which in turn reduces the TDH, and causes rarefaction waves to be

transmitted downstream and pressure waves to be transmitted upstream through the connected piping" (Wylie and Streeter, 1978).

In the event of a power failure, pumps would be quickly shut down which will often initiate a large transient event. Even for systems which have backup generators at the pump stations, there is a lag time before the generator will start, thus allowing time for the creation of extreme pressure waves. Power failures, although not common, are prone to happen occasionally. Natural disasters and harsh weather conditions are major causes of power failure, while smaller power loss events can be for reasons as minute as vandalism. Since a power failure is a fairly probable event, it was decided to be the transient event of choice for this study.

It should be noted that different systems will react to this type of transient event in different ways. For example, a pump that is positioned in an area of low elevation surrounded by higher elevations is more likely to experience a flow reversal soon after the pump is shutdown. Oppositely, a pump that is positioned in a relatively flat area with no tanks nearby is less likely to experience a sudden flow reversal since there are no forces encouraging the flow to reverse. In that sense, system design differences such as these are likely to warrant different responses to a pump shutdown.

It should also be noted that it does not take a power failure to induce extreme transient events in a system. Daily pump operations may include the starting and stopping of one or more pumps. If variable frequency drives are not installed at the pumps, or if transient protection devices are not used, extreme pressure situations may be present in the system on a regular basis. In that case, pipes may be exposed to sustained stresses over a

long period of time which may lead to pipe failures. Thus, transient modeling is essential in understanding stresses resulting from operational decisions.

For this study, a pump shutdown due to a power failure (i.e., a pump trip) is modeled as the initiated transient event. For each system, the pump closest to the water treatment plant was selected for modeling. This selection assumes a power failure at the water treatment plant. To model a sudden pump shutdown due to a power failure, the pump impeller's rotational speed was linearly decreased from 1 (i.e., fully operating) to 0 (i.e., fully stopped) over a 2 second time period. Pumps with inertial devices (e.g., a flywheel) would require a longer modeled time period for the impeller speed to fully stop rotating. It was assumed that all pumps for this study do not have inertial devices or transient protection devices installed at the treatment plant.

4.1.2   Valve Operations

The opening and closure of a valve is another commonly modeled transient event. There are many different types of valves in a water distribution system all with different purposes. Isolation valves are operated in the event of a pipe break, when that portion of the system requires separation from the rest of the network. Check valves, which close automatically upon flow reversal, are placed in areas of the system where flow reversal is undesirable such as the downstream side of a pump. Check valves often have a specified resistance associated with them such that they close over a specific time interval upon flow reversal. Although the instantaneous closure of a valve can produce extreme transient conditions in the system, general guidelines or design specifications are put in place to prevent transient conditions. For example, some valves have instructions to close the valve over a specific time interval. Another example is that pipes are appropriately sized during

the design such that energy (i.e., pressure) is conserved. High velocities in the line are directly related to high energy loss; thus, line velocities are typically low. Due to these natural transient protection measures, valve openings and closures were not selected for analysis for this study.

4.2   Pressure Analysis

Now that a pump shutdown has been defined as the transient event for this study, it is possible to analyze the system's response to the transient. Although extreme pressure and flow conditions are created during a transient event, the pressure results were selected as the most important factors in this study. High pressures may exceed a pipe's pressure rating, causing the pipe to burst. Low or negative pressures inside the pipe, along with the external loading of soil and traffic, may cause the pipe to fail by collapsing inward. Both maximum and minimum pressure, as well as the occurrence of cavitation, are weighted and included in the risk analysis. Pressures were calculated for each system using the Wave Characteristic Method, discussed in Section 2.3.4, which is embedded in both InfoWater and KYPIPE hydraulic modeling software.

It should be noted that the transient analysis was specified to run over a 90 second analysis period. This means that results were calculated for a 90 second period following the pump shutdown, although the amount of time required for the software to perform the calculations is considerably less. It should also be noted that specifications for the analysis such as wave speed and time of initial transient were predefined. The transient was specified to start at time t = 5 seconds, while the system was at steady-state for the first 5 seconds. Additionally, the wave speed "c" was defined as 3600 feet per second.

4.2.1 Maximum Pressure

Maximum pressures during transient events can destroy system components and result in the loss of human life in worst-case scenarios (Boulos et al., 2005). Repeated transients may also have a negative effect on the system by causing cracks in pipe liners, walls, and joints (Boulos et al., 2005).

After a transient event has been initiated, a period of rapid changes in flow and pressure occurs. The upstream side of the pump at the water treatment plant typically has only 1 pipe leading from the reservoir, while the downstream side of the pump leads to the rest of the pipe network. After a pump shutdown, the downstream side of the pump will experience an initial pressure drop due to the rarefaction waves from the impeller stoppage. These pressure waves will travel through the system, transmitting energy and reflecting energy at junctions and boundary conditions. Energy waves will continue to be transmitted and reflected until the end of the simulation or until a new steady-state condition is reached. A simple plot of pressure is shown in Figure 4.1 for part of a system following a pump shutdown.
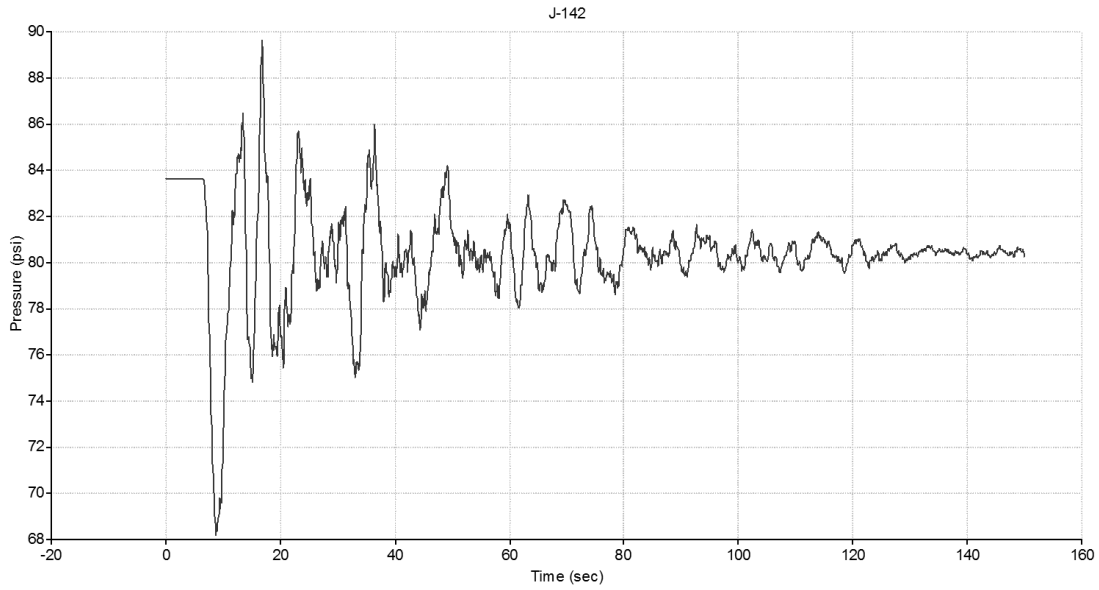
Figure 4.1: Transient Pressure Plot.

As shown in Figure 4.1, the steady-state pressure for this part of the system is recorded in the first 5 seconds of the transient simulation at approximately 83.8 psi. After 5 seconds, the pump shuts down and the pressure immediately drops to 68 psi. The pressure in the system then jumps from 68 psi to 86 psi over the course of about 5 seconds. Pressure continues to increase and decrease very rapidly for two minutes following the pump shutdown. After two minutes, the amplitude of the pressure jumps becomes less severe and the system is converging towards a new steady-state at approximately 80.5 psi. Embedded into the KYPIPE software is a "Maximum Pressure" results option which will output the maximum pressure for a given node during the transient simulation. For the transient at the junction shown in Figure 4.1, the maximum pressure result would read 89.5 psi, which was reached at approximately the 17 second mark.

The maximum pressure results from the transient analysis may be displayed as numerical output in table format which is helpful for quantitative analysis (e.g., how many

nodes in the system exceed the maximum pressure threshold). The results may also be displayed graphically by color coding the nodes based on their maximum pressure (e.g., lower maximum pressures displayed as blue; higher maximum pressures displayed as red). The graphical results may be useful in determining problematic areas in a system for which transient protection may be required. A color coded map is shown in Figure 4.2.
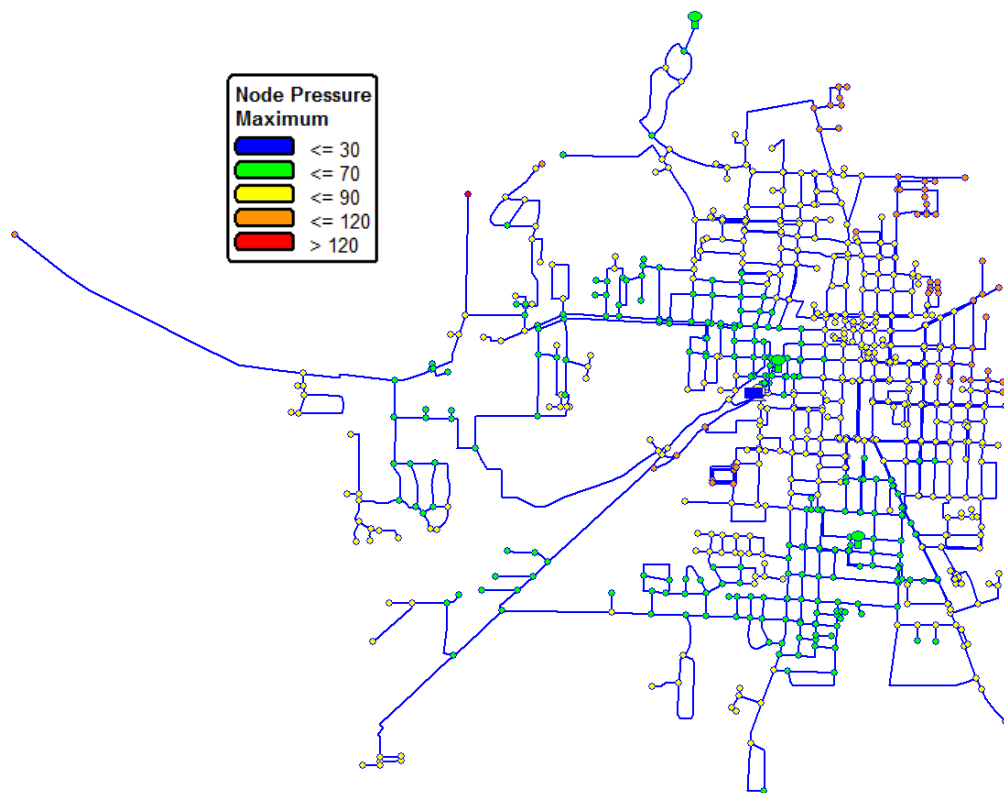
Figure 4.2: Color-coded Pressure Results.

4.2.2 *Minimum Pressure*

In addition to the maximum pressure results, the software also has an output option for "Minimum Pressure" results. As mentioned previously, the minimum pressure is a factor of concern in this analysis because the low or negative pressures, combined with the external load from the soil column and traffic, may cause the pipe to collapse inward. The

69

negative pressures also expose the system to contamination threat. If the pipe contains any discontinuities such as leaking joints or cracks in the pipe, these areas may allow contaminated groundwater to be sucked into the system when pressures go below zero. Where backflow preventers are not present, negative pressures may also pull in other contaminants through cross connections.

The software output of the minimum pressures may be specified as either tabular output or as graphical output. The graphical display of the results may be limited in the hydraulic modeling software as compared to that of GIS software. However, most of the modeling software has tools available to export results to other programs like ArcGIS. Within GIS, there are a number of great display features available as well as coding options to display algorithm results. For example, if the minimum pressure reaches the vapor pressure of water, then cavitation will occur. An "if" statement can be coded in binary representation to identify all pipes based on whether or not the pipe reaches cavitation pressure. The results can then be displayed as red and green; red pipes have cavitation occurring and green pipes do not. An example of this is shown in Figure 4.3.
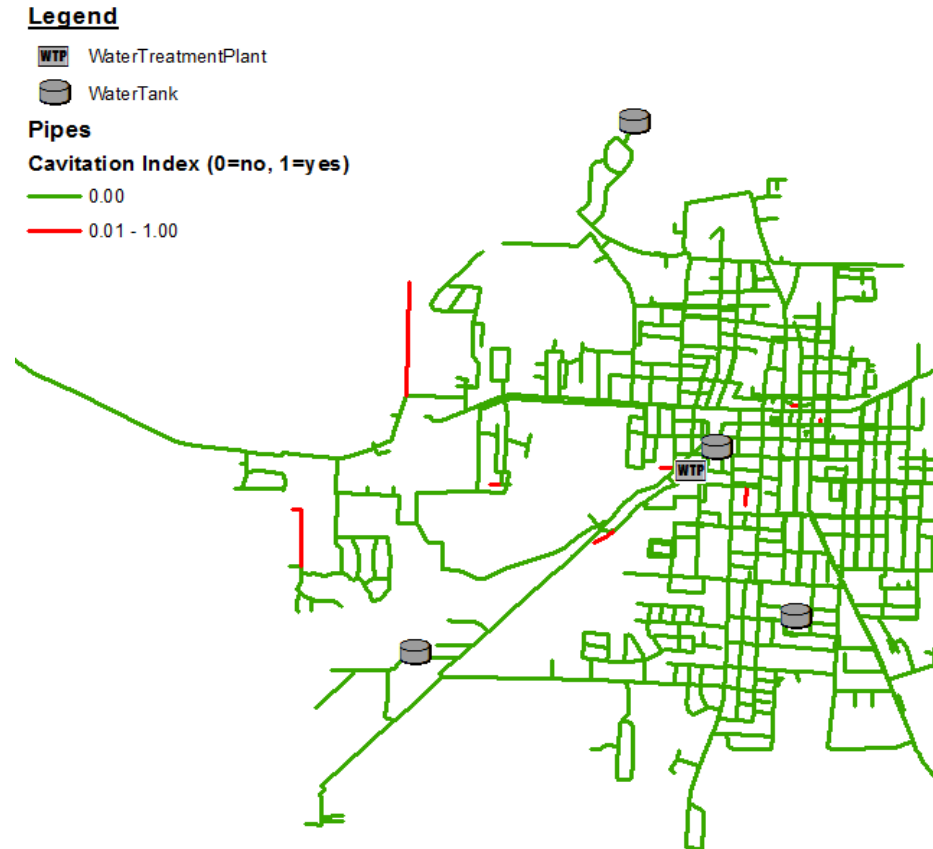
Figure 4.3: Color-coded Cavitation Results.

4.3   Risk Analysis

As mentioned in Section 2.1, the decision of whether or not to replace a water main is typically driven by economic factors. There are two things that go into this economic decision: 1) the cost of the project (i.e., how much it will cost to replace the main), and 2) the projected future costs associated with the pipe (i.e., how much it will cost to maintain this pipe in working condition). By comparing these two costs for all pipes in the system, a prioritization of which mains to replace can be established. Ideally, the main should be replaced when the total cost (i.e., sum of the capital investment per year and maintenance costs) is at a global minimum as shown in Figure 2.1. If one could see the future and know which pipes were going to break in each year, then it simply becomes an optimization

71

problem where the objective function is minimizing the total cost over "n" years. However, it is impossible to perfectly predict main breaks; therefore, there are many uncertainties involved in risk analysis.

The first and most obvious uncertainty is the remaining useful life of each pipe. Shamir and Howard (1979) showed that age and pipe breaks were exponentially related, where older pipes had a higher likelihood of failure. However, many studies have shown that age isn't very good at predicting breaks by itself (Ellison et al., 2014). There are many other factors that can play a role in when a pipe is likely to break. These factors are covered in Section 4.3.1. It should also be noted that even if the remaining useful life of each pipe could be accurately predicted, the cost of replacement and future maintenance costs would still have to be projected. A second uncertainty is the impact (or costs) associated with failure. There are a number of factors that can influence the impact of failure which are covered in Section 4.3.2.

Relative weighting has pros and cons when applied to risk analysis. One of the pros of relative weighting is that it allows for easy identification of pipes, regardless of system age. For example, if a completely new water distribution system was designed and installed, a relative weighting approach would still identify a group of pipes as having a higher probability of failure than the rest of the pipes, even though the overall probability of failure is likely going to be very low for all pipes in a new system. In this type of situation, this information could tell utilities which pipes should be monitored more closely.

In this study, the weighted-score method was used to calculate both probability of failure and impact of failure scores for each pipe. Each of the scores represents the pipe's probability or impact of failure relative to all other pipes in the system. Sections 4.3.1 – 4.3.3 discuss more specific details of the metrics used in this analysis.

4.3.1   *Probability of Failure*

As mentioned previously, a probability of failure score is assigned to each pipe in the system and represents a pipe's estimated likelihood of failure relative to all other pipes. All scores were scaled to values between 0 and 1 by dividing by the maximum possible score. Each probability of failure value was archived for later use in the composite risk metric calculations. Factors which were incorporated in the probability of failure value are generally classified into 3 categories: pipe factors, environmental factors, and loading factors. Each of the three categories is further discussed. Please note that this methodology was applied to System 1 as well as the 15 systems in the database. However, failure data was only available for System 1. Therefore, all relationships shown in Sections 4.3.1 are based on failure data from System 1. These relationships were used to validate System 1's behavior of pipe failures with findings of other studies in the literature (e.g., validate that smaller pipes break more frequently than larger ones, etc.).

Pipe Factors:

Part of the probability of failure score includes factors which come directly from information about the pipe itself. These factors are called pipe factors and include the following: material, class (or wall thickness), lining or wrapping, diameter, and age. Length of the pipe is not included in the pipe factors as it is commonly used to normalize the data.

Information on the pipe factors should have been documented by the utility company when the pipe was designed and installed.

With the exception of wall thickness, all other pipe factor information was obtained from the utility for this study. Pipe material, diameter, and year of installation were stored for each pipe in a geographic information system where all pipes were georeferenced. The lining or wrapping pipe factor was embedded in the pipe material factor. For example, unlined cast iron pipe and lined cast iron pipe were treated as two distinct pipe materials. Scores for each of the factors were determined from analyzing the relationship between a given factor and 9 years of historical break data obtained from the utility. For example, the number of breaks per foot of waterline was plotted against diameter as shown in Figure 4.4. This logarithmic relationship was used to assign score values for various pipe diameters.
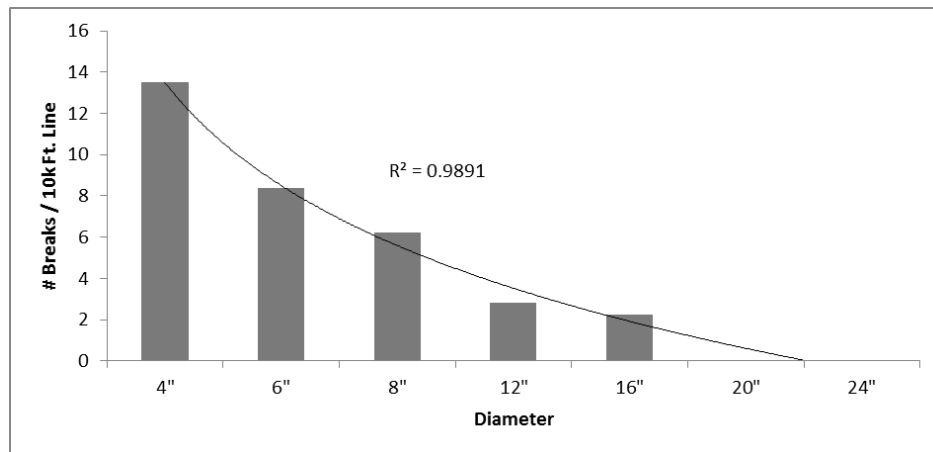
Figure 4.4: Breaks per Length vs. Diameter (2007-2015).

The same procedure was performed for each of the other pipe factors. The plots of breaks per foot of waterline vs. age and material are shown in Figure 4.5 and Figure 4.6, respectively.

74
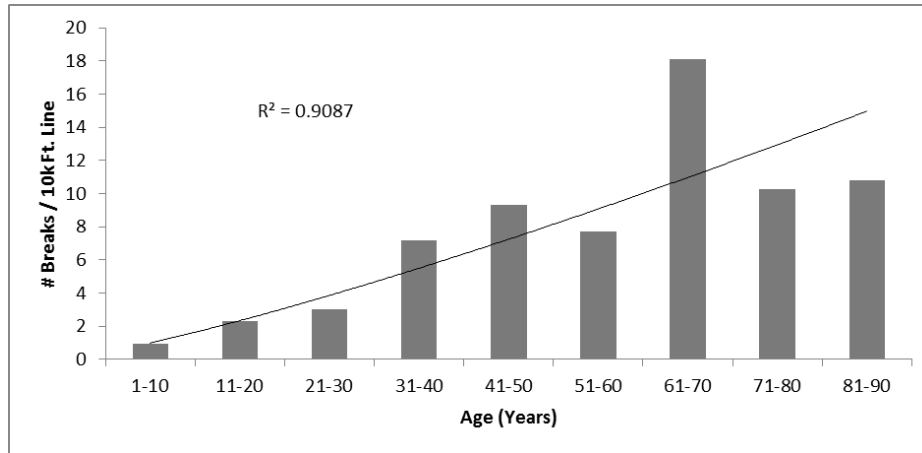
Figure 4.5: Breaks per Length vs. Age (2007-2015).
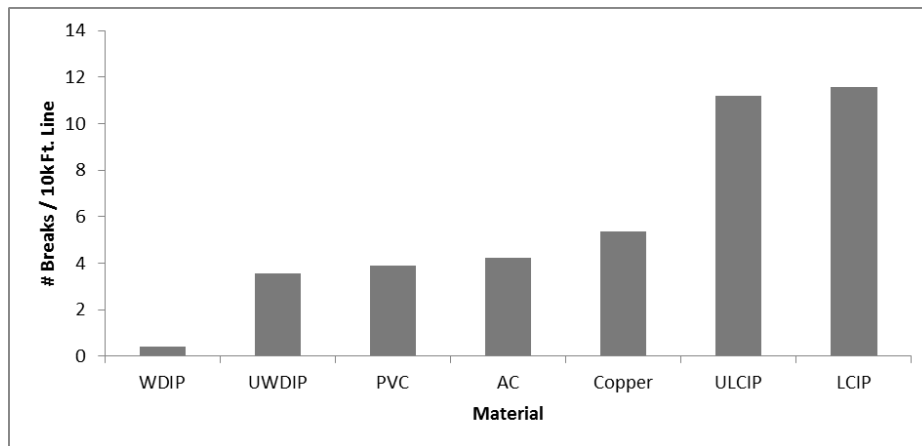
Figure 4.6: Breaks per Length vs. Material (2007-2015).

It should be noted that all relationships that were derived between pipe factors and the 9 years of break data, reasonably confirmed the relationship expectations. For example, it was expected that breaks would generally increase with age. It was also expected that the number of breaks per foot would decrease as the size (diameter) of the pipe increased. There are a couple of facts that may be deduced from Figure 4.6, the first being that adding a liner to the cast iron pipe is not a worthy economic decision for this utility. This is apparent by looking at the lack of difference in breaks between unlined cast iron pipe (ULCIP) and lined cast iron pipe (LCIP). Secondly, it appears that wrapping ductile iron

pipe is extremely effective at reducing the number of breaks for that pipe material. This is apparent by looking at the difference in the number of breaks per foot between wrapped ductile iron pipe (WDIP) and unwrapped ductile iron pipe (UWDIP). Other conclusions may be drawn from this graph such as the overall break rate between material types.

Another factor that may be included in the pipe factors is the number of previous failures experienced by a pipe. Previous pipe failures are generally used as the most helpful factor in predicting future failures (Ellison et al., 2014). The pipe break data from the utility was partitioned into two sets. The first set contained 5 years of break data from January 2007 to December 2011. The second set contained the remaining break data from January 2012 through July 2015. After partitioning the data, the two sets were used to establish a relationship between the number of previous failures and number of breaks per foot. The relationship obtained from this data is shown in Figure 4.7.
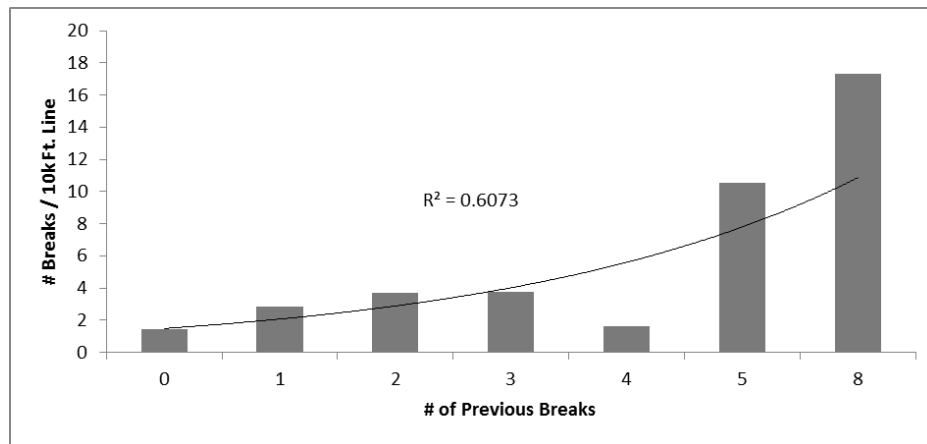
Figure 4.7: Breaks per Length (2012-2015) vs. Previous Breaks (2007-2011).

As shown in Figure 4.7, the number of breaks per foot of waterline increases exponentially with the number of previous breaks. This general direct relationship is expected and validated by many different studies as mentioned in Ellison et al. (2014).

76

However, the relationship may be stronger if a larger failure dataset was used for the analysis.

Environmental Factors:

Other factors that affect the probability of failure for an individual pipe segment are not dependent upon the pipe, but rather the pipe's environment. Thus, these factors are termed environmental factors. Ellison et al. (2014) lists the following potential environmental factors: soil corrosivity, groundwater, water aggressiveness, and stray current potential. Due to the fact that soil corrosivity is the most easily available data and has the most general agreement between these environmental factors, this was the only environmental factor included in this study.

Soil data was downloaded from the National Resources Conservation Service (NRCS) Web Soil Survey (WSS) website for the entire county. Embedded corrosion factors classify each soil type as "High" risk, "Moderate" risk, or "Low" risk of corrosion. After extracting this information to each pipe, the relationship between breaks per foot of waterline and soil corrosivity was obtained from the plot shown in Figure 4.8. As shown in the figure, the number of breaks per foot decreases linearly as the soil becomes less corrosive. This is the relationship that is generally expected.
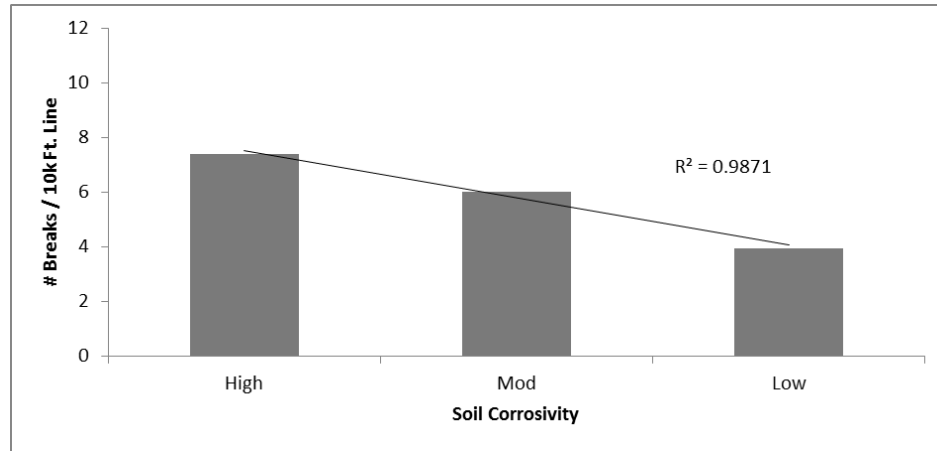
Figure 4.8: Breaks per Length vs. Soil Corrosivity (2007-2015).

Loading Factors:

The last group of probability of failure factors is the loading factors. Loading factors represent dynamic stresses that a pipe experiences over the course of its useful life. These factors consist of both internal and external loads. Potential loading factors include gradual pressure changes, transient pressures, ground or soil movement, changes in the water table, and traffic loading. The main focus of this study is transient pressures, therefore transient pressures were the only loading factors considered.

Three transient pressure factors were considered for this analysis. The first factor is the maximum transient pressure which is discussed in Section 4.2.1. The second is the minimum transient pressure which is discussed in Section 4.2.2; a cavitation index is embedded in the minimum pressure factor. The third factor is called the transient pressure range and is defined as the difference between the maximum and minimum pressure during a transient event. For example, if the maximum pressure reached 100 psi and the minimum pressure dropped to -5 psi, then the transient pressure range would be equal to 105 psi (100 psi minus -5 psi). This factor represents the combined amplitude of the positive and

negative pressure waves experienced by a waterline during a transient event. The relationship between breaks per foot of waterline and the transient pressure factors are shown in Figures 4.9 – 4.11.
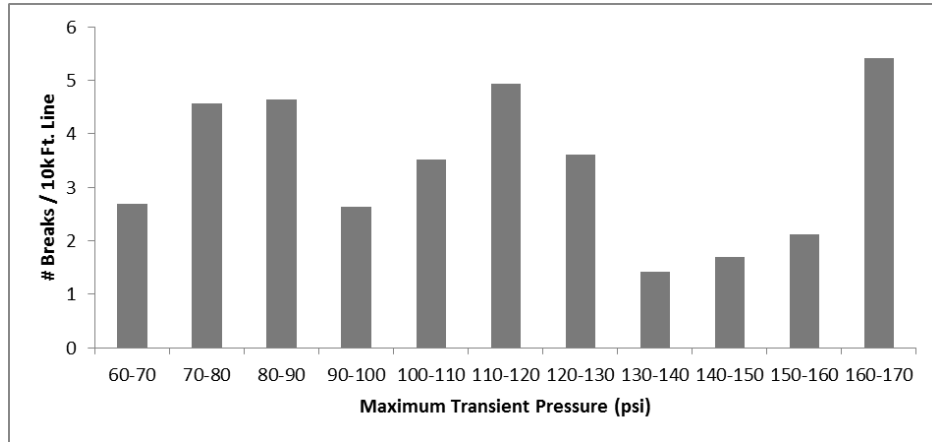
Figure 4.9: Breaks per Length vs. Maximum Transient Pressure (2007-2015).
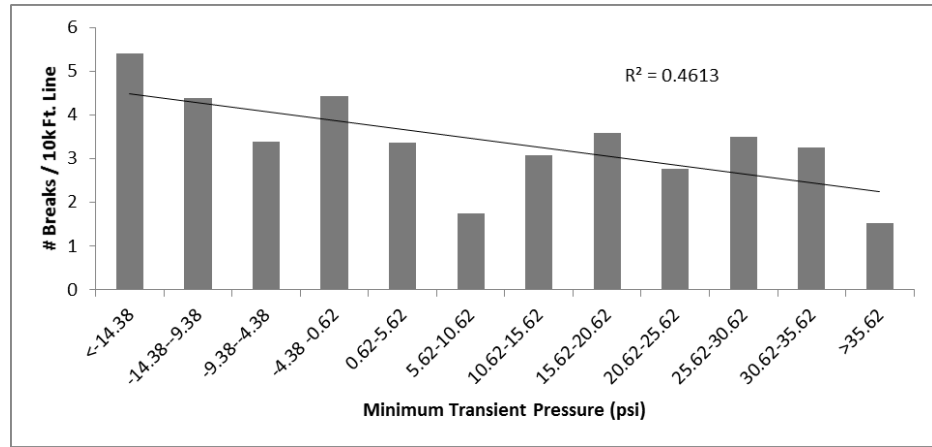
Figure 4.10: Breaks per Length vs. Minimum Transient Pressure (2007-2015).
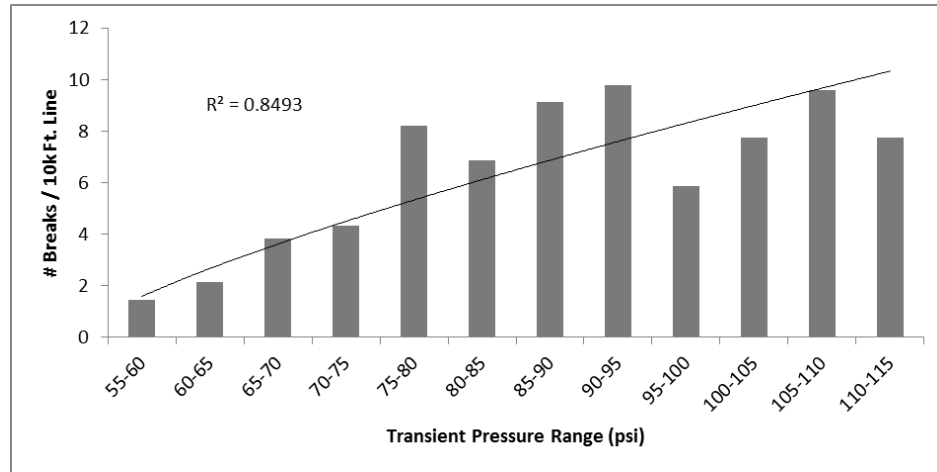
Figure 4.11: Breaks per Length vs. Transient Pressure Range (2007-2015).

As shown in Figure 4.9, the maximum transient pressure seems to have no correlation with pipe failures. The minimum transient pressure has an overall negative correlation with pipe failures as shown in Figure 4.10; however, the correlation is weak with an R^2 value of approximately 0.46. Lastly, Figure 4.11 shows the plot of breaks per foot of waterline against the transient pressure range. This plot shows a strong positive relationship between the independent and response variable. Figure 4.11 suggests that pipes which have a higher transient pressure range break more often than pipes in lower ranges.

It should be noted that the transient pressure factors were compared with the entire pipe failure dataset. Therefore, the relationship shown in Figure 4.11 would imply that there is a relationship between many of the failures from 2007 to 2015 and transient pressures resulting from a pump trip. However, according to the data from Brock (2014), there were only 6 power outages in this utility's region between 2007 and 2015 for which the failure data was obtained. Therefore, it is unreasonable to assume that many breaks were a direct result of extreme transient pressures from a power outage. Thus, the author does not wish to draw such conclusions. However, the author did hypothesize that the

transient pressure range factor can be directly related to the day to day pressure fluctuations resulting from daily pump operation transients or daily tank level fluctuations. This assumption was verified two ways.

First, a random system was drawn from the database and used to analyze a small transient event (representing daily pump operations) and a large transient event (representing the pump trip used in this study). Pressure ranges were recorded for each pipe in the system and a cumulative distribution function was created for each run. A short MATLAB code was written to compare pipe id's between cumulative distribution functions. A commented version of this code can be viewed in Appendix B. Results from comparing the cumulative distribution functions showed that 75% of all pipes in the system fell within the same quarter of the distribution for both large transient events and small transient events. When looking at the spatial distribution of the 25% of pipes which fell into different segments of the distribution function, almost all of the pipes in that 25% were concentrated in a small, isolated part of the system. After excluding that isolated part of the system, the pipe id cumulative distribution functions were very similar for the large and small transient events.

To verify the assumption a second way, maximum and minimum pressure values were recorded for each pipe in System 1 from a 24-hour extended-period simulation (EPS) in which tank levels were allowed to reach their minimum and maximum levels. The relationships between the number of breaks per foot of waterline and each of the two factors, transient pressure range and EPS pressure range, were compared and determined to be similar. The plot of breaks per foot vs. EPS pressure range is shown in Figure 4.12.
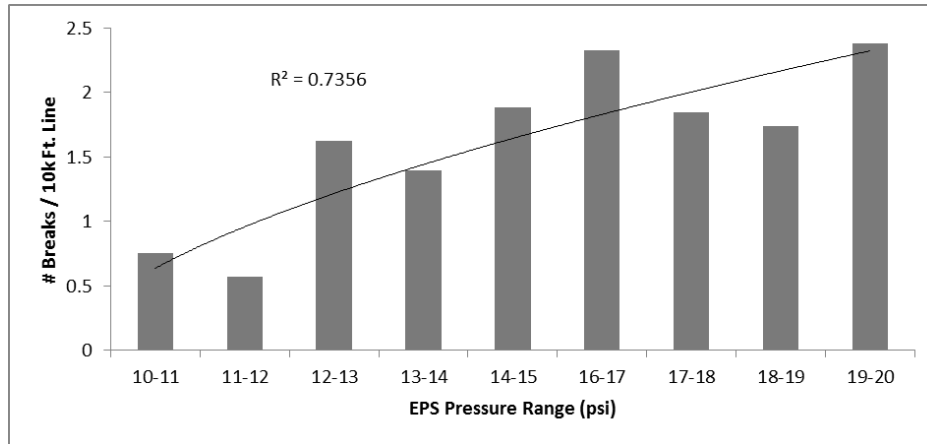
Figure 4.12: Breaks per Length vs. EPS Pressure Range (2007-2015).

As shown in Figure 4.12, there is a strong positive relationship between breaks per length of waterline and EPS pressure range. Although this relationship is not as strong as the relationship found between the transient pressure range and breaks per length, it is still shows that the magnitude of normal pressure fluctuations have an effect on pipe failures and it also validates the assumption mentioned previously.

Composite Probability of Failure Score:

In order to include each of the factors discussed in this section into a weighted-score model for probability of failure, a scoring chart needed to be derived from the relationships between "Breaks per Foot" and each of the factors. The scoring for each factor was scaled between 0 and 100 in order to simplify calculations for the composite probability of failure metric. Scores for various diameters, soil corrosion risks, number of previous breaks, and materials are shown in Table 4.1. Age and transient pressure range are not shown in Table 4.1 as pipe factors due to their large number of unique values; however, the factors are included in the scoring process.

Table 4.1: Probability of Failure Factor Scoring.

Pipe Factor	Values	Score	Pipe Factor	Values	Score
Diameter			*Material*		
	1"	100.00		ULCIP	100.00
	1.5"	87.50		LCIP	96.52
	2"	79.17		Copper	46.40
	3"	70.83		AC	36.55
	4"	56.23		PVC	33.76
	6"	34.95		UWDIP	30.90
	8"	25.85		WDIP	3.43
	10"	18.75		Polyethylene	0.00
	12"	11.75	*# Previous Breaks*		
	16"	9.34		8	100.00
	20"	0.42		7	87.50
	24"	0.42		6	75.00
	>=30"	0.00		5	62.50
Soil Corrosivity				4	50.00
	High	100.00		3	37.50
	Moderate	81.29		2	25.00
	Low	53.37		1	12.50
				0	0.00

Note that the scores in Table 4.1 are derived from the pipe break behavior of System 1 over a 9 year period from 2007 to 2015. In reality, pipe break behavior will likely vary from system to system and over time as well. Therefore, it would be ideal to use the most recent historical break data to calibrate the scoring for each factor. However, if that data is unavailable, then results of other studies from literature or results from other systems in a similar geographical region may be an appropriate alternative.

Each pipe was assigned a score for each of the six factors, four of which are shown in Table 4.1 (note that 2 of the 6 factors - i.e., age and transient pressure range, were excluded from Table 4.1 due to the large number of unique values). In order to combine these factors into a single probability of failure score, appropriate weighting values needed to be applied to each factor. These weighting values are represented by the symbol W_j, where W is the scalar weighting value for the jth factor. Weighting values must be greater

than or equal to 0 and less than or equal to 1, and all weights must sum to equal 1. The equation used to calculate the probability of failure value for each pipe is shown in Equation 44 where POF_i is probability of failure for the ith pipe, W_j is the weight of jth factor (the factors being diameter, soil corrosivity, material, # of previous breaks, age, and transient pressure range), F_j is the score for the jth factor, K is the total number of non-zero weighting values, and MAX( ) is the maximum value of all values within the parentheses.

$$POF_i = \left(\frac{\sum_{j=1}^{6}(W_j \times F_j)}{K}\right) \times \left(\frac{1}{MAX\left(\frac{\sum_{j=1}^{6}(W_j \times F_j)}{K}\right)}\right) \tag{44}$$

Using Equation 44 to calculate the relative probability of failure score for each pipe is a very simple process assuming all of the required data inputs are available. A much more complicated part of the process is calculating appropriate or even optimal weighting values for each factor. The methodology for obtaining weighting values is further discussed.

Weighting Values:

Scalar weighting values (weights) are assigned to each factor in the weighted-score method. Each weighting value must be between 0 and 1 and all of the weights must sum to equal 1. These weights represent the relative percent impact of each factor on the most recent pipe break behavior of the system. These weights are then applied to the factors in order to project which pipes are more likely to break in the near future. It should be noted that the impact of factors can and will likely vary between systems. Therefore, it is logical

84

to optimize the weighting values for each system to obtain the best possible prediction performance.

The following general procedure is used to optimize the weighting values for each factor. The pipe failure database is divided into two groups by year. For System 1, the first group contains all pipe failures from January 2007 to December 2011; this will be referred to as Dataset 1. The second group contains all pipe failures from January 2012 through June 2015; this will be referred to as Dataset 2. Note that almost all of the factors do not require this division of data since they are not necessarily time dependent; however, the number of previous failures is time dependent and therefore requires different two datasets from different time periods for calibration. All pipes are assigned scores for each factor from Table 4.1 using Dataset 1. The scores are then multiplied by weighting values which all have equal initial values of j^{-1}, where j is the number of factors. A relative probability of failure is calculated for each pipe using Equation 44. Each pipe in Dataset 2 are assigned a 1 if that pipe broke during the time period January 2012 to June 2015, or a 0 if the pipe did not break during that time period. The sum of squared errors (SSE) is then calculated for the entire pipe dataset using Equation 45 where POF_i is the calculated relative probability of failure for pipe i, CAL_i is the calibration value from Dataset 2 (either 0 or 1), and n is the total number of pipes.

$$SSE = \sum_{i=1}^{n}(POF_i - CAL_i)^2 \tag{45}$$

The SSE is then used in the objective function of a global optimization problem. The single objective of this optimization algorithm is minimizing the SSE by adjusting the weighting

values subject to the following constraints: 1) all weighting values must be non-negative and less than or equal to 1, and 2) the sum of all weighting values must equal 1.

This general procedure was performed in Microsoft Excel in order to obtain optimal weighting values for System 1's relative probability of failure model. The global optimization was performed using Excel's Solver add-in which utilizes the Generalized Reduced Gradient (GRG) algorithm to find the best possible combination of weights. Due to the complexity of the optimization problem, the solution space contains many local optima which are problematic for the GRG algorithm. Therefore, a multi-start approach is used to help find the global solution.

It should be noted that using a system's historical data should theoretically provide the best insight into the pipe break behavior of that particular system. However, this data may not always be readily available. In such instances, weighting values may be pulled from the results of other studies in literature. Systems that are geographically nearby may also be a good reference for obtaining appropriate weighting values due to similar factors that affect pipe failures such as freeze-thaw cycles, weather patterns, topography, etc.

Once optimal weights have been obtained, the resulting POF values can be checked to see how well the calibration was able to predict pipe failures. After the optimal weights are utilized, there is a resulting distribution of POF values between 0 and 1 for the entire pipe dataset. The user may then specify a threshold value between 0 and 1 for which all pipes with a greater POF value are considered as pipes which are predicted to break. Conversely, all pipes less than the threshold value are considered as pipes which are predicted not to break. This binary classification of the predicted pipes, along with the

binary calibration data of pipe failures results in a confusion matrix as shown in Figure 4.13 where there are a certain number of true positives (correct predictions of failure), false positives (incorrect predictions of failure), true negatives (correct predictions of no failure), and false negatives (incorrect predictions of no failure).

		Predicted Results	
		TRUE	FALSE
Actual Results	TRUE	*True Positive*	*False Negative*
	FALSE	*False Positive*	*True Negative*

Figure 4.13: Confusion Matrix.

There are many different metrics which can be used to evaluate the results in a confusion matrix. Sensitivity, precision, and accuracy are all different metrics that are used to describe results in a confusion matrix. For this study, the Matthew's Correlation Coefficient (MCC) as calculated by Equation 46 is used to describe the confusion matrix results where TP is the number of true positives, TN is the number of true negatives, FP is the number of false positives, and FN is the number of false negatives (Powers, 2007).

$$MCC = \frac{(TP \times TN) - (FP \times FN)}{\sqrt{(TP + FP)(TP + FN)(TN + FP)(TN + FN)}} \qquad (46)$$

The MCC is a scalar value between -1 and +1 and describes the predictive results of the confusion matrix as follows: +1 means the model has perfect predictive capabilities, 0 means the model does no better than a random prediction would do, and -1 means the model's predictive capabilities are completely opposite of reality. The GRG optimization algorithm can be used to maximize the MCC by changing the threshold variable subject to the constraint that the threshold value must be between 0 and 1.

Since no additional failure data were available for this study, the weighting values needed to be validated with values for the same factors from literature. In order to do this, the analysis was performed both with and without the transient pressure range included as a factor. Once the weighting values are compared with literature values and validated, then the transient factor is added and the results are analyzed.

4.3.2   Impact of Failure

As mentioned previously, the risk associated with pipe failure has two dimensions: the probability of failure and the impact of failure. Section 4.3.1 discussed the probability of failure metric and how the metric was calculated to be a scalar value between 0 and 1. Similarly, a scalar value will be calculated as the impact of failure for each pipe. The impact of failure score will be between 0 and 100 and will represent the impact (or cost) the utility or community will experience if a specific pipe fails. There are a number of different factors that play a role in the overall impact of a pipe failure. These factors are broken down into two general categories which are further discussed: Pipe Factors and Environmental Factors.

Pipe Factors:

Part of the impact of failure score includes factors which come directly from information about the pipe itself. These factors are called pipe factors. The diameter of the pipe is the only pipe factor included in the impact of failure metric for this study. In general, the larger the pipe, the larger impact the pipe will have upon failure. However, there has been very little research done in quantifying (i.e., costing) the effects of diameter on impact of failure. Therefore, only a general relationship may be applied. The general relationship shown in Figure 4.14 was obtained from a proactive main replacement program utilized by the same utility company which operates the System 1 pressure zone.
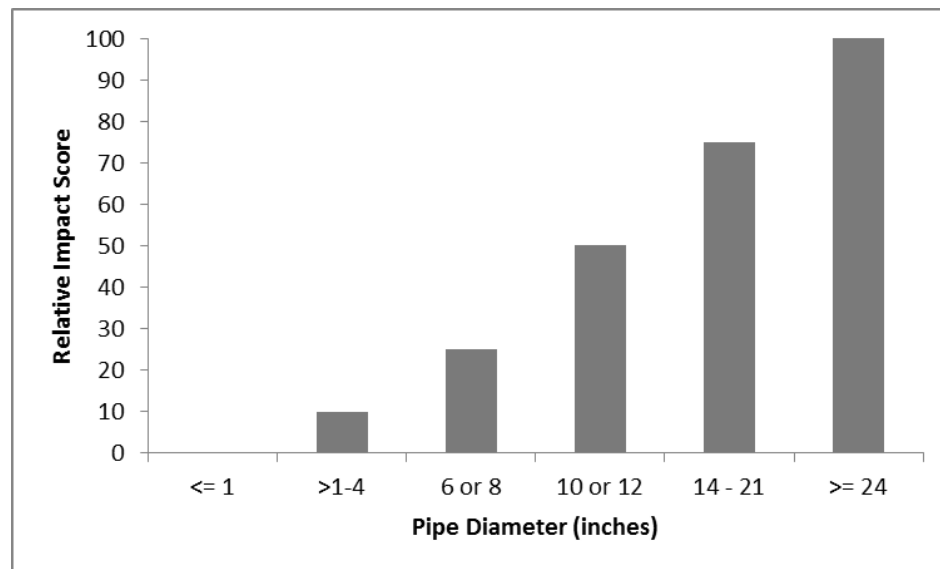
Figure 4.14: Relative Impact Score vs. Pipe Diameter.

As shown in Figure 4.14, larger pipes have a higher relative impact score as compared to smaller pipes. Pipes that are greater than or equal to 24 inches are assigned a score of 100 for this factor. Oppositely, pipes that are less than or equal to 1 inch are assigned a score of 0. Note that this relationship is opposite of the probability of failure vs.

diameter relationship shown in Figure 4.4. In this regard, small diameter pipes will have a larger probability of failure score relative to larger pipes; however, their relative impact of failure score will be low. Note that this relationship is not backed up by published literature since there has not been a comprehensive study performed on this topic to date. However, the same methodology that a real utility uses was deemed suitable for this study.

Environmental Factors:

Other factors that affect the impact of failure for an individual pipe segment are not dependent upon the pipe, but rather the pipe's environment and location. Thus, these factors are termed environmental factors. Ellison et al. (2014) lists potential environmental factors which affect the impact of failure for a given pipe: potential for property damage, repair difficulty (i.e., access depth, groundwater, etc.), traffic conditions, business and other community impacts, loss of service, and loss of critical customer service (e.g., hospitals, nursing homes, etc.).

Each of these factors has the potential for significant direct and societal costs. However, these costs are very difficult to quantify as they will likely be different for every pipe in the system. Little research has been performed to quantify these impacts. Therefore, relationships used by the utility from System 1 are also used for this study. Two factors are used in this study which can arguably incorporate many of the factors listed by Ellison et al. (2014). These factors are road class and customer criticality. Figure 4.15 shows the relative impact scores for different road classes.
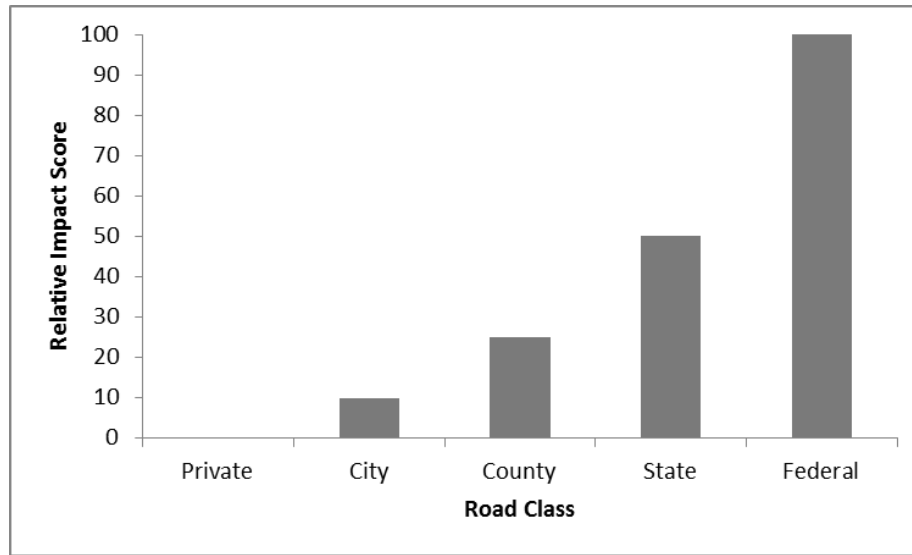
Figure 4.15: Relative Impact Score vs. Road Class.

As shown in Figure 4.15, the relative impact score increases as the roads get larger, with interstates and highways dominating the scoring chart at a score of 100. It can be argued that road class incorporates certain factors listed by Ellison et al. (2014) such as business and community impacts and traffic conditions. Businesses are more often located in downtown or commercial districts and less often located on unpaved roads. Likewise, there is much more traffic on larger roads than on smaller ones. However, there will likely be anomalies to those general rules in each city. The nearest road class was extracted to each pipe in the system using the ArcGIS built-in tool "Near". This road class file was taken from the Kentucky Transportation Cabinet and last updated in 2014.

Customer criticality was incorporated for this study by assigning a score of relative importance for varying customers. Hospitals were assigned a score of 100 and nursing homes were assigned a score of 75 which suggests that service to the hospital is more critical than service to the nursing home. Pipes were assigned an impact score manually based on their importance in delivering water to the various customers shown in Figure

4.16. A relative impact of failure score for each factor was assigned to every pipe from Table 4.2. Note that relative impact scores may be adjusted by the user to account for their opinion as to which factors are most important.
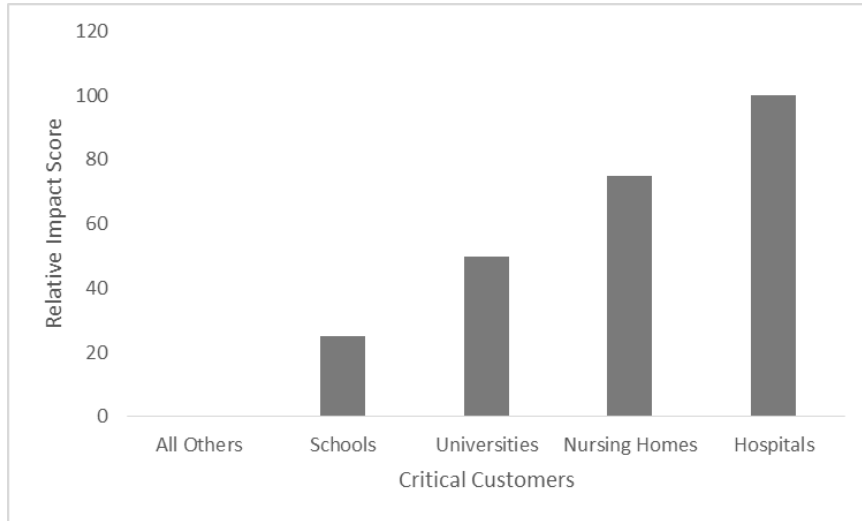
Figure 4.16: Relative Impact Score vs. Customer Criticality.

Table 4.2: Impact of Failure Factor Scoring.

Impact Factor	Values	Score
Diameter		
	<= 1"	0.00
	>1" to 4"	10.00
	6" or 8"	25.00
	10" or 12"	50.00
	14" to 21"	75.00
	>= 24"	100.00
Road Class		
	Private	0.00
	City St.	10.00
	County Rd.	25.00
	State Rd.	50.00
	Federal Hwy.	100.00
Customer Criticality		
	All Others	0.00
	Schools	25.00
	Universities	50.00
	Nursing Homes	75.00
	Hospitals	100.00

92

Composite Impact of Failure Score:

Now that each of the pipes in the system has been assigned a relative impact score for each factor, a composite impact of failure score may now be calculated. Similar to the composite probability of failure score, the composite impact of failure score has weights which are multiplicatively assigned to each factor. All of the weights must be between 0 and 1 and must sum to equal 1. However, these weighting values may not be optimized since there is no real data to calibrate the model. Therefore, the user must use engineering judgement in assigning weights. For this study, all weights were assumed equal (which is also what the utility uses for their pipe replacement program). Each weight is equal to j^{-1}, where j is the number of impact of failure factors. The composite impact of failure score for each pipe may be calculated using Equation 47 where IOF_i is impact of failure score for the ith pipe, W_j is the weight of jth factor, F_j is the score for the jth factor, K is the total number of non-zero weighting values, and MAX( ) is the maximum value of all values within the parentheses. Note that all composite impact of failure scores are values between 0 and 100.

$$IOF_i = \left(\frac{\sum_{j=1}^3 (W_j \times F_j)}{K} \right) \times \left(\frac{100}{MAX\left(\frac{\sum_{j=1}^3 (W_j \times F_j)}{K} \right)} \right) \qquad (47)$$

4.3.3   Composite Risk Score

As defined in Section 2.1.4, risk is a term used to describe the influence of the following two dimensions on any given event: 1) the probability that the event will take place, and 2) the impact of the event once it has taken place. In this study, the aforementioned event is a pipe failure. This section will discuss the combination of the two

dimensions into a composite risk metric which can be used to analyze a system and subsequently make informed decisions.

Section 4.3.1 discussed the probability dimension of risk. This dimension represents the likelihood that a given pipe will fail, relative to all of the other pipes in the system; therefore, this is a relative probability of failure. Various factors were combined to arrive at a composite probability of failure score for each pipe. All probability of failure scores were scaled between 0 and 1 to make composite risk calculations simpler.

Section 4.3.2 discussed the impact dimension of risk. This dimension represents the impact (or cost) the utility or community will experience if a specific pipe fails. These costs can be both direct costs (e.g., system damage, property damage, etc.) and societal costs (e.g., loss of work productivity, loss of life, etc.). Each composite impact of failure score was scaled between 0 and 100 for the simplicity of composite risk calculations.

Once both dimensions of risk had been covered for every pipe in the database, it was time to combine those dimensions to produce a composite risk score. Equation 48 was used to calculate a composite risk score for each pipe where ROF_i is the risk of failure for the ith pipe, POF_i is the relative probability of failure for the ith pipe, and IOF_i is the relative impact of failure for the ith pipe.

$$ROF_i = POF_i \times IOF_i \tag{48}$$

This resulted in a risk of failure score between 0 and 100 for each pipe in the system. Pipes with lower scores had a lower risk of failure and pipes with higher scores had a higher risk of failure.

CHAPTER 5 RESULTS

5.1   Database Risk Analysis

The results of the risk analysis performed for each system in the database are presented in this section. As mentioned previously, the database consists of 15 water distribution system models which represent actual systems in the state of Kentucky. Each of these models was generated for research application using the methodology presented in Chapter 3; hence, pipe failure data was not available for systems in the database. Due to this lack of data, and the fact that the systems are not calibrated, a complete risk analysis was not performed for the database systems. Rather, the effects (i.e., pressures) of the initiated transient events were analyzed for general patterns and differences between system configurations.

5.1.1   Transient Analysis Results

The results of the transient analysis for each system may be summarized by the following metrics: 1) Average Steady-State Pressure (the static pressure before the transient event was imitated), 2) Maximum Pressure (the highest pressure reached during the transient event), 3) Minimum Pressure (the lowest pressure reached during the transient event, 4) Transient Pressure Range (the difference between highest pressure reached and lowest pressure reached during the transient event), 5) Positive Pressure Deviation (the difference between the highest pressure reached during the transient event and the static pressure prior to the transient event), and 6) Negative Pressure Deviation (the difference between the static pressure prior to the transient event and the lowest pressure reached during the transient event). Each of these metrics was calculated for the 15 systems. The

scores of the metrics were then color coded onto schematics of the systems so that the results could be analyzed graphically. Figures 5.1 – 5.6 show examples of the results of each of these metrics for system KY2.
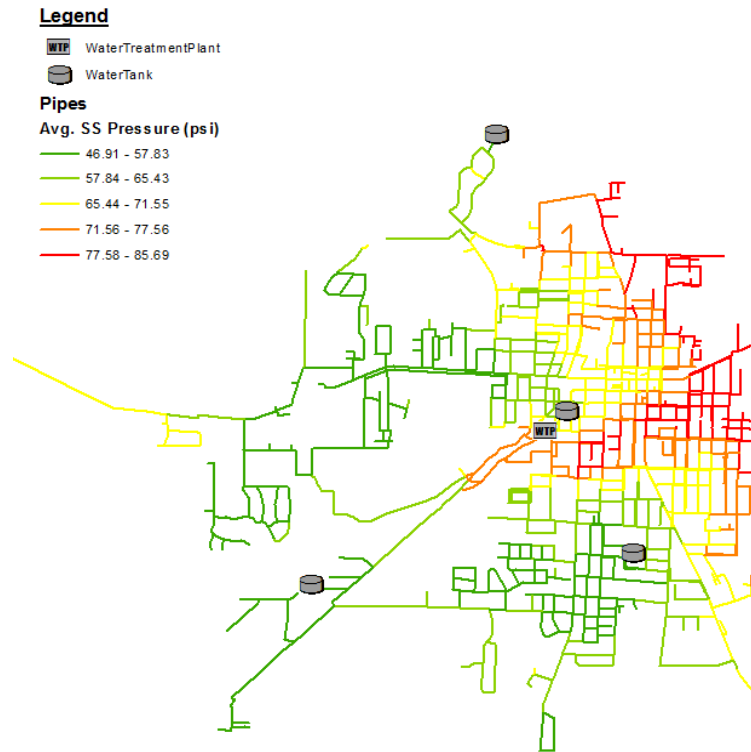
Figure 5.1: Average Steady-State Pressure for KY2.
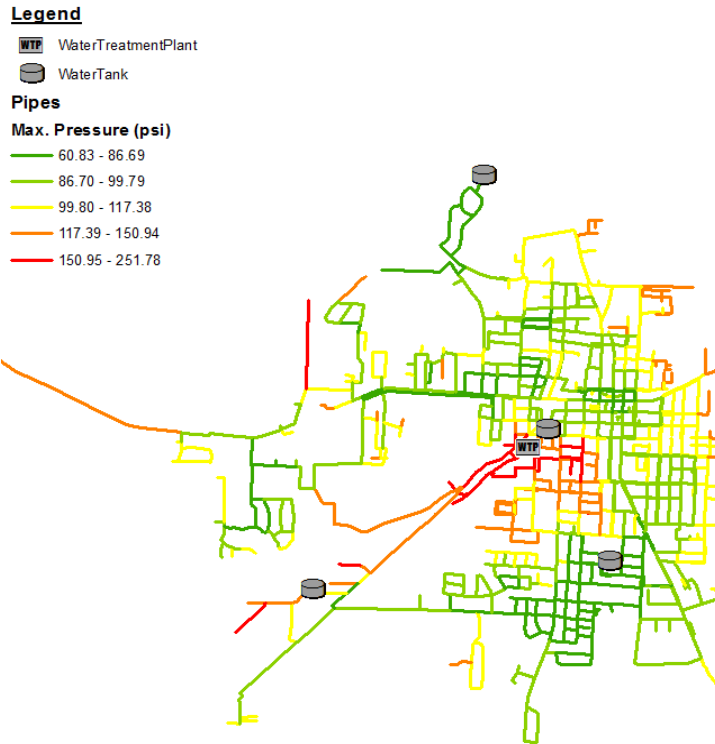
Figure 5.2: Maximum Pressure for KY2.
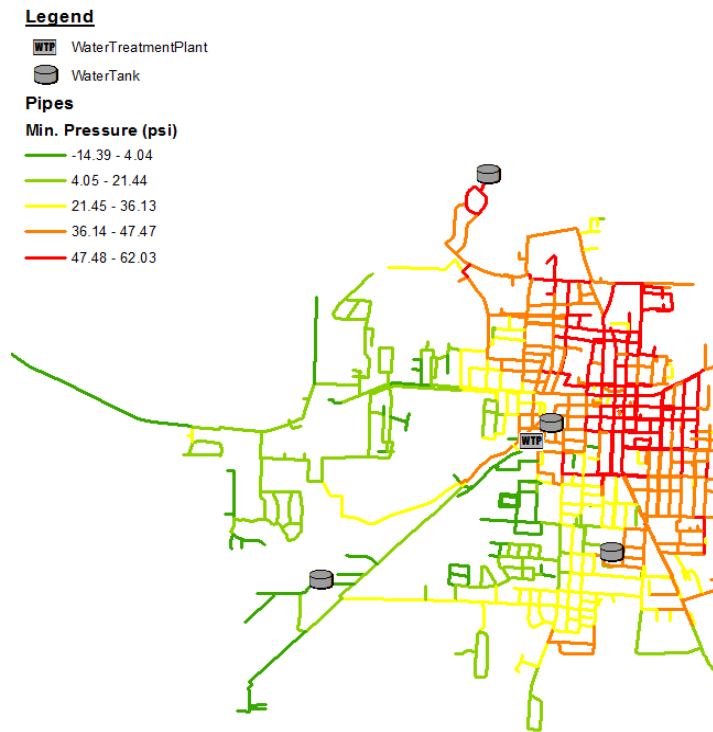
Figure 5.3: Minimum Pressure for KY2.
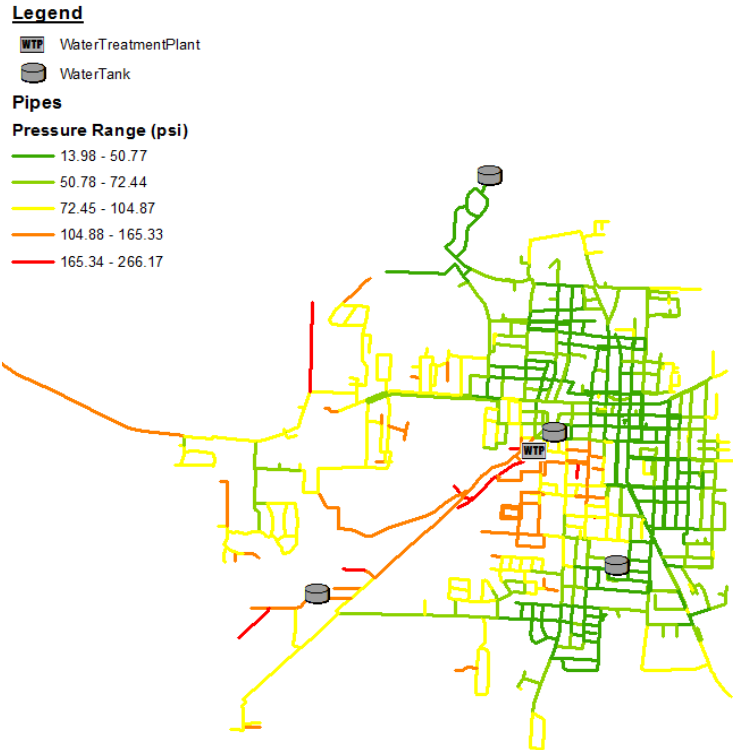
Figure 5.4: Transient Pressure Range for KY2.
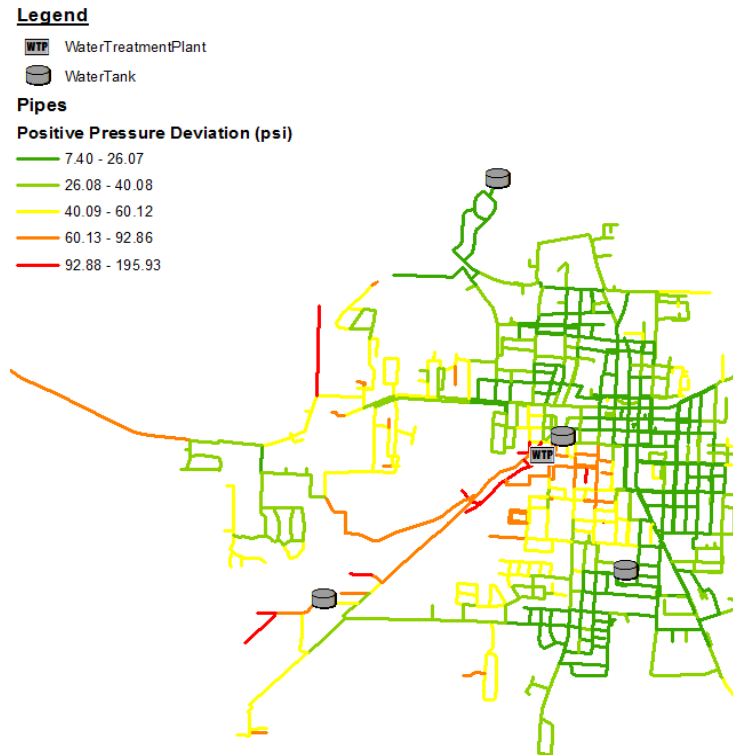
Figure 5.5: Positive Pressure Deviation for KY2.
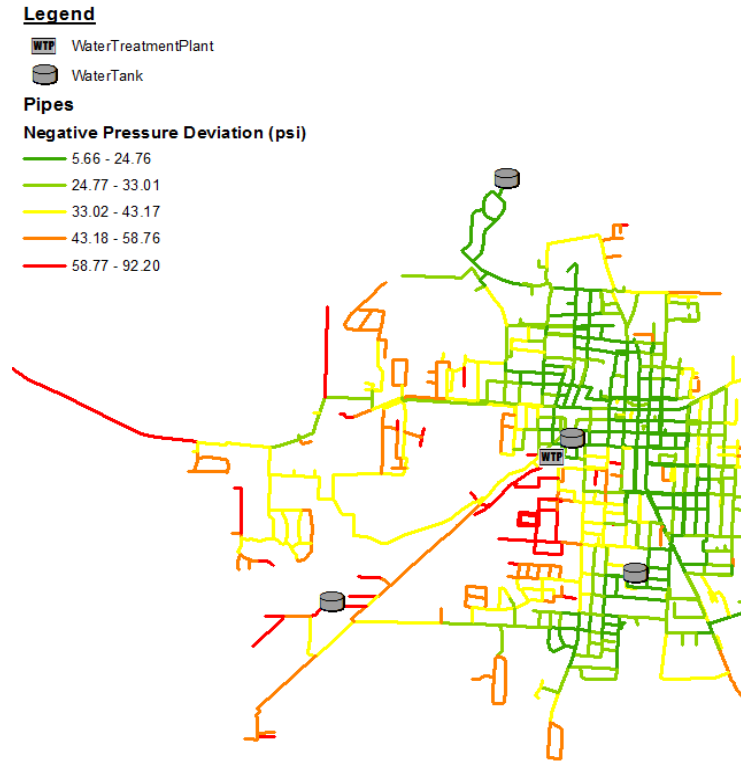
Figure 5.6: Negative Pressure Deviation for KY2.

The presentation of results as shown in Figures 5.1 – 5.6 for KY2 was kept consistent for the other 14 systems in the database. The complete set of system results for the transient analysis metrics is presented in Appendix C. The significance of the results that were presented in this section and Appendix C are discussed in Section 6.1.3.

5.2.2   Elevation Results

In addition to the results of the transient analysis, other system-specific factors such as elevation may be able to provide insight into the transient effects. Therefore, the average pipe elevation was calculated for each pipe. The elevations were then used to color code the schematic of the system in order to view the results graphically. An example of the results for an average pipe elevation schematic of system KY2 is shown in Figure 5.7.

99
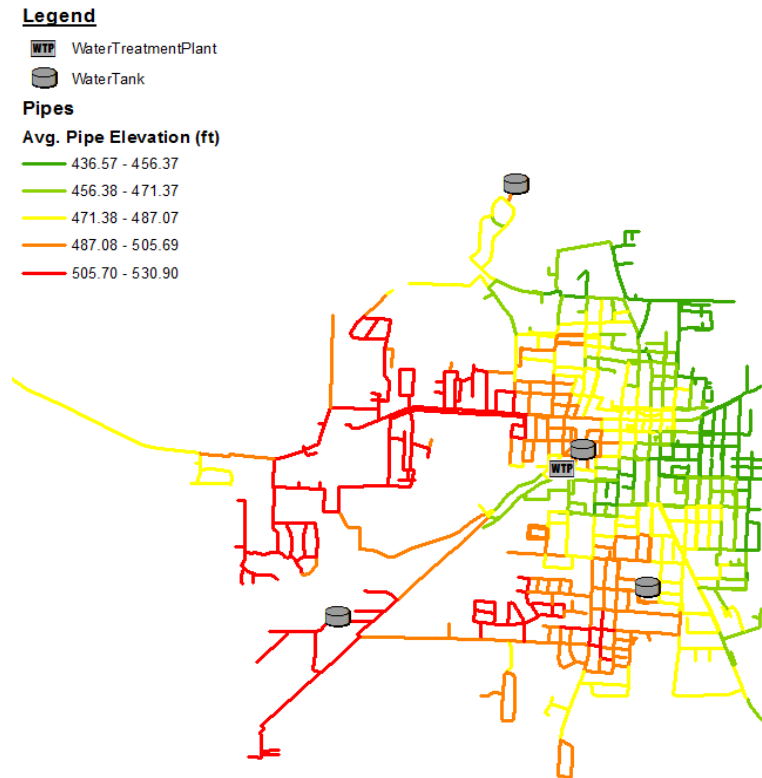
Figure 5.7: Average Pipe Elevation for KY2.

The presentation of results as shown in Figure 5.7 for KY2 was kept consistent for the other

14 systems in the database. The complete set of system results for average pipe elevation

is presented in Appendix C. The significance of the results that were presented in this

section and Appendix C are discussed in Section 6.1.3.

5.2   System 1 Risk Analysis

The results of the various aspects of the risk analysis for System 1 are presented in

this section. As mentioned previously, System 1 is a calibrated model provided by a utility

in Kentucky. Along with the model, the utility also provided 8.5 years of pipe failure data

which was used to calibrate the model for System 1. As this was the only system for which

historical failure data was available, the validity of the methodology presented in Chapter

4 is entirely dependent on the results of the model for System 1. The probability of failure

(POF), impact of failure (IOF), and overall risk of failure (ROF) results are presented in the following subsections.

5.2.1 POF Results

The relative probability of failure (POF) score was calculated for each pipe based on the methodology presented in Section 4.3.1 by using derived relationships to determine pipe scoring and a global optimization algorithm to optimize the weighting values. The relationships derived between breaks per length of water main and various prediction parameters (i.e., diameter, material, age, soil corrosivity, # of previous breaks) all agreed with relationships obtained from other studies in literature. These relationships are not technically results of the risk analysis and therefore are not listed in this section; they are shown in Section 4.3.1.

As mentioned, the weights first needed to be validated using accepted literature values. This meant initially excluding the transient pressure range as a factor since no previous studies have included it as a factor. With pressure range excluded, the optimal weights are shown in Table 5.1. Note that multiple runs of the same optimization may result in different solutions due to the randomness of the starting points from Multistart and the many local optima in the solution space. Therefore, multiple trial runs were performed for each optimization to account for the random selection of starting points in the Multistart algorithm.

Table 5.1: Optimal Weighting Values (Excluding Transients)

Factor	Weighting Value
Age	0.0012
Soil Corrosiv.	0.0134
Diameter	0.0205
Material	0.0609
# Prev. Breaks	0.9040

Results of the optimization showed that the number of previous breaks was the most important factor used to predict breaks with a weighting value of 0.9040. All other factors had minor effects on the prediction capabilities of the model: material with a weight of 0.0609, diameter at 0.0205, corrosivity of the soil at 0.0134, and age with a weight of 0.0012. These weighting factors produced true positives (TP), true negatives (TN), false positives (FP), and false negatives (FN) as shown in Confusion Matrix 1 in Table 5.2. The Matthews Correlation Coefficient (MCC), which is used to summarize the predictive capabilities of the confusion matrix in a single number, was calculated to be 0.2412.

Table 5.2: Confusion Matrix 1.

Class	# in Class
True Positive	42
False Positive	94
True Negative	1526
False Negative	101

Next, these weighting values needed to be compared to accepted values in literature. Vanrenterghem-Raven (2007) studied the effects of similar factors on the structural degradation of New York City's water distribution system using 20 years of historical break data. The relative effects of all factors were analyzed using a Cox Proportional Hazards Model (CPHM) since no baseline function was required for the analysis (Vanrenterghem-Raven, 2007).

Results from the CPHM applied to the New York City dataset showed that the factors diameter, material, and number of previous breaks obtained the highest impact scores (Hazard Ratios) on average. The material "Steel" ended up skewing the results to heavily favor the impact of material. After removing steel as a factor (there is no steel pipes in System 1), averaging the Hazard Ratios, and scaling the ratios to values between 0 and 1, the relative impacts are shown in Table 5.3.

Table 5.3: Relative Impact of Factors from Literature

Factor	Weighting Value
Age	0.0000
Diameter	0.1720
Material	0.3430
# Prev. Breaks	0.4850

The CPHM results of the New York City dataset showed that the number of previous breaks had the highest impact on pipe failures, with a relative weighting value of 0.4850. The material factor scored the second highest impact at 0.3430, followed by diameter at 0.1720 and age at 0.0000. A discussion of the comparison between the experimental results (i.e., Table 5.1) and results from literature (i.e., Table 5.3) is presented in Chapter 6.

Next, the optimization procedure was used to derive the weighting values, this time including transient pressure range as a factor. Results of the optimization are shown in Table 5.4.

Table 5.4: Optimal Weighting Values (Including Transients)

Factor	Weighting Value
Age	0.0000
Diameter	0.0000
Soil Corrosiv.	0.0056
Transient Range	0.0437
Material	0.0593
# Prev. Breaks	0.8914

As shown in Table 5.4, the number of previous breaks received the highest weighting value of 0.8914. The transient pressure range factor and material factor received weighting values of 0.0437 and 0.0593, respectively. Soil corrosivity received a weight of 0.0056 while diameter and age received weighting values of 0.0000. These weights produced the confusion matrix shown in Table 5.5 and resulted in a MCC of 0.2613. The number of true positives actually decreased from 42 to 41 between the first and second run (i.e., Table 5.2 and 5.5), and the number of false positives increased from 94 to 95. However, the number of false negatives decreased from 101 to 83, which is the most significant difference between the two runs. This improvement is reflected in the increased MCC, from 0.24 to 0.26. The significance of these results is further discussed in Section 6.1.1.

Table 5.5: Confusion Matrix 2.

Class	# in Class
True Positive	41
False Positive	95
True Negative	1544
False Negative	83

The weights presented in Table 5.4 were the final weighting values used to calculate the POF score for each pipe. All POF scores were between values of 0 and 1 as calculated by Equation 44. These scores were then used to color code the system schematic so that the results could be analyzed graphically. This method allows the user to identify patterns in the system which may previously have gone unrecognized. The POF results for System 1 are presented in Figure 5.8. In this figure, the highest POF pipes are shown in red while the lowest POF pipes are shown in green.
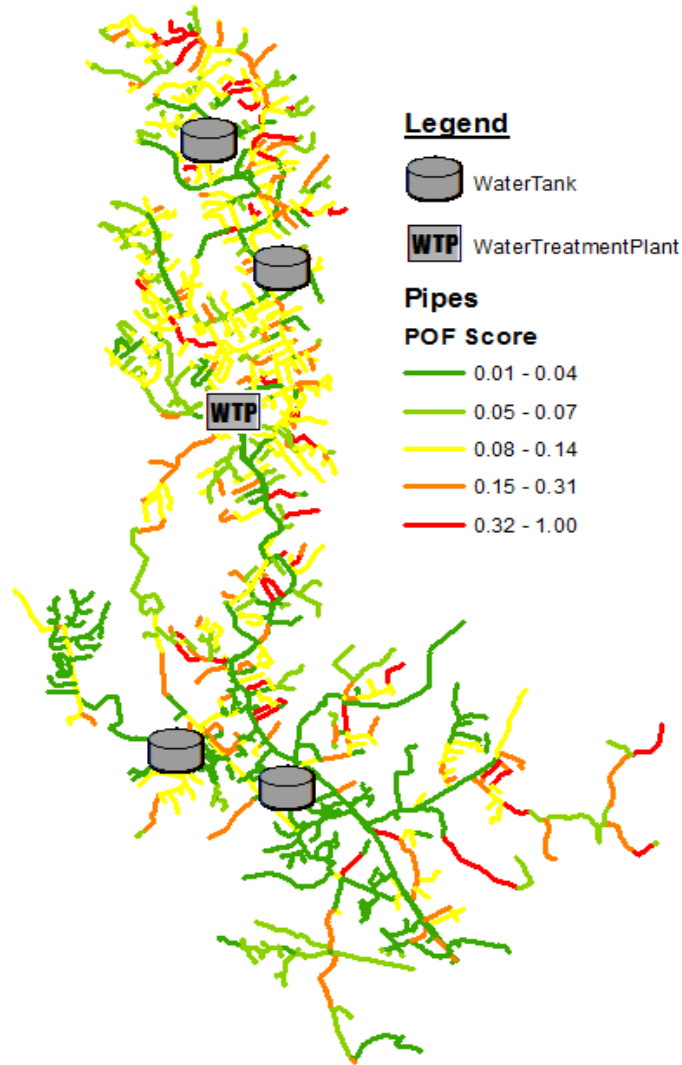
Figure 5.8: POF Results for System 1.

In addition to the POF results shown in Figure 5.8, the results of the confusion matrix shown in Table 5.5 were plotted on the system schematic. Figure 5.9 shows the true and false positives in green and red, respectively, and Figure 5.10 shows the true and false negatives shown in green and red, respectively. The significance of these results are discussed in Section 6.1.2.
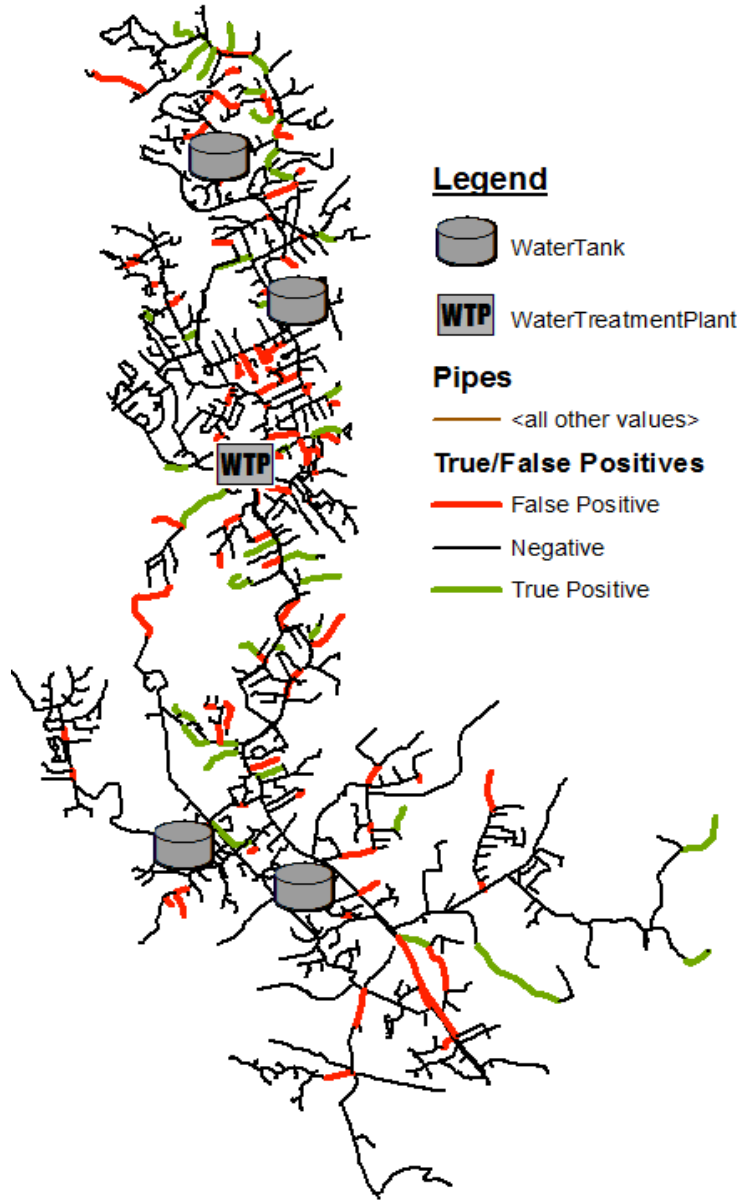
Figure 5.9: True and False Positives for System 1.
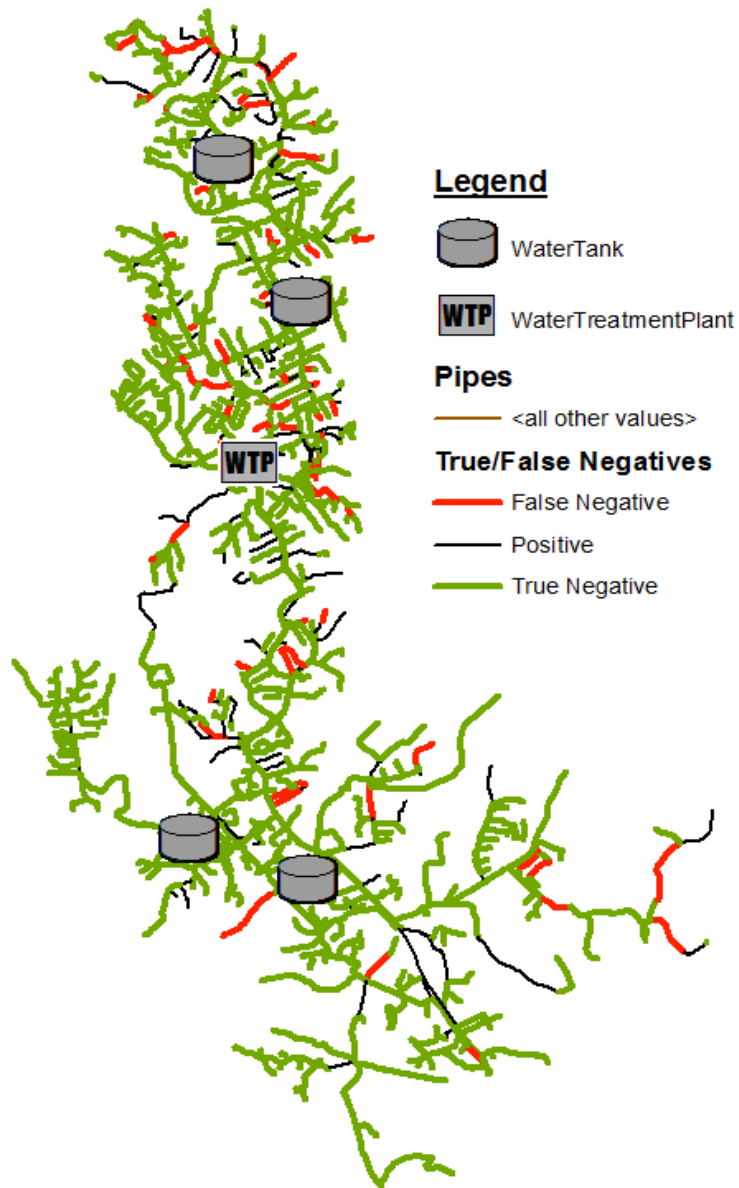
Figure 5.10: True and False Negatives for System 1.

5.2.2 IOF Results

The relative impact of failure (IOF) score was calculated for each pipe in System 1 based on the methodology presented in Section 4.3.2 by using relationships between various factors and their estimated impacts to score the pipes. The relationships between the factors and their impacts were obtained from a utility company in the state of Kentucky

which are used in the utility's proactive main replacement and monitoring program. These relationships are not technically results of the risk analysis and therefore are not listed in this section; they are shown in Section 4.3.2.

Before assigning IOF scores to each pipe, weighting values were required to be specified for each factor. Since there was no impact data available to calibrate the model, the weighting values could not be optimized. Therefore, the same weighting values which were used by the utility company were applied to the IOF model for this study. This resulted in equal weights being applied to each of the 3 factors. Using the methodology from Section 4.3.2 and the specified weights, an IOF score was assigned to each pipe. The IOF scores were then used to color code the system schematic so that the results could be analyzed graphically. The IOF results for System 1 are presented in Figure 5.11 and the significance of those results are discussed in Section 6.1.2.
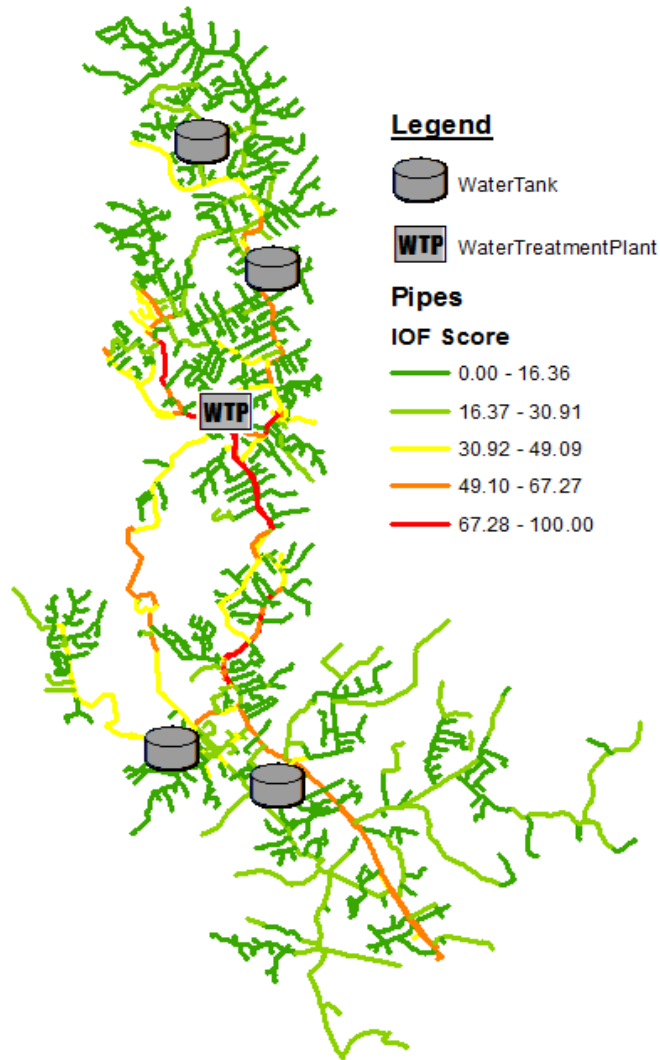
Figure 5.11: IOF Results for System 1.

5.2.3 System 1 Risk of Failure

Once POF and IOF scores have been calculated for each pipe, the total risk of failure (ROF) score for each pipe may be calculated using the methodology presented in Section 4.3.3 which involves multiplicatively combining the POF and IOF scores to produce a composite score between 0 and 100. The composite ROF scores were then used to color code the schematic for System 1 in order to display the results graphically. The

ROF results for System 1 are presented in Figure 5.12 and the significance of the results are discussed in Section 6.1.2.
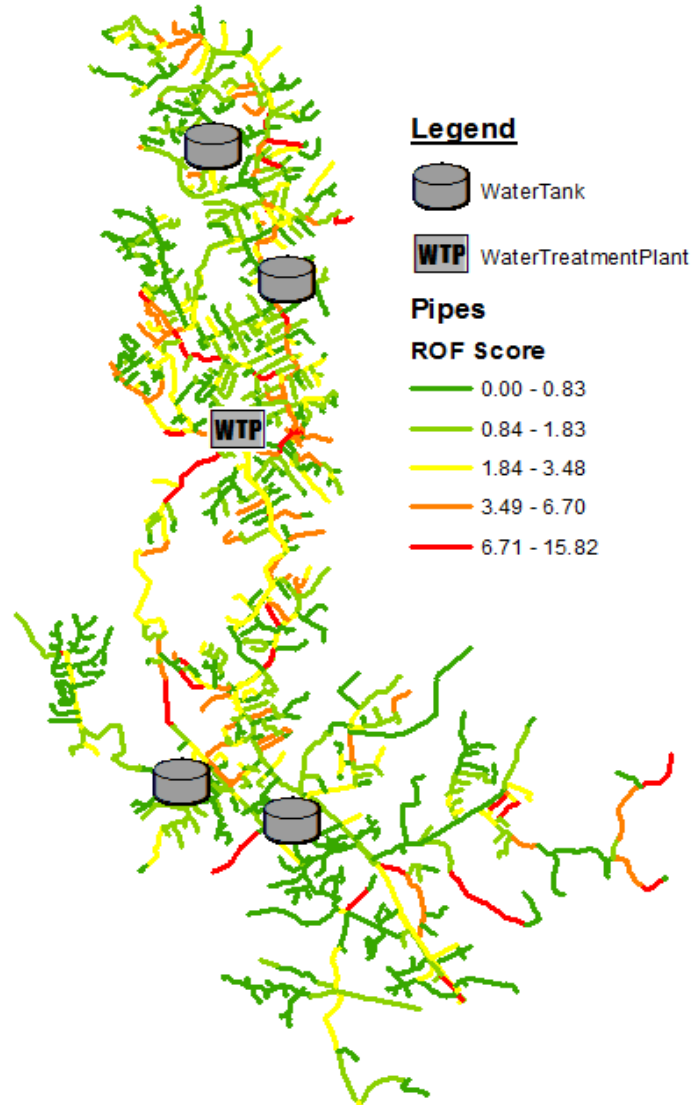
Figure 5.12: ROF Results for System 1.

CHAPTER 6 DISCUSSION

This chapter provides a discussion of the results of this study which were presented in Chapter 5. These results include the weighting results for the probability of failure (POF) model, the POF results, the impact of failure (IOF) results, and the total risk of failure (ROF) results for System 1. This chapter also includes the results of the transient analysis which was performed for each system in the database. Any trends or patterns that emerged in the results are also discussed.

6.1   Database Analysis Discussion

Results of the database analysis, which are presented in Appendix C, consisted of the maximum transient pressure, minimum transient pressure, transient pressure range, positive pressure deviation (from steady-state), and negative pressure deviation. Average steady-state pressures and average pipe elevations were also included in the results to compare to the transient pressures. All results were displayed graphically on a schematic of the distribution network, which included the location of WTPs and storage tanks, and were color coded for easy visual inspection. These results are further discussed for each pressure factor.

The spatial distribution of average pipe elevation was fairly consistent for all systems. Pipes in close proximity to tanks generally had higher elevations than pipes which were further away from tanks. This made intuitive sense due to the fact that most storage tanks are placed in areas of high elevation within the system. By comparing the average steady-state pressure results with the schematic of average pipe elevation, it can be observed that pipe elevation has a significant impact on the standard operating pressure.

However, this is not the only factor which has an impact. Other competing factors include the proximity to storage tanks and proximity to pumping stations.

The results of the maximum and minimum transient pressure factors were also fairly consistent for each system. The maximum transient pressures were found in areas of close proximity to the WTP (i.e., area where the transient event was initiated), in areas of low elevation, and in areas of high standard operating pressure. Minimum transient pressures were also found in areas of close proximity to the WTP, as well as areas of high elevation, and areas of low standard operating pressure. In both the maximum pressure and minimum pressure factors, the standard operating pressure had significant influence in the results. Analyzing the positive pressure deviation and negative pressure deviation eliminates the influence of standard operating pressure by looking more at the relative amplitude of the pressure wave. Therefore, when analyzing the schematics in grid and loop systems, where the transient pressure wave has a more significant effect on pipes furthest from the WTP, there is not much difference between the maximum pressure and the positive pressure deviation results. However, in branch systems, the pressure wave does not have a significant effect on the pipes furthest from the WTP. This means that the positive pressure deviation would be limited to areas of close proximity to the WTP while the maximum pressure results would vary across the map.

The last factor which will be discussed is the transient pressure range factor. This factor is critically important since a relationship was found between the transient pressure range and the number of pipe breaks. In essence, this factor takes into account both the positive deviation and the negative deviation from steady-state pressure. High transient pressure ranges were found in areas of close proximity to the WTP as well as areas where

112

cavitation occurred. Lower transient pressure ranges were found further away from the WTP and around tanks, which are not often mutually exclusive.

In general, proximity to the WTP was found to be the factor which accounted for the largest difference in transient pressure range between system configurations. In grid and loop systems, the proximity to the WTP was not often a significant factor. However, in branch systems, the proximity to the WTP had a significant impact on the results. Pipes in close proximity to the WTP had a much higher pressure range than pipes which were spatially further away. This makes intuitive sense due to the large spatial footprint of branch systems. Another general trend which was found across all system configurations is more extreme pressure conditions in branching pipes. This trend was observed in a visual assessment of the schematics presented in Appendix C.

6.2   Weighting Values Discussion

The probability of failure (POF) model assigns a relative POF score to each pipe which separates the pipes that are more likely to fail in the near future from those that are less likely to fail. Part of creating a good POF model is understanding which factors play an important role in pipe failures, as well as understanding the relationships between those factors and pipe failures. There are many relationships that were derived between various factors and pipe failures for System 1. These factors include diameter, age, material, number of previous breaks, and soil corrosivity, for which the relationships are shown in Figures 4.3 – 4.7. In addition to these relationships, a number of transient-related factors were investigated and their relationships to pipe failures are shown in Figures 4.8 – 4.11. These relationships are further discussed.

Figure 4.8 shows the relationship between pipe breaks per length of waterline and the maximum transient pressure experienced in a given pipe. From a first glance, there is no relationship between these two factors. However, if the standard operating pressure range (60-120 psi) is eliminated, the exponential relationship shown in Figure 6.1 is derived between pipe breaks and high transient pressures (130-170 psi). This relationship is much stronger and should be verified by other studies.

The chart shows a bar graph titled with y-axis "# Breaks / 10k Ft. Line" ranging from 0 to 6, and x-axis "Maximum Transient Pressure (psi)" with categories 130-140, 140-150, 150-160, 160-170. The trend line equation is $y = 0.7921e^{0.4245x}$ with $R^2 = 0.8444$.
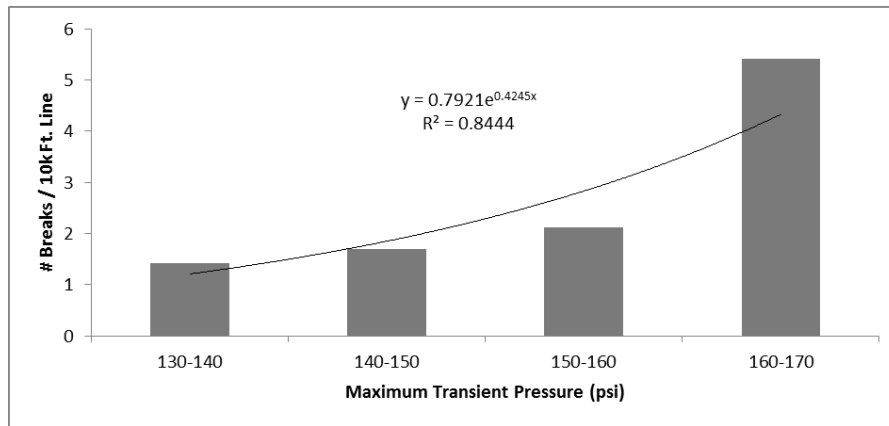
Figure 6.1: Breaks per Length vs. High Transient Pressures.

Figure 4.9 shows the relationship between pipe breaks per length of waterline and the minimum transient pressure experienced in a given pipe. This figures reveals a weak negative relationship. However, this negative trend was expected (i.e., pipes which are closer to cavitation pressure are more likely to break than pipes with higher normal pressures), and therefore this result must be noted.

Figure 4.10 is the most significant relationship between pipe failures and a transient-related factor. This figure shows the relationship between breaks per length of waterline and the transient pressure range (i.e., the combined amplitude of the positive and negative transient pressure waves). Figure 4.10 suggests that pipes with a higher combined

amplitude of pressure waves will break more often than pipes with a lower combined amplitude. However, in Section 4.3.1 the author hypothesized that the breaks in the system were due to sustained pressure fluctuations over time as opposed to acute transient events. Therefore, the author compared the pipe failures with pressure fluctuations from an extended-period simulation (EPS) which is representative of standard pressure fluctuations from daily system operations. This relationship was shown in Figure 4.11, which was remarkably consistent with Figure 4.10. The author believes the relationship between pressure fluctuations and pipe failures to be a significant finding of this study.

Once the relationships were established between pipe failures and the various factors, these relationships needed to be included in the POF model. The difference in relative importance of each factor is represented by the weighting values; higher weighting values meant a factor was more important while lower values meant a factor was less important. In this study, the author used 3.5 years of pipe failure data to derive the weights which minimized the error between the predicted pipe failures and the actual pipe failures. The results of the weighting values between the different optimization trials are presented in a composite table in Table 6.1.

Table 6.1: Composite Table of Weighting Value Results.

From Table 5.1		From Table 5.3		From Table 5.4	
Factor	Weighting Value	Factor	Weighting Value	Factor	Weighting Value
Age	0.0012	Age	0.0000	Diameter	0.0000
Soil Corrosiv.	0.0134	Diameter	0.1720	Age	0.0000
Diameter	0.0205	Material	0.3430	Soil Corrosiv.	0.0056
Material	0.0609	# Prev. Breaks	0.4850	Transient Range	0.0437
# Prev. Breaks	0.9040			Material	0.0593
				# Prev. Breaks	0.8914

Starting with Table 5.1, a summary of the weighting value results of the first optimization trial which excluded transient pressure range as a factor, the number of previous breaks received the highest weighting value of 0.9040. This result is consistent with other studies in literature as shown in Table 5.3, which was taken from Vanrenterghem-Raven (2007). This is also corroborated by Ellison et al. (2014) which states that the first of 3 general areas of agreement among nearly all statistical studies of main breaks is that once a failure has occurred on a particular pipe, a model's ability to predict future failures on that pipe is greatly improved. The second highest weighting value was assigned to the pipe material factor which is followed by diameter and soil corrosivity. Ellison et al. (2014) go on to say that the last of the 3 general areas of agreement is that pipes in more corrosive soils break sooner. The validity of the weighting value results for material and soil corrosivity from the first optimization trial is confirmed by other studies such as Vanrenterghem-Raven (2007) and those cited by Ellison et al. (2014).

The weighting value results of the second optimization trial, which included transient pressure range as a factor, were summarized in Table 5.4. As shown in the results, the number of previous breaks also received the highest weighting value followed by material. This is consistent with the first optimization trial, which was consistent with results published in the literature. The addition of transient pressure range as a factor changed the weights of the other two factors as expected. However, the fact that the second optimization trial did not produce illogical results (i.e., results that substantially deviated from both the first trial and literature) shows a degree of consistency in the optimization procedure. The transient pressure factor received a minor weight of approximately 4.37%. This minor weight should not be discarded as unimportant. The prediction capabilities of

the model with the weighting values from the second optimization trial was improved from a Matthew's Correlation Coefficient (MCC) of approximately 0.24 to 0.26. This improvement, although small, shows an improvement in a model's capability to predict whether a pipe will fail or not by including transient pressure fluctuations. Specifically, the inclusion of transient pressure fluctuations as a factor reduces the number of false negatives.

The statistical significance of including transient pressure fluctuations as a factor in the POF model is unknown due to the lack of data available for this study, which is also discussed as a limitation in Section 7.3.1. A minimum of three different calibrated distribution system models and pipe failure data is required in order perform hypothesis testing to identify the statistical significance of including transient pressure fluctuations as a factor. However, the results of this study may be useful in corroborating future research in this field.

6.3   System 1 Risk Analysis Discussion

Results of the risk analysis for System 1 were heavily dependent on the POF and IOF scoring. The POF scores were dependent on the relationships between the factors and the number of pipe failures per length of waterline which were presented in Section 4.3.1, and the weighting values applied to those factors which were discussed in Section 6.1.1. From a purely theoretical standpoint, this should be the optimal approach to assigning a probability of failure to each pipe for a couple of reasons: 1) it takes into account system variability (i.e., a system in California may have entirely different factors than a system in Kentucky), 2) it allows the user to define the amount of data and time frame of the data for which the analysis is run (i.e., user could use a 5,000 break dataset over the past 50 years

117

or a 500 break dataset over the past 5 years), and 3) it allows an optimization procedure to determine which factors are the most important to pipe failure prediction. This method should also consistently improve with time as more data is collected and the research community gains a better understanding of why pipes fail.

The IOF scores for the risk analysis were determined solely by the user. For most of the factors included in the IOF analysis, this determination seemed appropriate. For example, an engineer at a water utility will know how the system operates and thus will know which pipes are vitally important for carrying water to a hospital or nursing home. However, the impact scores assigned to factors such as road class and diameter are not derived from real world data. This is another area of research which could help to improve asset management and is further discussed in Section 6.2.3.

The ROF scores were the final results of the risk analysis for System 1. These results ultimately tell the user which pipes are most at risk by taking into account both the probability of failure and the impact of failure. It is difficult to assess the effectiveness of a risk analysis as it pertains to asset management. The purpose of risk analysis is to assist the user or utility in making optimal decisions regarding asset management. However, if a decision is made to replace a main proactively, then the true optimal decision for that pipe will never be known for certain. Only in hindsight (i.e., after the pipe breaks) will the optimal course of action be apparent to the user. Nevertheless, the utility's budget is probably the only way of assessing the effectiveness of a risk analysis or optimal system rehabilitation strategy over time.

From a visual assessment of Figures 5.1-5.3, the only trend that seems to emerge is that there are many True Positives and False Negatives (i.e., breaks) on dead end pipes (i.e., pipes which do not loop back into the system). From a theoretical standpoint, a dead end pipe will have lower static pressures than pipes which are looped back into the system. This is because pipes which are looped back into the system have multiple paths which the water can take which reduces the total head loss and increases the static pressure. Other than dead end pipes, there are no other spatial patterns or groupings of breaks that are apparent from the visual assessment.

CHAPTER 7 CONCLUSIONS AND RECOMMENDATIONS

7.1   Review of Research Objectives

This section provides a discussion on each of the research objectives listed in Section 1.3. This discussion includes objectives that were achieved in this study, as well as objectives that were not achieved.

7.1.1   Research Objective 1

The author's first research objective is as follows: to investigate system responses to transient events for various system configurations. Research objective 3 was completely fulfilled in this study. A database of 15 water distribution system models developed at the University of Kentucky was used in this study. The database contained 5 systems for each configuration type (e.g., branch, loop, and grid), and the results of the transient analysis were compared between system configurations.

In general, the author found that proximity to the WTP was the factor which accounted for the largest difference in transient pressure range between system configurations. In grid and loop systems, the proximity to the WTP was not often a significant factor. However, in branch systems, the proximity to the WTP had a significant impact on the results.

7.1.2   Research Objective 2

The author's second research objective is as follows: to determine if pressure fluctuation factors are a significant contributor to a simple pipe failure prediction model. Research objective 2 was partially fulfilled in this study. The author identified strong

relationships between both transient pressure fluctuations and pipe breaks, and daily pressure fluctuations from standard system operations and pipe breaks. Transient pressure fluctuations were included in the probability of failure model as an input factor and improved the overall accuracy of the predictions by reducing the number of false negatives.

However, the statistical significance of adding pressure fluctuations to the probability of failure model was not calculated due to the lack of available data for this study. Only 1 calibrated model and set of pipe failure data were available to the author. Therefore, the author could not replicate his results other systems. A minimum of 3 calibrated models and failure datasets would be required to test the statistical significance of the author's findings. Therefore, the author could not fulfill the second part of research objective 2. If more time were allotted for this research project, the author would try to obtain two other distribution system models with approximately 10 years of failure data to repeat the analysis performed in this study.

7.1.3   Research Objective 3

The author's third research objective is as follows: to develop and test a transient-based risk analysis methodology to aid utilities in making optimal decisions regarding water main rehabilitation and replacement, and to test the effectiveness of the methodology by executing the risk analysis on a real distribution system with pipe failure data. Research objective 1 was partially fulfilled in this study as the author developed a transient-based risk analysis methodology. This methodology was tested on a real water distribution system in the state of Kentucky (i.e., System 1) with real pipe failure data. The results of the analysis were displayed graphically on a schematic of the system for easy visual assessment.

However, the effectiveness of the methodology was not tested in this study due to time constraints on the research project. The most appropriate way to test the effectiveness of this methodology is to compare the actual cash flow of the water utility for a given year with the projected cash flow in the same year using the proposed methodology.

7.2   Summary of Major Findings

The following is a summary of the findings:

- A strong relationship was discovered between the frequency of pipe failures and the magnitude of both transient and normal pressure fluctuations,

- The performance of the probability of failure (POF) model was improved by including the magnitude of pressure fluctuations,

- The largest transient fluctuations were observed near supply pump stations.

Two notable relationships were derived from this study. The first is the relationship between the transient pressure range and pipe failures. Transient pressure range represents the combined amplitude of the positive and negative pressure waves experienced by a pipe during a transient event. The strong, positive relationship between transient pressure range and pipe failures is shown in Figure 4.10. The second notable relationship that was derived for this study is between EPS pressure fluctuations and pipe failures. The EPS pressure fluctuations represent the daily fluctuations resulting from standard system operations. This strong, positive relationship is shown in Figure 4.11. Each of these relationships reveal that pipes are more likely to break in System 1 as the pressure fluctuations increase, whether those fluctuations are due to standard operations or transient events. The author

suggests that this is a key finding of this study and that the results should be verified by other studies.

A simple POF model was used in this risk analysis methodology to assess which of the pipes were most likely to break based on a set of input variables. Traditional variables were used in this model such as age, diameter, material, soil corrosivity, and number of previous breaks. The author analyzed the model results for 2 trials. The first trial used only the traditional variables, and the second trial used the traditional variables plus the transient pressure range. The model results marginally improved with the addition of the transient pressure range by decreasing the number of false negatives by approximately 20%. The improvement of the model results is the 2nd major finding in this study. It reveals to the author that transient pressure range helps to explain a portion, however small, of the individual pipe failures. Pressure fluctuations should be included in other studies to verify the improvement in the failure prediction models.

Lastly, a database of 15 water distribution system models was used to analyze the effects of acute transient events between different system configurations. Five branch, loop, and grid systems were analyzed by simulating a pump failure and recording the resulting transient pressures. Various transient pressure metrics were color-coded onto the system schematics in order to visually assess the results. The most notable difference between the configurations was due to the distance between the pipes and the source of the transient event. In branch systems, which have a much larger footprint than grid and loop systems, only pipes in close proximity to the water treatment plant (i.e., where the pump shutdown occurred) experienced significant pressure fluctuations. Therefore only a small portion of the pipes in the branch systems were affected by the transient. Oppositely, in

grid and loop systems, a much larger percentage of the system was at risk to large pressure fluctuations due to the relatively small distance from the transient source. This is the 3rd major finding of this study.

7.3   Limitations, Application, and Future Research

7.3.1   Limitations

The most significant limitation in this study was the lack of available data. This study did not require any field work; it only required the participation of utilities in letting the author analyze the data which they have collected. After contacting multiple utility companies, a single utility agreed to participate in this study. This utility provided the author with a calibrated model of a pressure zone in their system, approximately 8.5 years of georeferenced pipe failure data, and the general approach to their proactive main replacement and monitoring program. This data was very useful in determining the most recent pipe failure behavior in that pressure zone. However, the data did not provide insight into historical pipe failure behavior (i.e., behavior prior to 2007). In order to fully understand the factors behind pipe failures, a more robust dataset should be analyzed.

Another limitation of this study is the optimization solver which was used to obtain the weighting values for the prediction factors. Microsoft Excel's solver add-in was used to perform the constrained global optimization of the weighting values. This solver employs the Nonlinear General Reduced Gradient algorithm to arrive at the optimal solution. While this algorithm works well for smooth, convex problems, the algorithm will often find a local optima close to the starting points rather than a global optima if the problem is not convex and not smooth. In order to overcome this problem, the Multistart

function was employed which generates a user-defined number (e.g., 1000 in this study) of random starting points for which to run the algorithm. While this extends the computational time significantly, it also increases the robustness of the optimization which makes it more likely to find the global optima. However, the solver add-in is not as strong an optimization program as many other software packages. Other packages employ more robust algorithms such as genetic algorithms which work very well to find global optimal solutions for non-smooth, non-convex problems.

7.3.2 *Application*

This research is directly applicable to most asset management programs employed by water utility companies. The methodology of this study is simple and may be easily understood. There are various pieces of software which are extremely helpful for parts of this analysis. This includes spreadsheet software such as Microsoft Excel, geographic information systems software such as ArcMap, academic computer programming software such as MATLAB, hydraulic modeling software such as KYPIPE and InfoWater, and optimization programs such as the Excel Solver add-in. Overall, this research could be employed by a utility company to help assess the at-risk parts of their system and make optimal rehabilitation decisions.

There are also various standalone parts of this study which may be applicable such as the derived relationships between various factors and breaks per length of waterline, the POF and IOF models, and the results of the transient analysis for the database systems. The derived relationships between various factors and breaks per length of waterline can help to corroborate results of other studies, they can be tested in future studies to improve the general understanding of pipe failures, and they can be used by the utility company who

provided the break data to increase the effectiveness of their main replacement program. The POF model can be used by utility companies to assess which of their pipes are most likely to break based on designated factors and weights. The IOF model can also be used by utilities to analyze which parts of their system would have the greatest impact if failure occurred. Lastly, the results of the transient analysis on the 15 database systems may be used in the research community to better understand the behavior of transient pressure waves in a large-scale distribution system analysis.

7.3.3   Future Research

The author acknowledges that this research has room to be expanded upon and improved. The search for an adequate prediction model for individual pipe failures is ongoing and has much room for improvement. Many of the relationships between various pipe factors and the number of breaks per length of waterline have been derived and verified by other studies. However, there has still been limited research performed in the relationship between transient events (both acute and those which cause daily pressure fluctuations) and pipe failures.

The author also recommends that a quantitative analysis be performed on transient pressure results for each system in the database. While a visual analysis of the results may show general differences, a quantitative analysis would help to analyze the interdependency of factors such as elevation, standard operating pressure, proximity to tanks, and others.

There is also a considerable amount of future research to be performed in analyzing the impact of pipe failures. While general rules and relationships have been presented in

this study, a quantification of the impact of failure for various pipe diameters and locations has not been performed to the author's knowledge. A quantification of the impact of failure due to loss of service is another area of future research that would be helpful to this study.

Appendix A: Derivations

Continuity Equation:

The continuity equation is based on the law of conservation of mass which states that matter cannot be created or destroyed. To derive the continuity equation, the law of conservation of mass is applied to a control volume for steady flow as shown in Figure A.1.
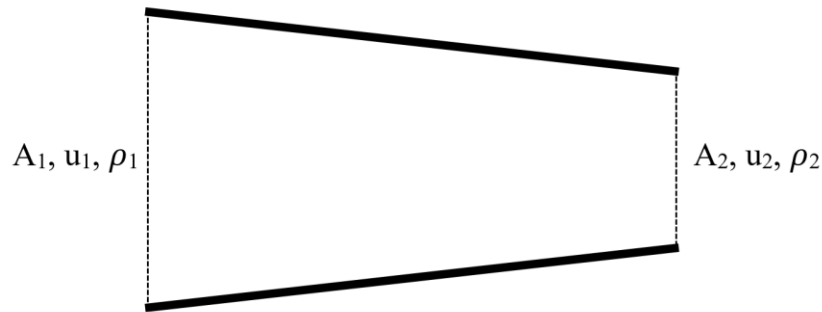
Figure A.1: Control Volume.

Where:
A_1 = Area at the entrance of the control volume,
u_1 = Fluid velocity at the entrance of the control volume,
ρ_1 = Fluid density at the entrance of the control volume,
A_2 = Area at the exit of the control volume,
U_2 = Fluid velocity at the exit of the control volume,
ρ_2 = Fluid density at the exit of the control volume.

Using the variables and the control volume depicted in Figure A.1, the law of conservation of mass is represented in the following equation:

$$A_1 u_1 \rho_1 = A_2 u_2 \rho_2$$

For steady-state and extended-period simulations in water distribution system analysis, a constant fluid density is assumed ($\rho_1 = \rho_2$) which means that density can be removed from the equation altogether which results in the following equation:

$$A_1 u_1 = A_2 u_2$$

Since flowrate, shown in the previous equation as "$A_n u_n$", may also be represented by the letter "Q", the continuity equation may be simplified to the following form for a controlled volume as shown in Figure A.1:

$$Q_1 = Q_2 \qquad \text{or} \qquad Q_{in} = Q_{out}$$

Bernoulli's Equation for Incompressible Fluids:

Bernoulli's equation for an incompressible fluid may be derived from the conservation of energy law which states that the total energy of an isolated system remains constant, and the work-energy theorem which states that the net work done (ΔW) is equal to the change in system energy (ΔE).

$$\Delta W = \Delta E$$

Consider a profile section of fluid flowing to the right as shown in Figure A.2. In the figure, P_1 and A_1 are the pressure and area of the fluid at point 1, P_2 and A_2 are the pressure and area of the fluid at point 2, and x_1 and x_2 are the distances of which point 1 and point 2 of the fluid moved, respectively.
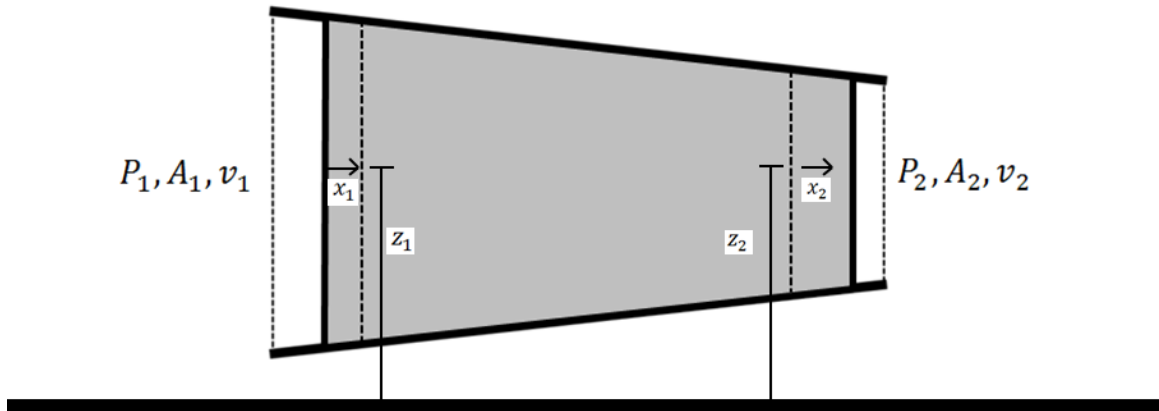
Figure A.2: Profile Section of Fluid.

The work done on the fluid is equal to the force (F) acting on the fluid times the distance which the fluid moved (x) for both points in the confined system. This is shown in the equation below.

$$\Delta W = W_1 + W_2 = P_1 A_1 x_1 - P_2 A_2 x_2$$

The fluid volume is assumed to be constant as shown by $V = A_1 x_1 = A_2 x_2$, therefore the equation simplifies to the following form.

$$\Delta W = (P_1 - P_2)V$$

The change in energy (ΔE) between position 1 and position 2 is given by the following equation, where U is potential energy and K is kinetic energy.

$$\Delta E = E_2 - E_1 = (U_2 + K_2) - (U_1 + K_1)$$

The kinetic energy of the fluid is equal to $\frac{mv^2}{2}$ where m is the fluid mass and v is the fluid velocity. The potential energy of the fluid is equal to mgz where m is the fluid mass, g is gravitational acceleration, and z is relative fluid height.

Therefore, work-energy theorem after rewriting is shown by the equation below.

$$(P_1 - P_2)V = \left(mgz_2 + \frac{mv_2^2}{2}\right) - \left(mgz_1 + \frac{mv_1^2}{2}\right)$$

After reorganizing terms in the equation, the modified Bernoulli equation for incompressible fluids is arrived at and shown below.

$$\frac{P_1}{\gamma} + z_1 + \frac{v_1^2}{2g} = \frac{P_2}{\gamma} + z_2 + \frac{v_2^2}{2g}$$

Momentum Equation:

According to Newton's second law of motion, the time rate of change of momentum of a system is equal to the resultant of the forces exerted on the system by its surroundings.

Picture a free body of fluid with a cross sectional area A and thickness dx. Area is a function of the position along the horizontal axis (x) of the pipe. Forces on the fluid slice include the pressure forces (p) on both ends of the fluid slice, the shear forces (τ) from contact with the pipe wall, and gravitational force which also has an x component due to the pipe's incline angle (α).

In reference to the above figure, the summation of forces on the fluid slice is as follows:

$$pA - [pA + (pA)_x \delta x] + \left(p + \frac{p_x \delta x}{2}\right) A_x \delta x - \tau_0 \pi D \delta x - \gamma A \delta \sin(\alpha) = \rho A \delta x (VV_x + V_t)$$

After dropping the negligible δx^2 term and simplifying, the following equation is obtained:

$$p_x A + \tau_0 \pi D + \rho g A \sin(\alpha) + \rho A (VV_x + V_t) = 0$$

The shear stress τ_0 is assumed to be the same as steady flow, therefore it is written in terms of the Darcy-Weisbach friction factor f.

$$\tau_0 = \frac{\rho f V |V|}{8}$$

Once the shear stress is equation is substituted, the momentum equation is as follows:

$$\frac{p_x}{\rho} + VVx + V_t + g \sin(\alpha) + \frac{f V |V|}{2D} = 0$$

130

This is the momentum equation and may also be written as follows:

$$\frac{1}{\rho}\frac{dp}{dx} + V\frac{dV}{dx} + \frac{dV}{dt} + gsin(\alpha) + \frac{fV|V|}{2D} = 0$$

This equation may be simplified to the equation shown in Section 2.2.1 which is also shown below.

$$\frac{\partial H}{\partial x} = -\frac{1}{gA}\frac{\partial Q}{\partial t} + \frac{fQ|Q|}{2DA}$$

Appendix B: Code

B.1: MATLAB Code

Legend:

Green Text = Comments

Black text = variables, values, and operators

Blue text = statement begin or end

```matlab
%Import CDF for Large Transient Event
importmajor;

%Import CDF for Small Transient Event
importminor;

%Set column for CDF value
check=5;

%User define how much of CDF to check for PipeID
cdfrange = 0.125;

%Create results matrix and PipeID matrix
rm(1:1124,1:1)=0;
pm(1:1124,1:1)=0;

%Introduce PipeID variable
pipeid=0;

%Initiate for Loop: For each pipe in 1 CDF
for i=1:1124;
    %Establish upper and lower CDF check limits
    ulrange=minor(i,check)+cdfrange;
    llrange=minor(i,check)-cdfrange;
    %Initiate IF statement: If PipeID is within set range then 1 or 0
    if(llrange < 0);
        llrange=0;
    end
    if (ulrange>1);
        ulrange=1;
    end
    pipeid=minor(i,1);
    %Last part exports results for each pipe to results matrices
    for j=1:1124;
        if (major(j,check)<=ulrange && major(j,check)>=llrange);
            if (major(j,1)==pipeid);
                rm(i,1)=1;
            end
        end
```

```
        end
    if (rm(i,1)==1);
        rm(i,1)=1;
    else
        pm(i,1)=pipeid;
    end
end

%Display pipe IDs which fell outside defined CDF range
unique(pm)

%Display percentage of pipes in defined CDF range
sum(rm)/1124*100
```

Appendix C: Additional Figures
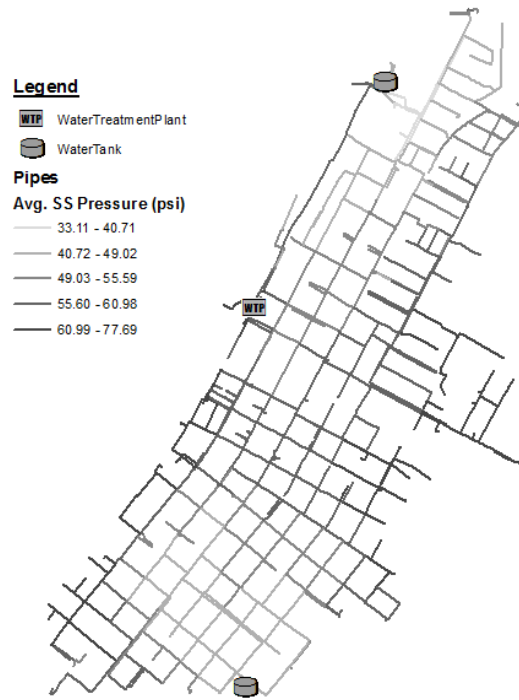
Figure C.1: Average Steady-State Pressure for KY1.
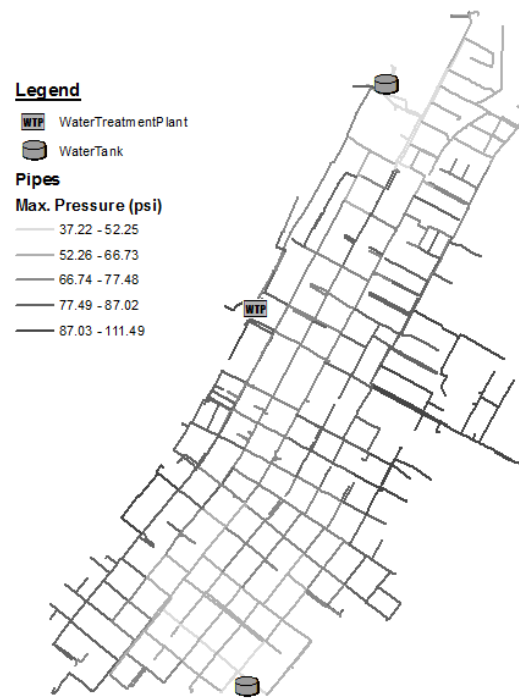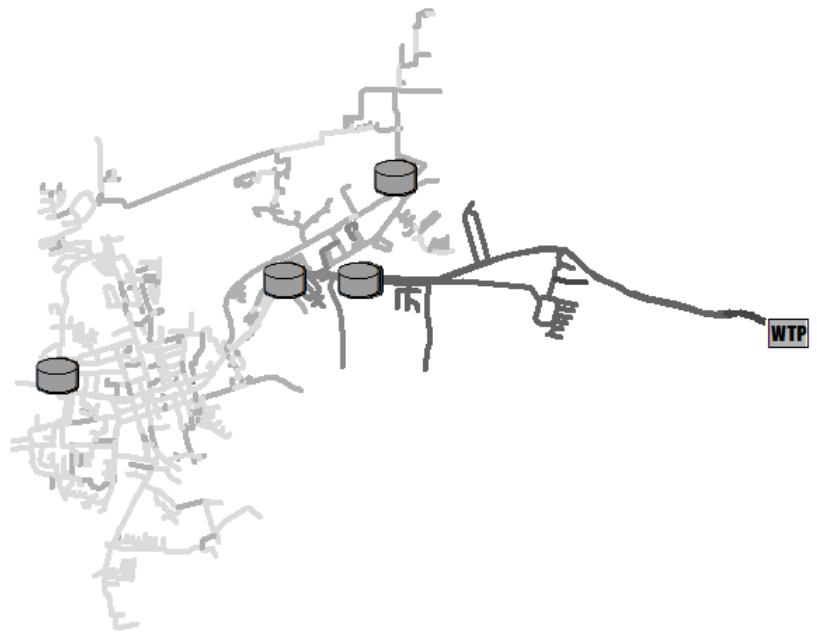

Figure C.2: Maximum Pressure for KY1.
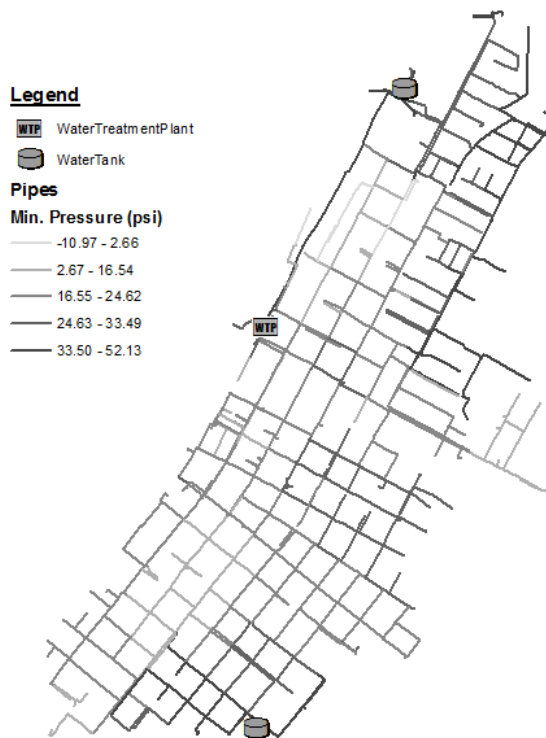
Figure C.3: Minimum Pressure for KY1.
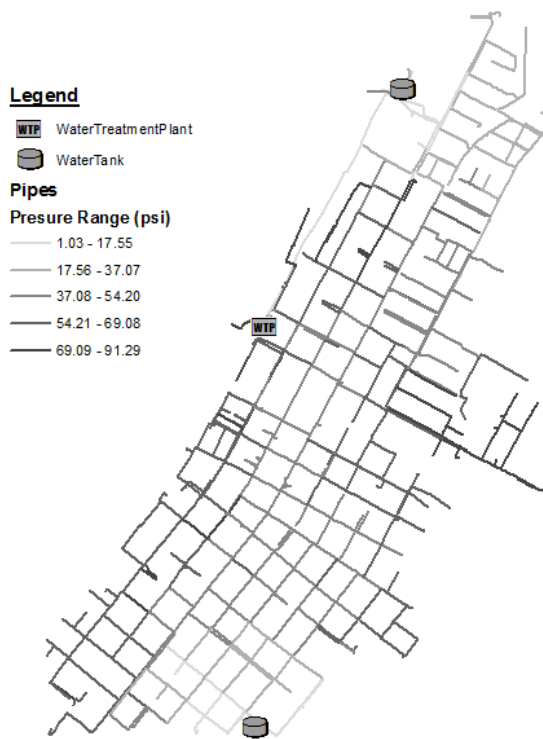
Figure C.4: Transient Pressure Range for KY1.
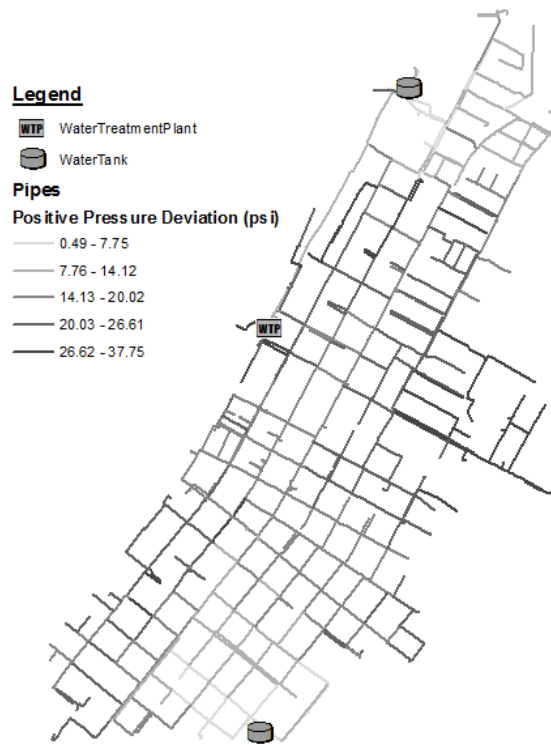
Figure C.5: Positive Pressure Deviation for KY1.
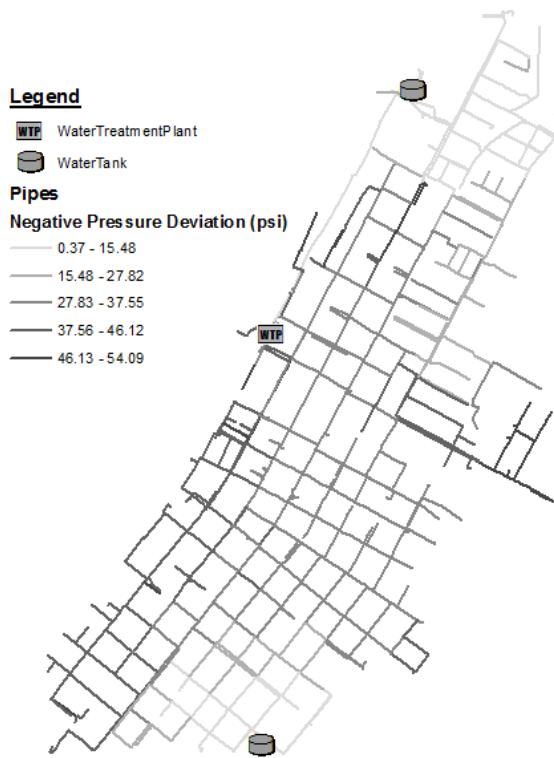
Figure C.6: Negative Pressure Deviation for KY1.

Figure C.7: Average Pipe Elevation for KY1.
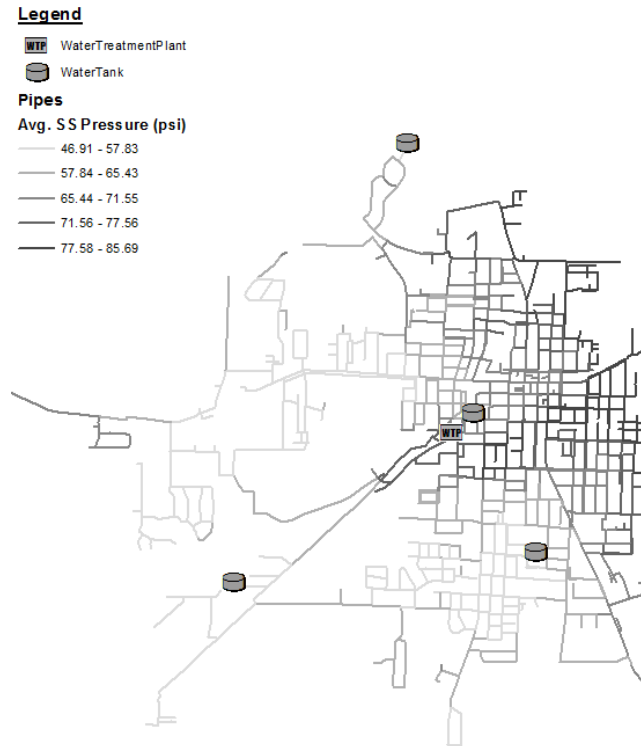
Figure C.8: Average Steady-State Pressure for KY2.

137
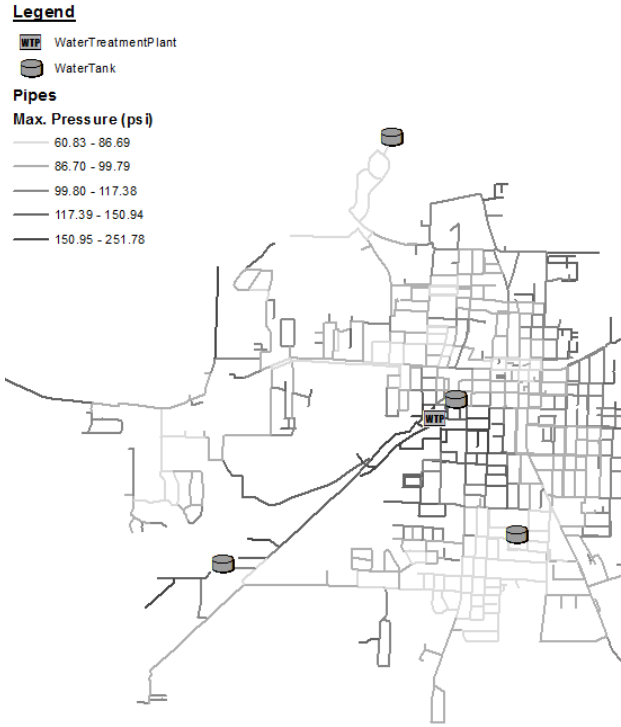
Figure C.9: Maximum Pressure for KY2.
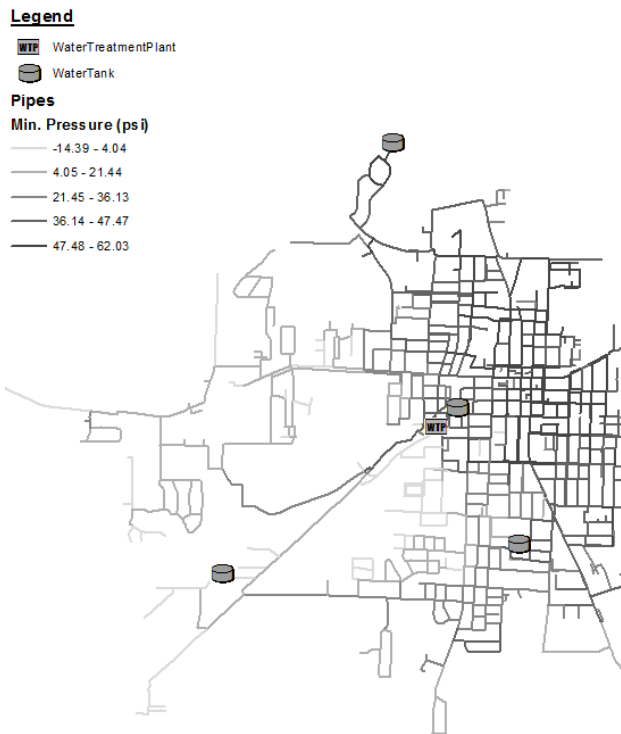
Figure C.10: Minimum Pressure for KY2.

138

WTP WaterTreatmentPlant

WaterTank

Pipes

Pressure Range (psi)

— 13.98 - 50.77
— 50.78 - 72.44
— 72.45 - 104.87
— 104.88 - 165.33
— 165.34 - 266.17
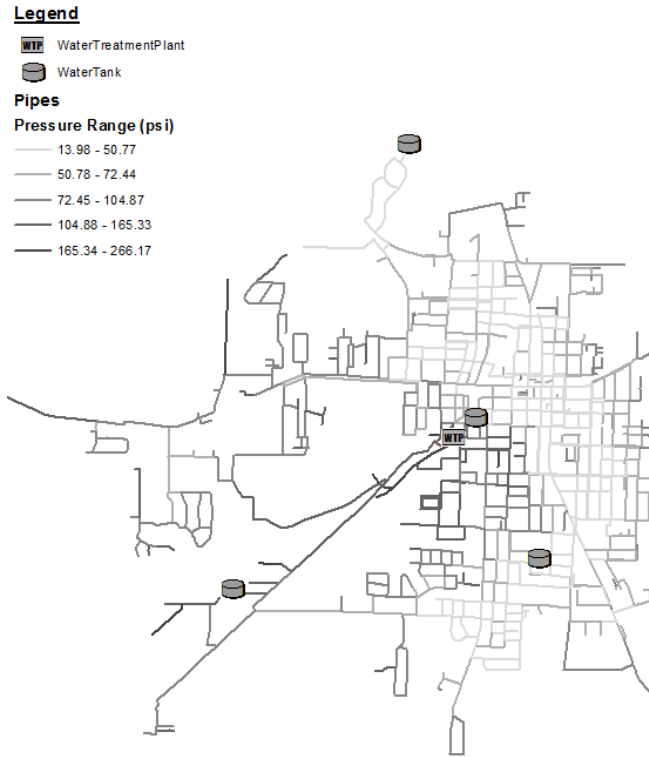
Figure C.11: Transient Pressure Range for KY2.

Legend

WTP WaterTreatmentPlant

WaterTank

Pipes

Positive Pressure Deviation (psi)
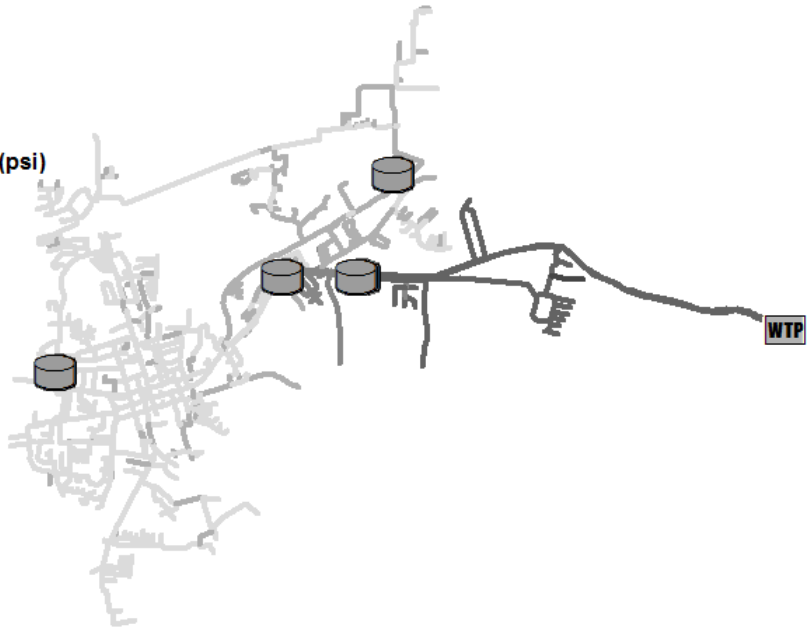
— 7.40 - 26.07
— 26.08 - 40.08
— 40.09 - 60.12
— 60.13 - 92.86
— 92.88 - 195.93
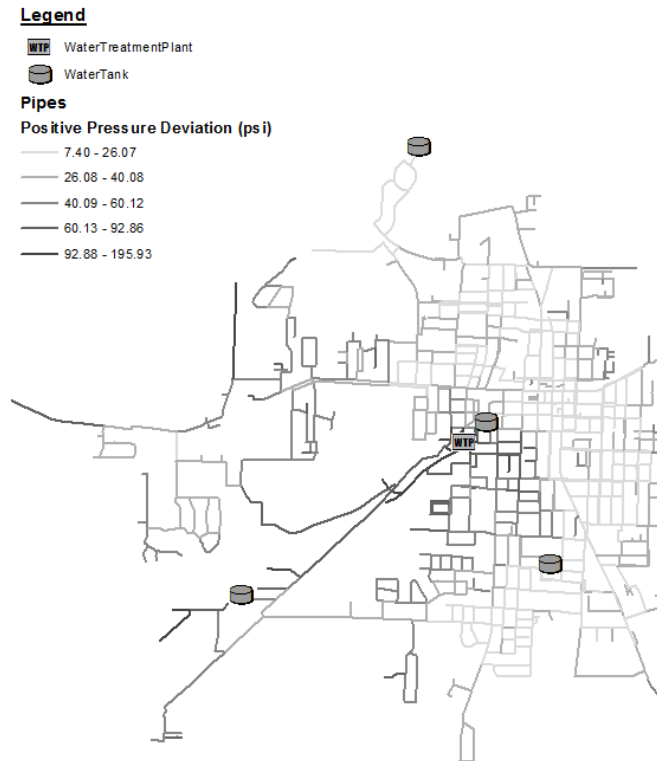
Figure C.12: Positive Pressure Deviation for KY2.
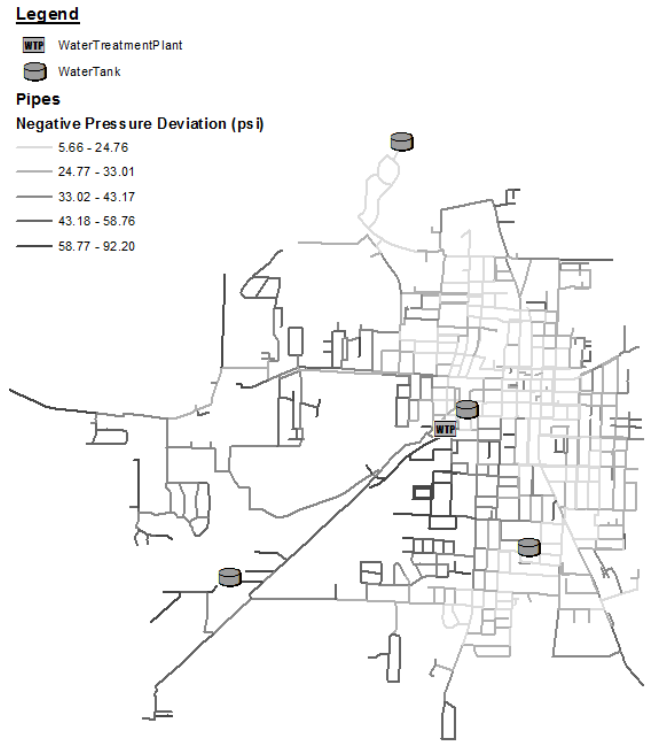
Figure C.13: Negative Pressure Deviation for KY2.
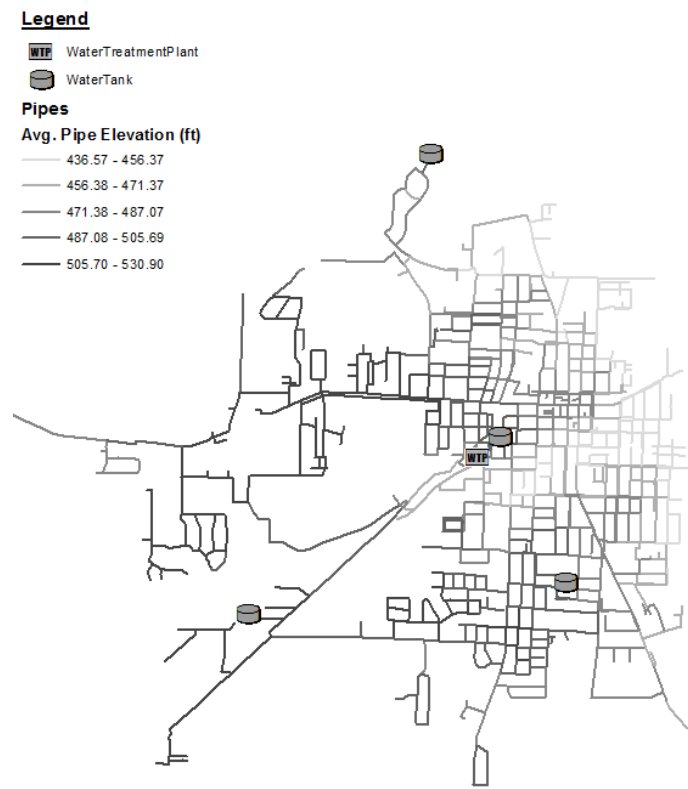
Figure C.14: Average Pipe Elevation for KY2.

140
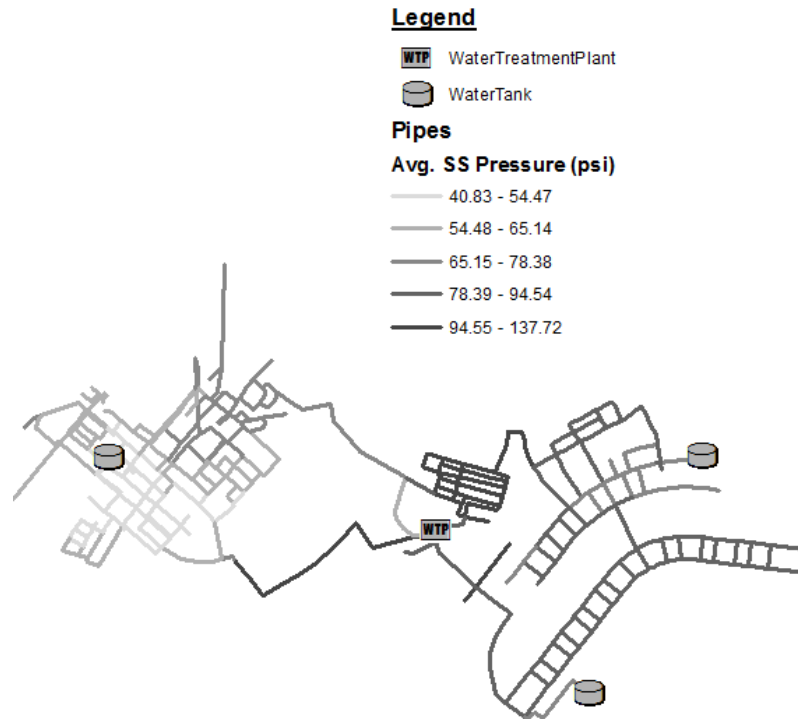
Figure C.15: Average Steady-State Pressure for KY3.
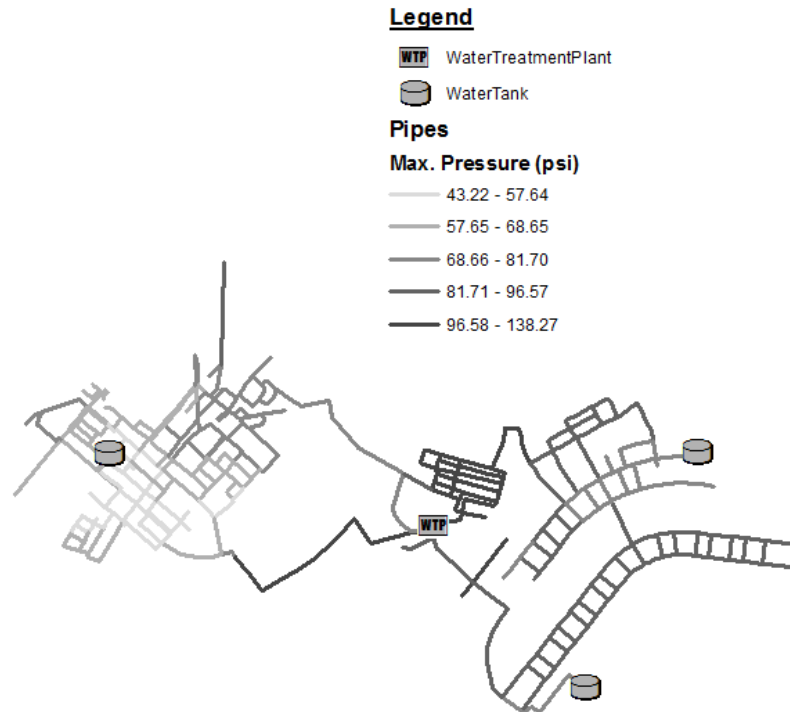
Figure C.16: Maximum Pressure for KY3.

141
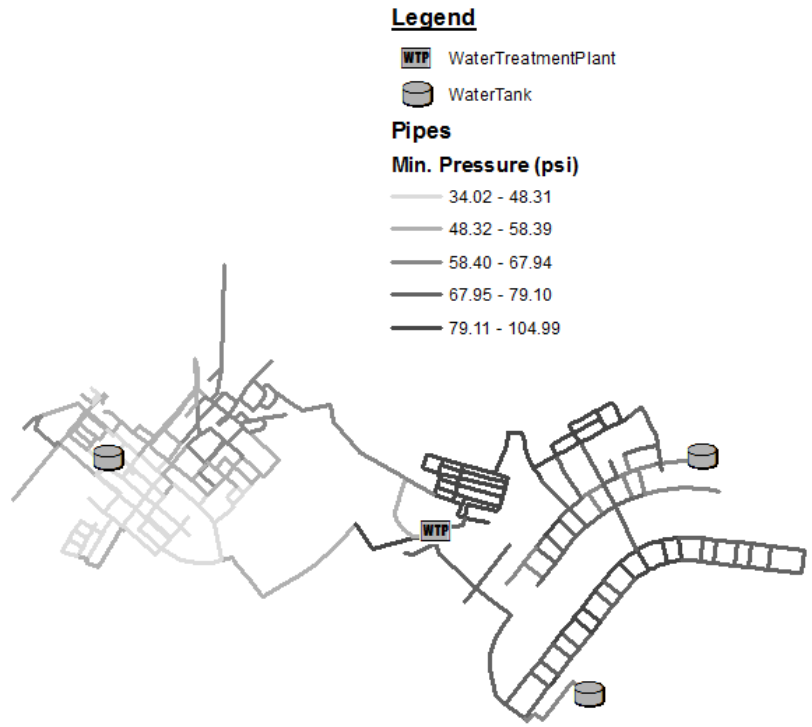
Figure C.17: Minimum Pressure for KY3.
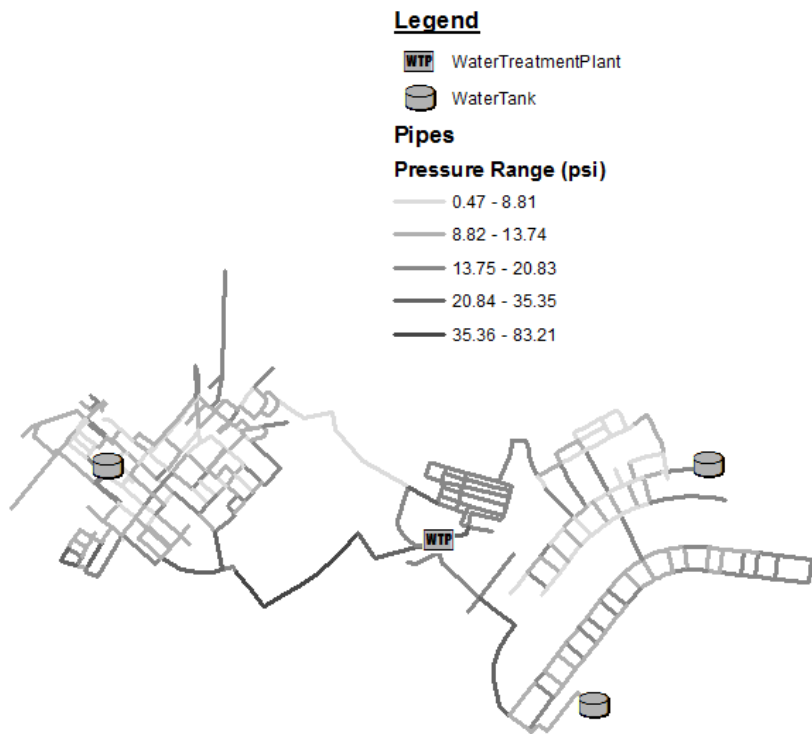
Figure C.18: Transient Pressure Range for KY3.
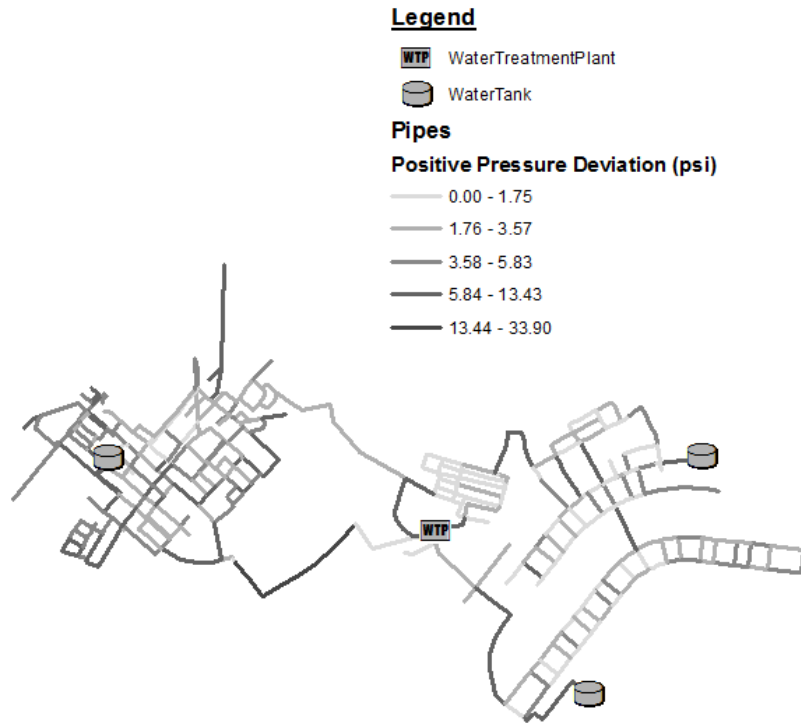
Figure C.19: Positive Pressure Deviation for KY3.
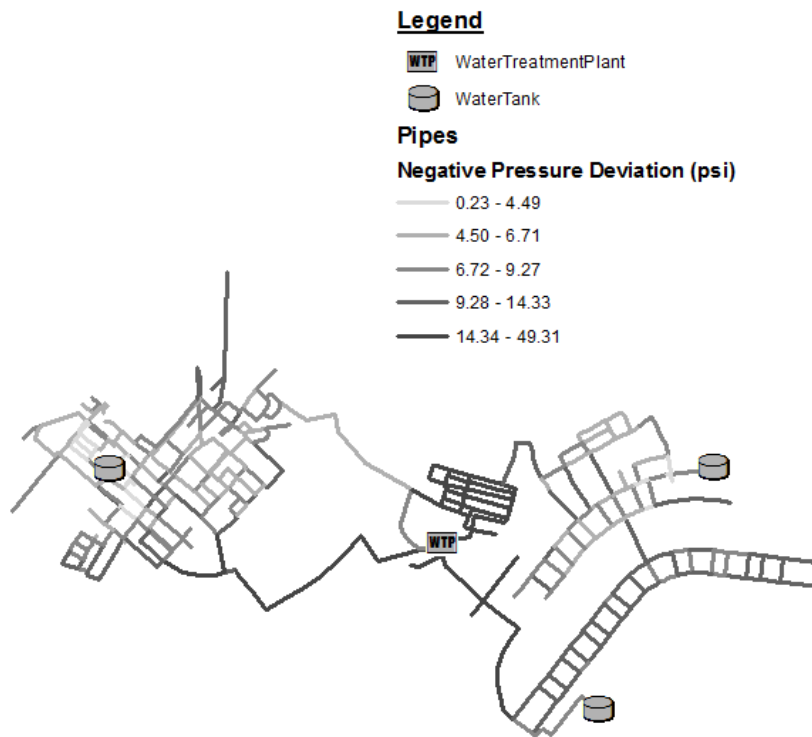
Figure C.20: Negative Pressure Deviation for KY3.
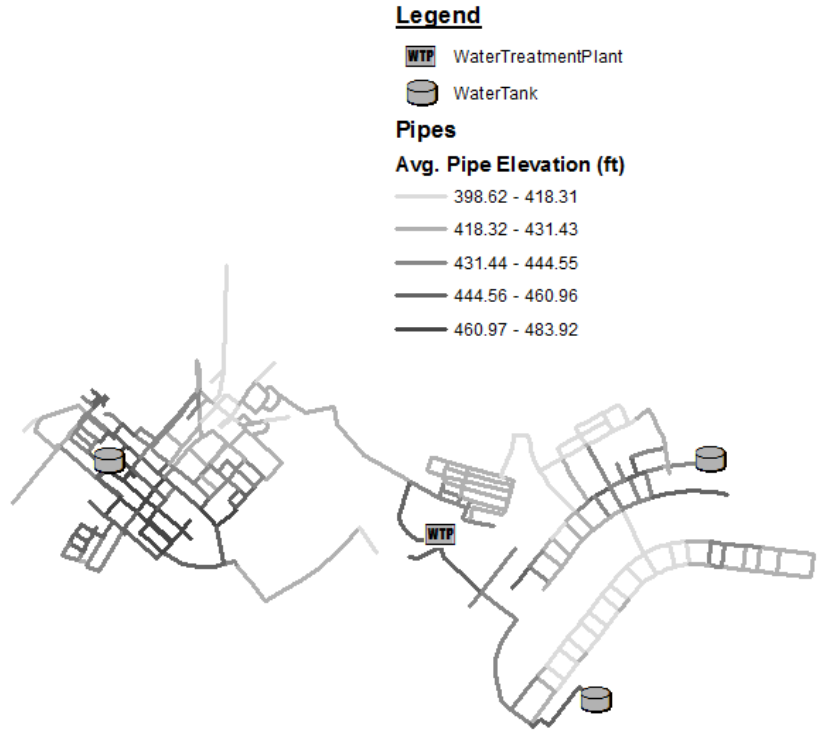
Figure C.21: Average Pipe Elevation for KY3.
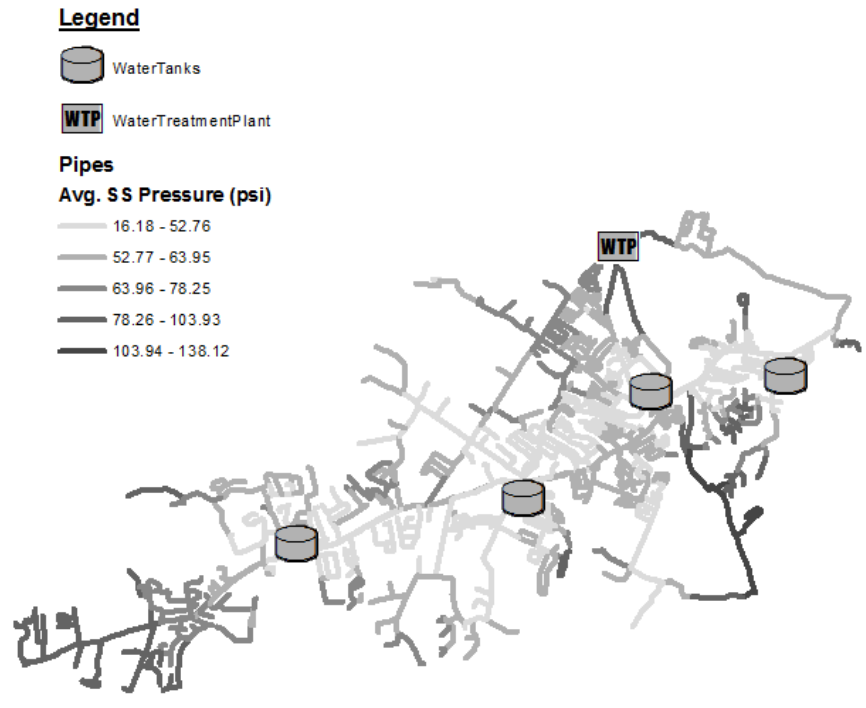
Figure C.22: Average Steady-State Pressure for KY4.
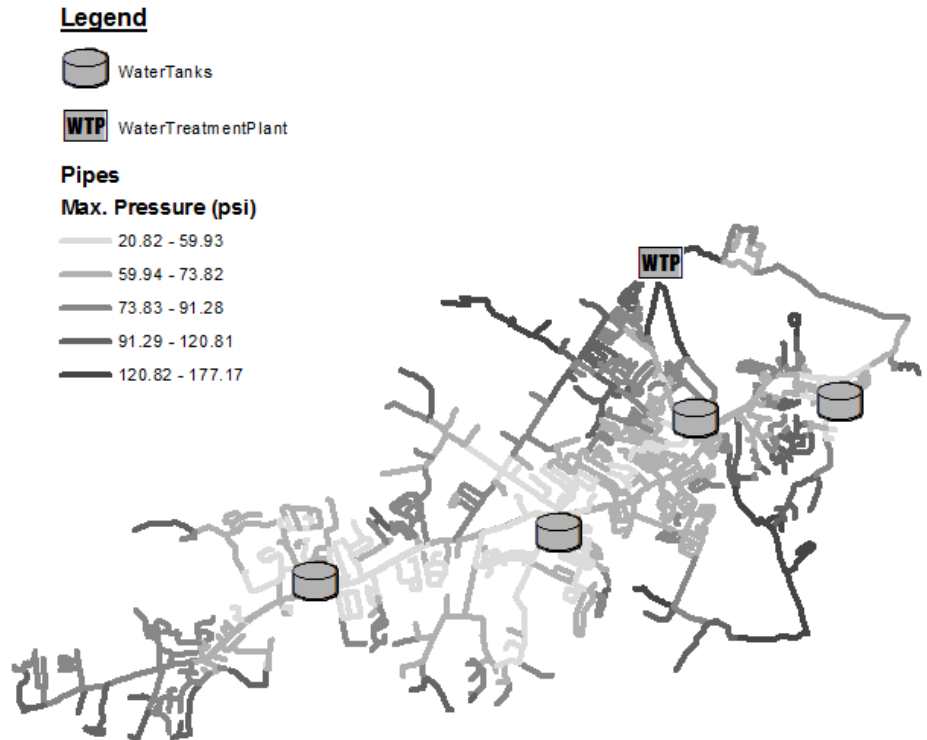
Figure C.23: Maximum Pressure for KY4.

Figure C.24: Minimum Pressure for KY4.

WaterTanks

WTP WaterTreatmentPlant

Pipes
Pressure Range (psi)

— 1.16000000 - 17.6000000
— 17.6000001 - 34.6100000
— 34.6100001 - 54.7900000
— 54.7900001 - 96.1100000
— 96.1100001 - 185.810000
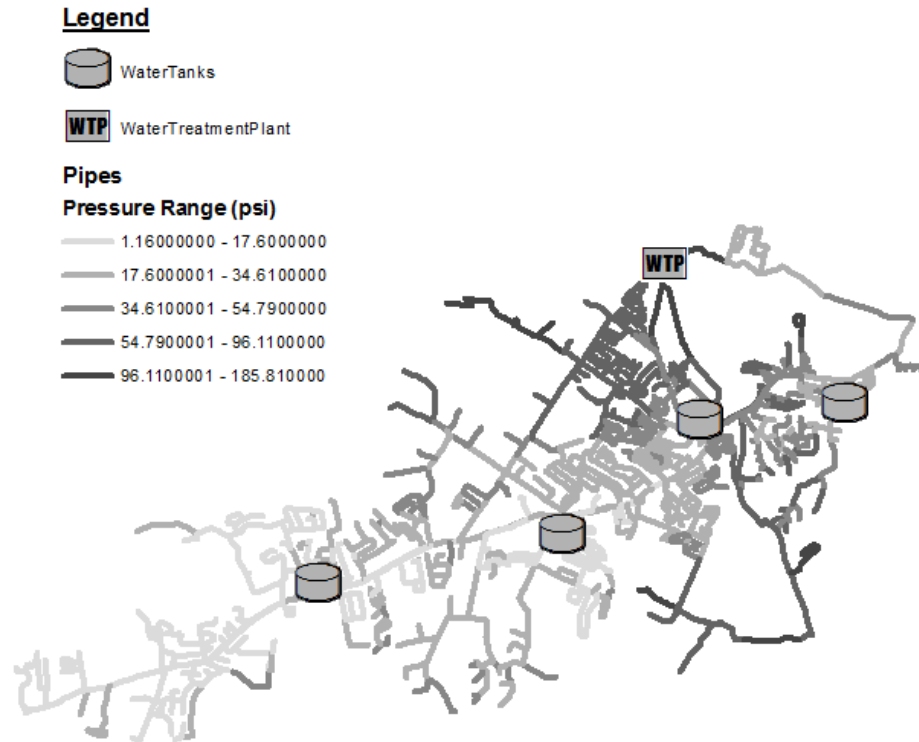
Figure C.25: Transient Pressure Range for KY4.

Legend

WaterTanks

WTP WaterTreatmentPlant

Pipes
Positive Pressure Deviation (psi)

— 0.56 - 9.31
— 9.32 - 19.03
— 19.04 - 34.41
— 34.42 - 64.05
— 64.06 - 110.61
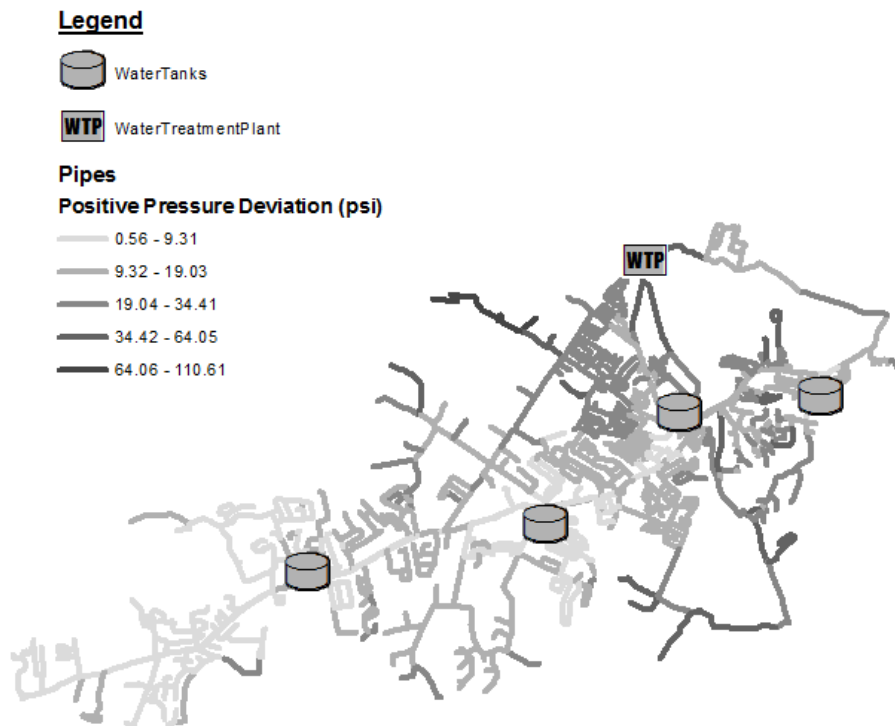
Figure C.26: Positive Pressure Deviation for KY4.

146
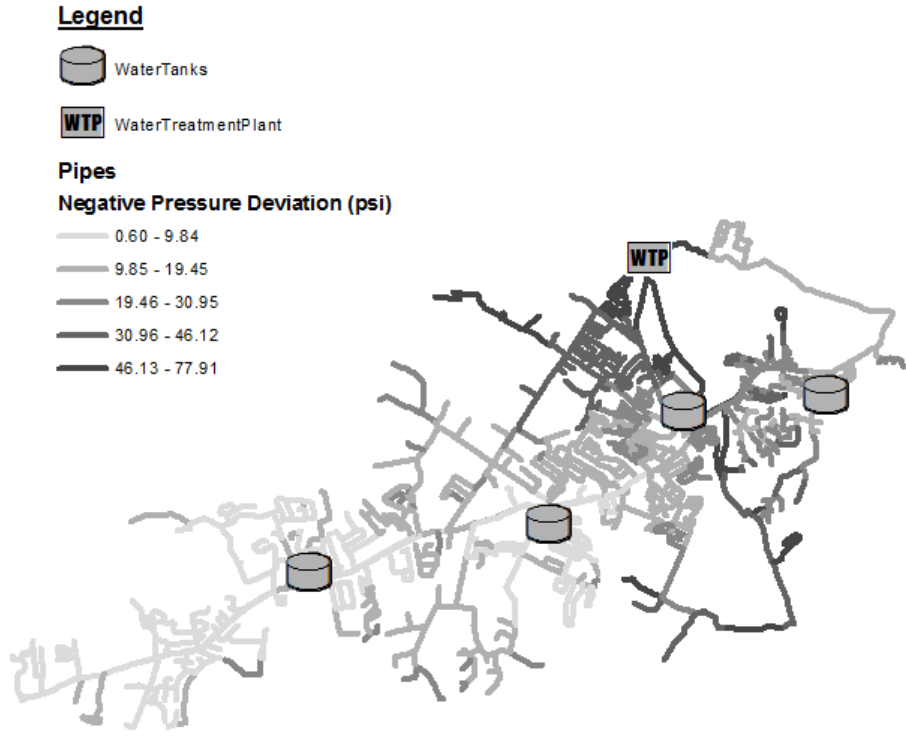
Figure C.27: Negative Pressure Deviation for KY4.
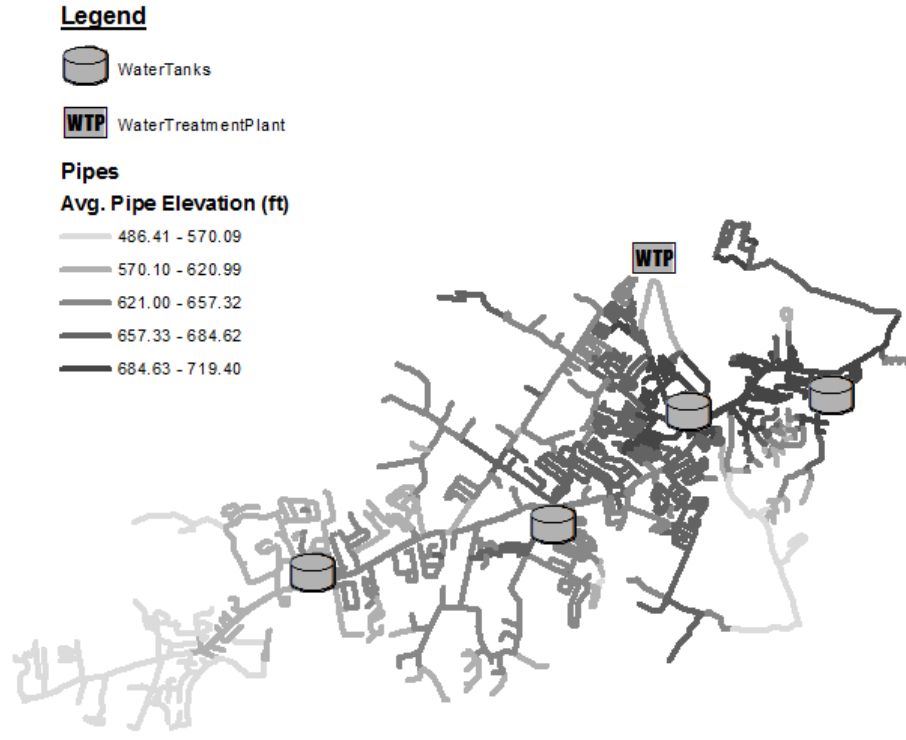
Figure C.28: Average Pipe Elevation for KY4.

Figure C.29: Average Steady-State Pressure for KY5.

Figure C.30: Maximum Pressure for KY5.

Figure C.31: Minimum Pressure for KY5.

Figure C.32: Transient Pressure Range for KY5.

Figure C.33: Positive Pressure Deviation for KY5.

Figure C.34: Negative Pressure Deviation for KY5.
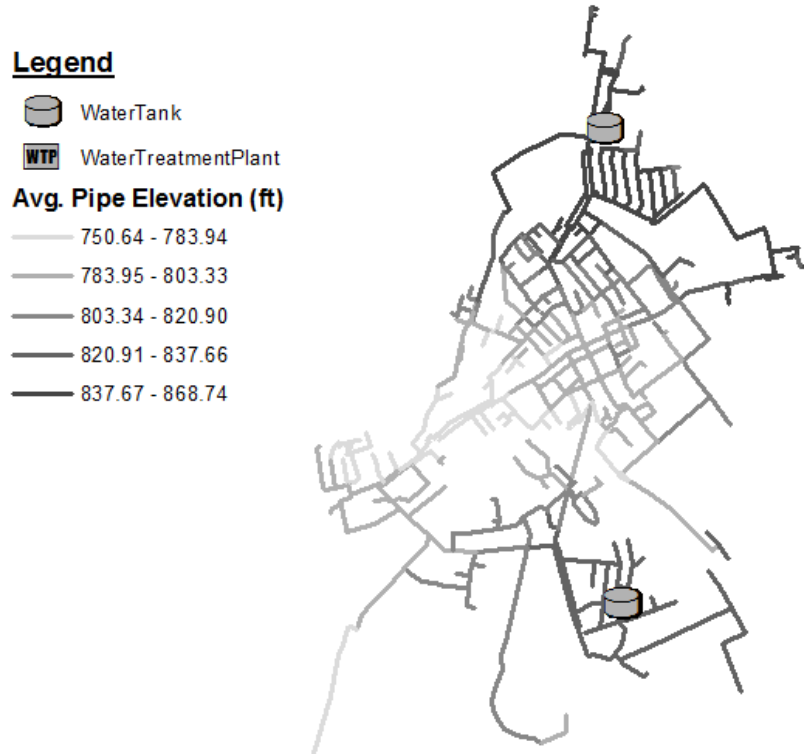
Figure C.35: Average Pipe Elevation for KY5.
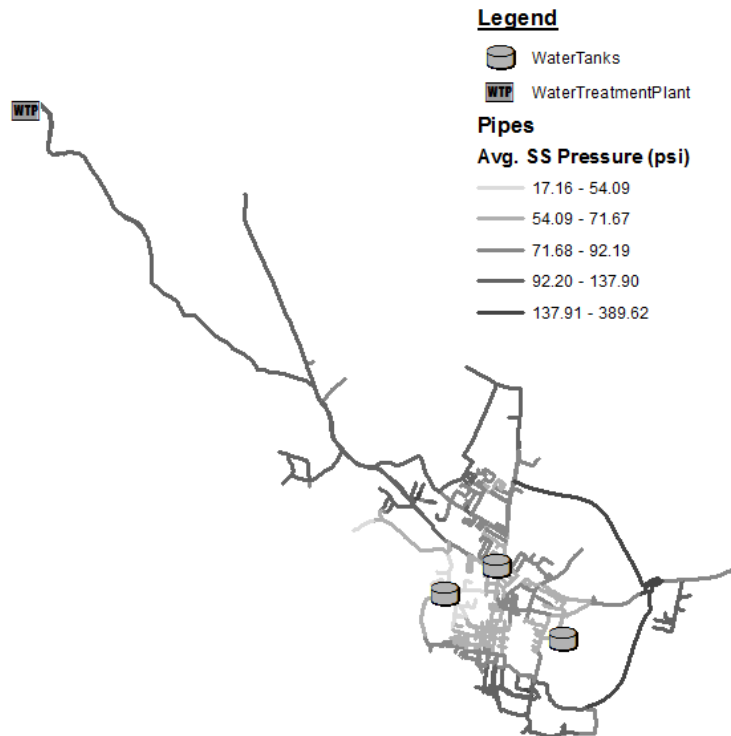
Figure C.36: Average Steady-State Pressure for KY6.
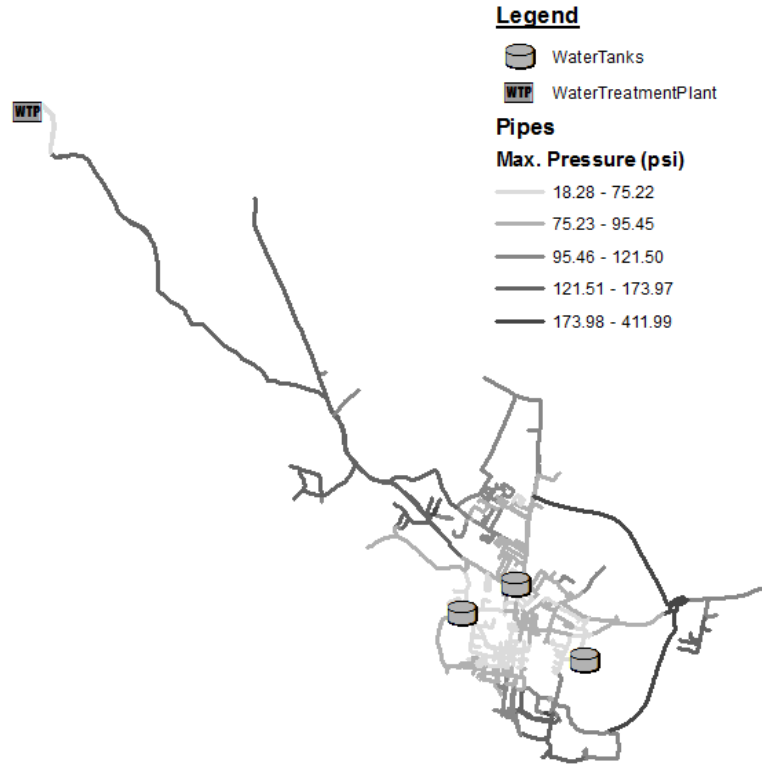
Figure C.37: Maximum Pressure for KY6.
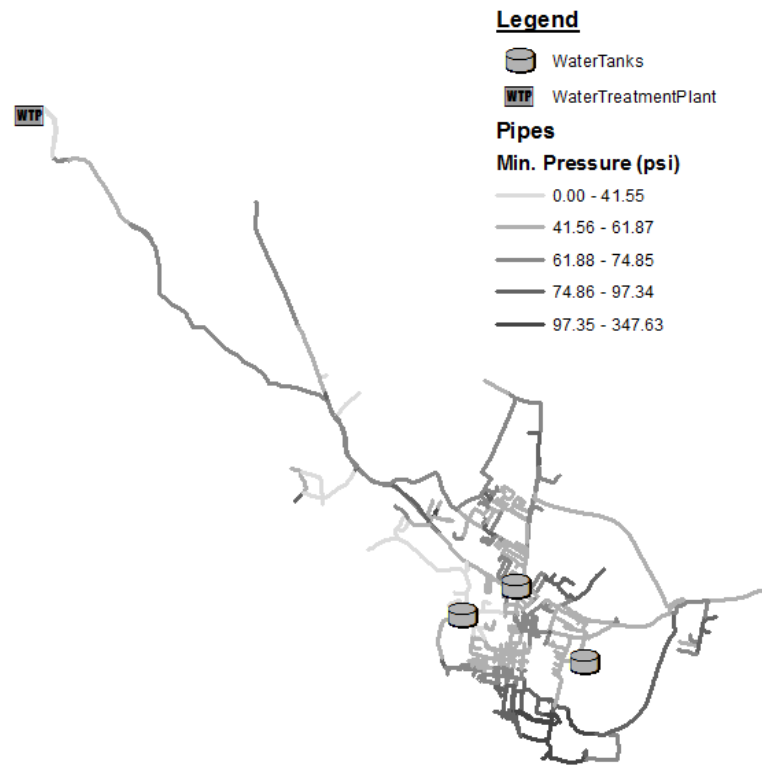
Figure C.38: Minimum Pressure for KY6.

152
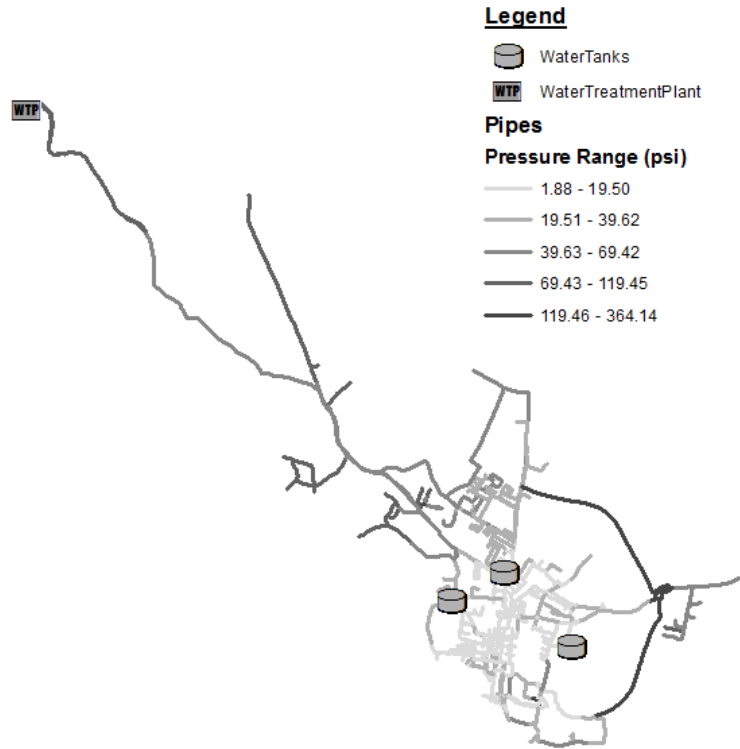
Figure C.39: Transient Pressure Range for KY6.
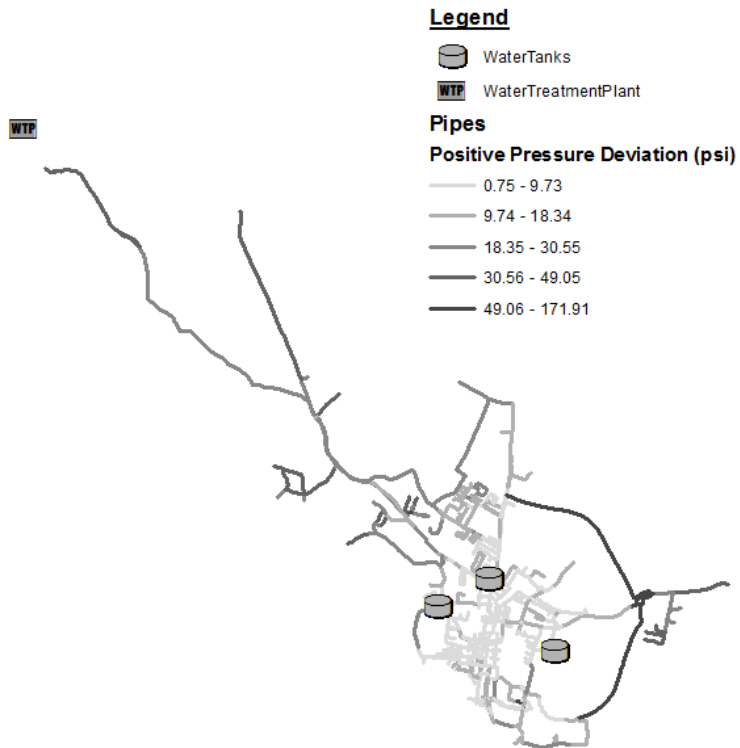
Figure C.40: Positive Pressure Deviation for KY6.

153
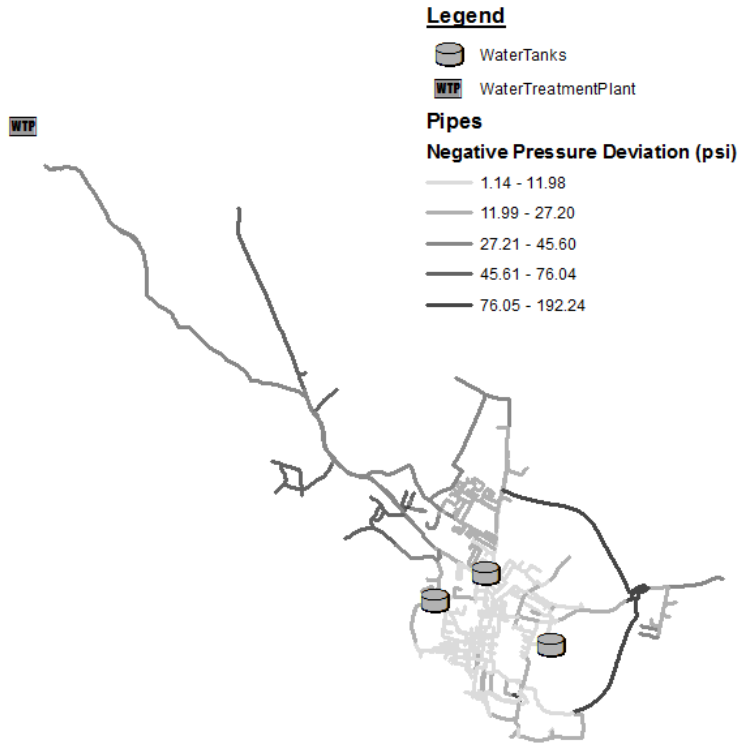
Figure C.41: Negative Pressure Deviation for KY6.
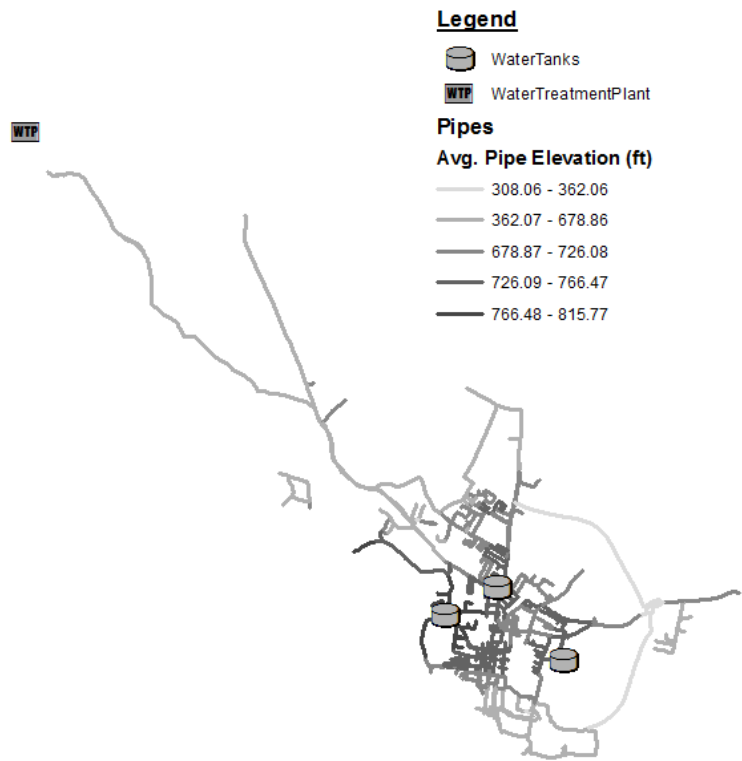
Figure C.42: Average Pipe Elevation for KY6.

154
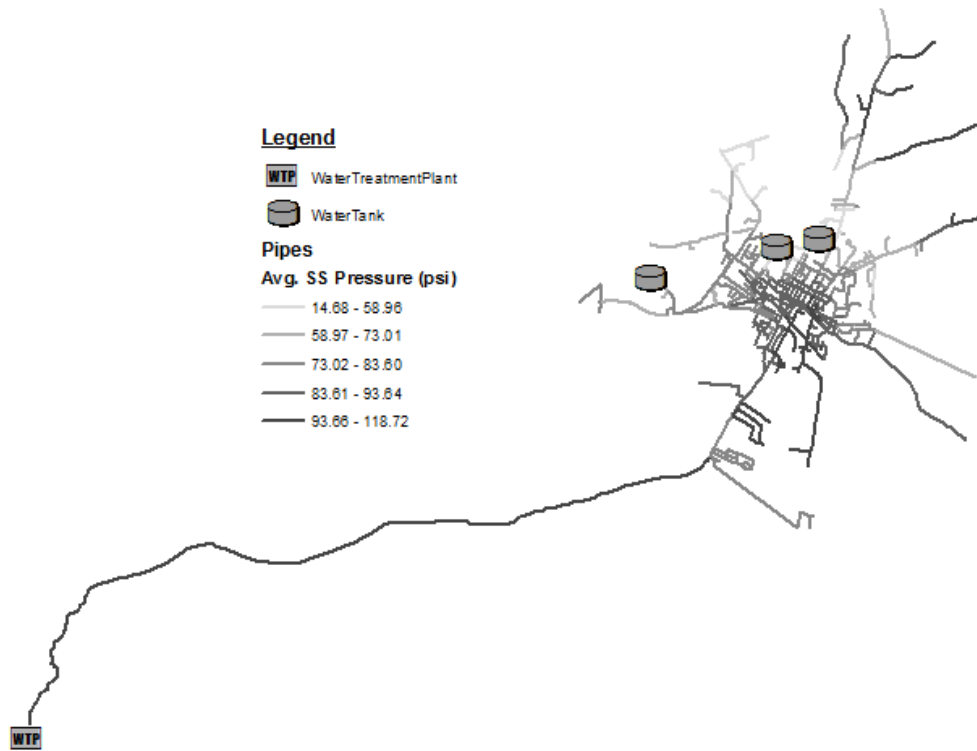
Figure C.43: Average Steady-State Pressure for KY7.
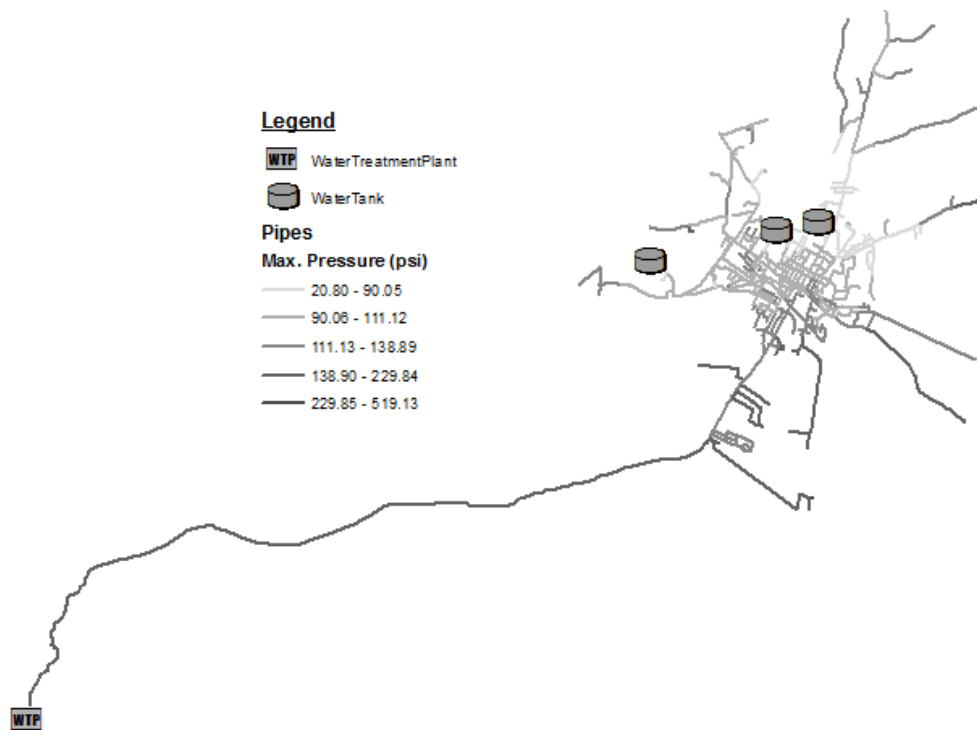
Figure C.44: Maximum Pressure for KY7.

155
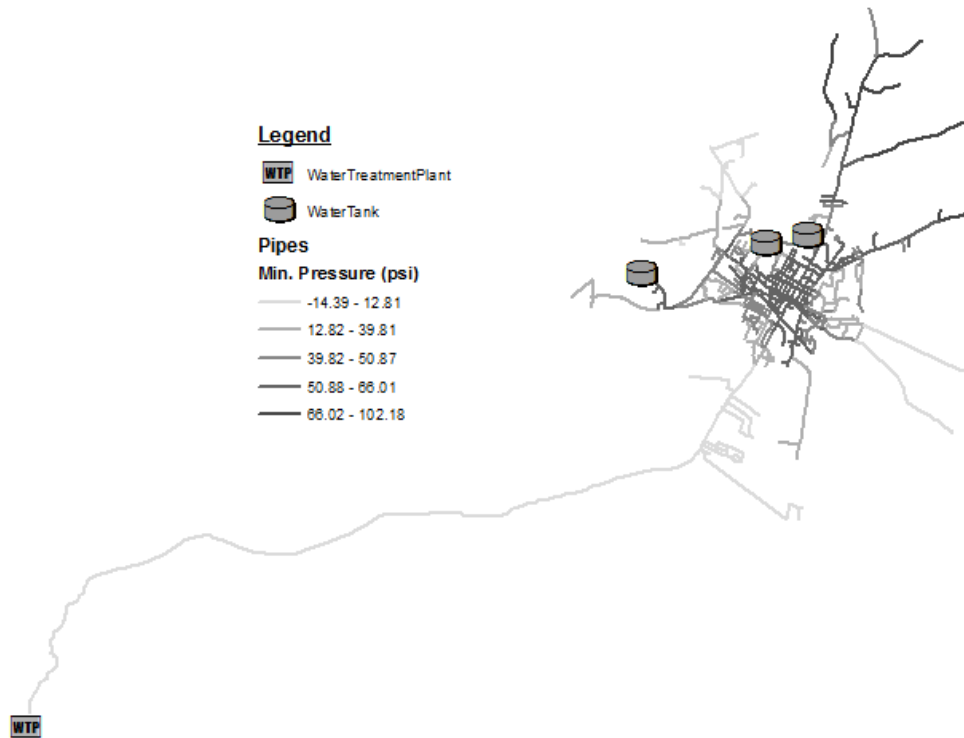
Figure C.45: Minimum Pressure for KY7.
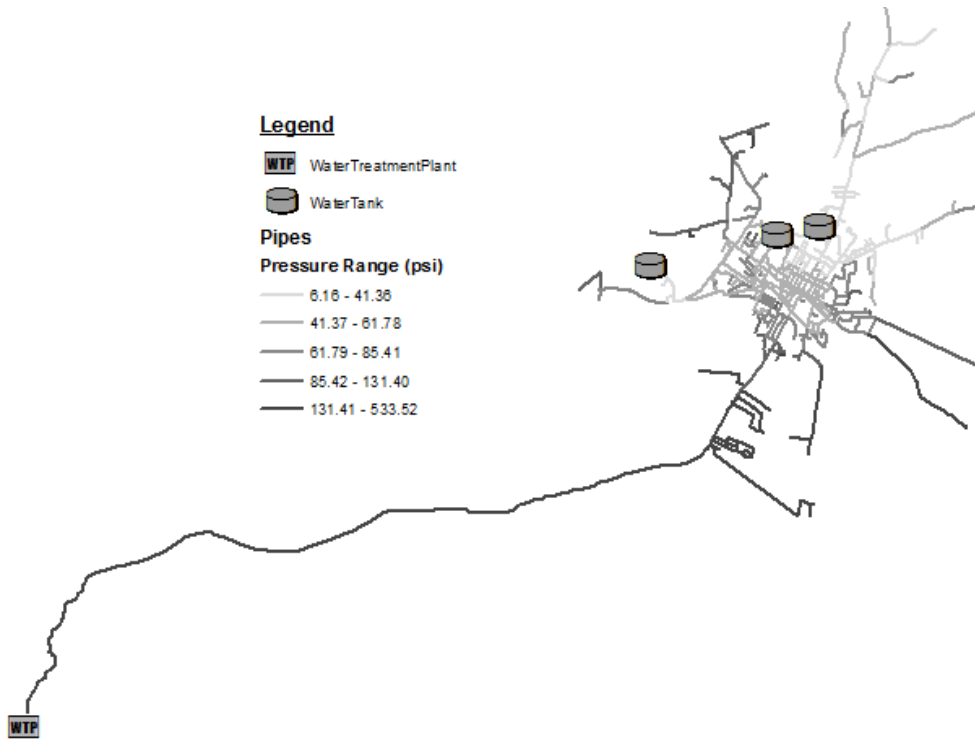
Figure C.46: Transient Pressure Range for KY7.
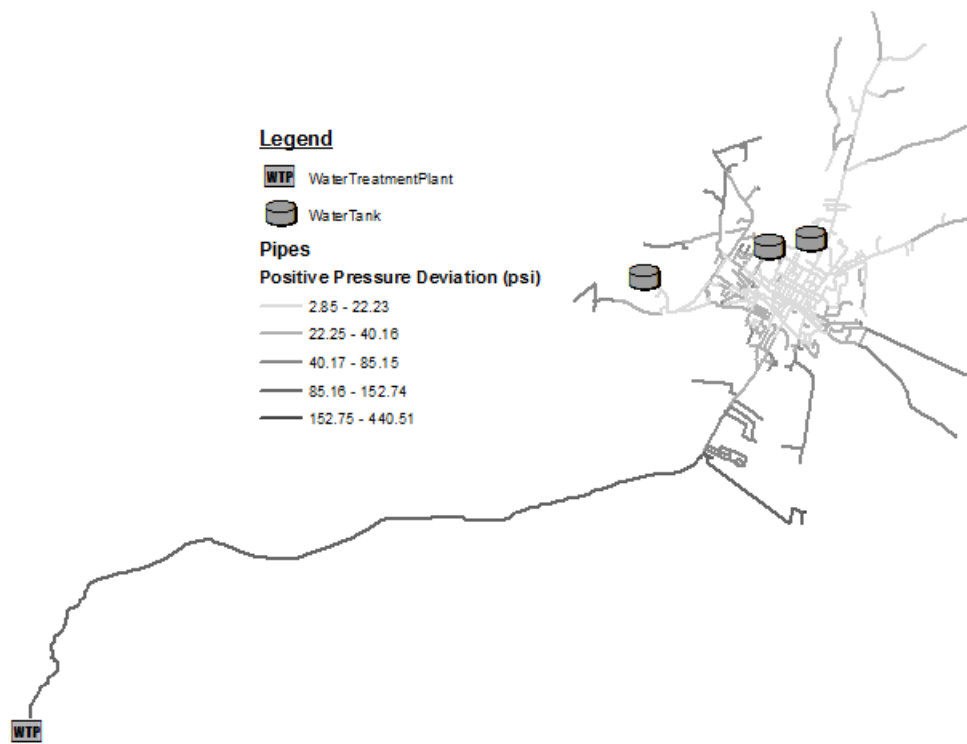
Figure C.47: Positive Pressure Deviation for KY7.
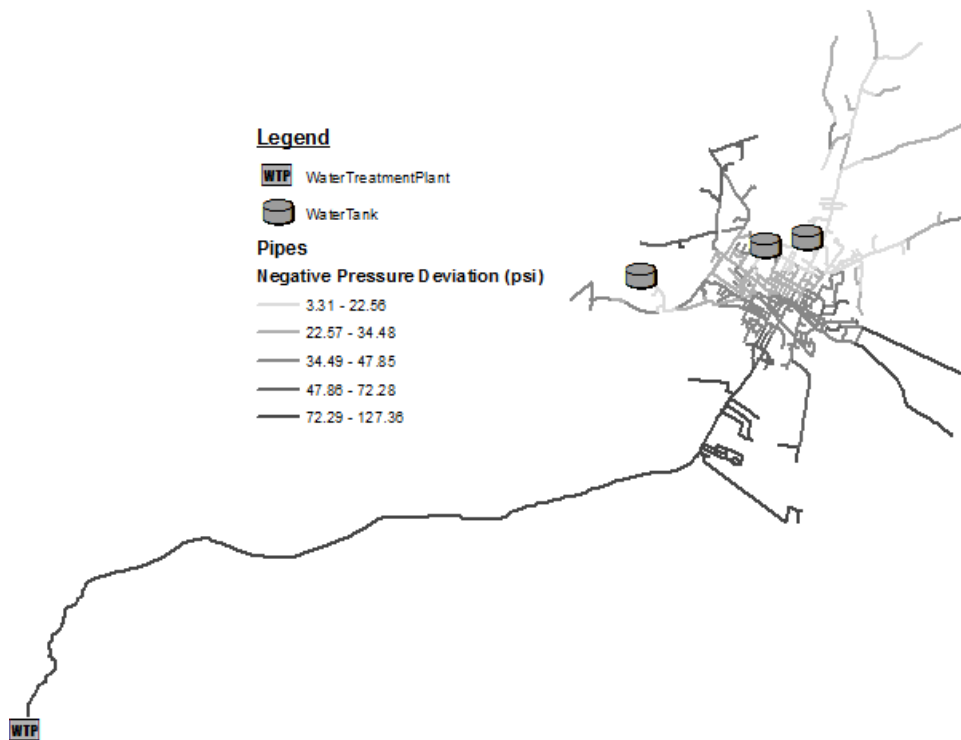
Figure C.48: Negative Pressure Deviation for KY7.
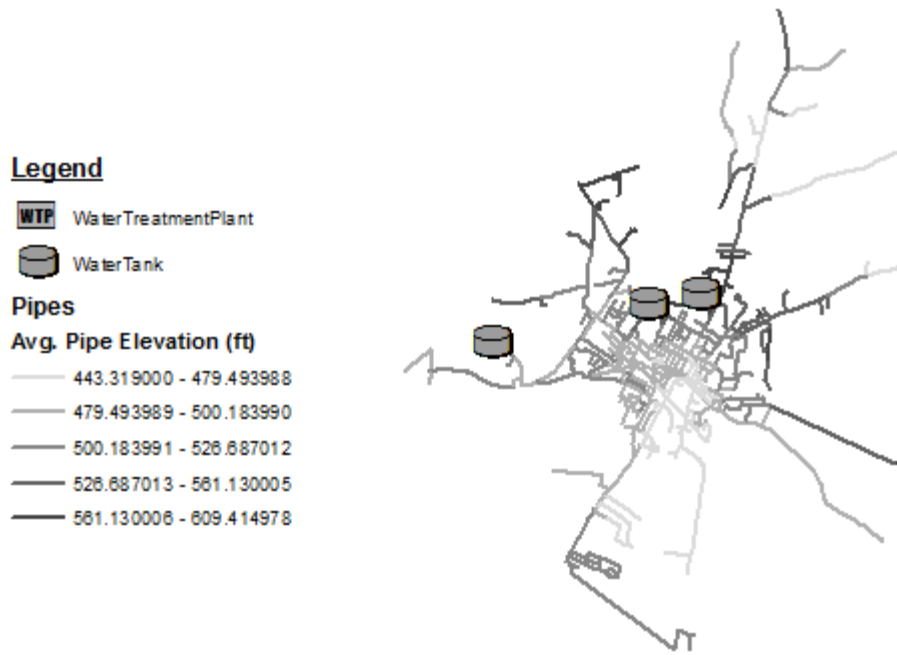
Figure C.49: Average Pipe Elevation for KY7.
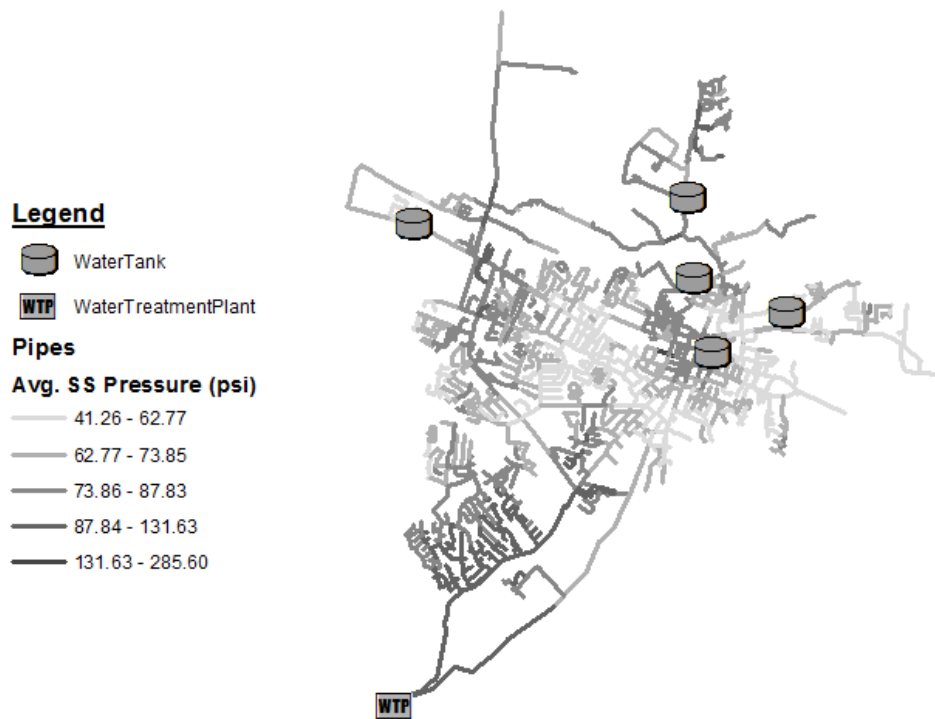
Figure C.50: Average Steady-State Pressure for KY8.

158

Figure C.51: Maximum Pressure for KY8.

Figure C.52: Minimum Pressure for KY8.

159
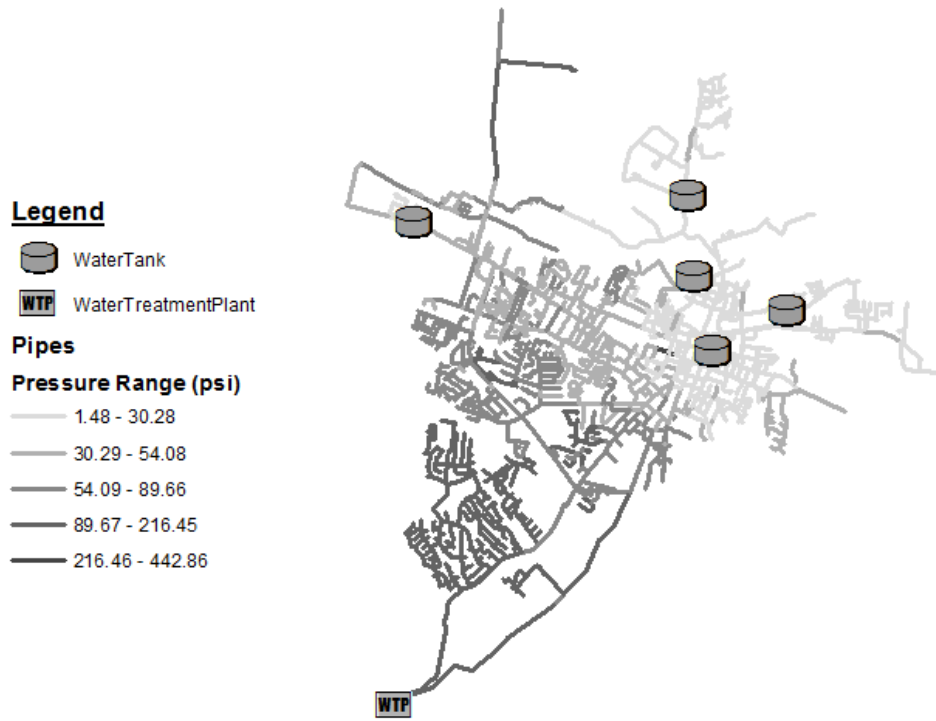
Figure C.53: Transient Pressure Range for KY8.
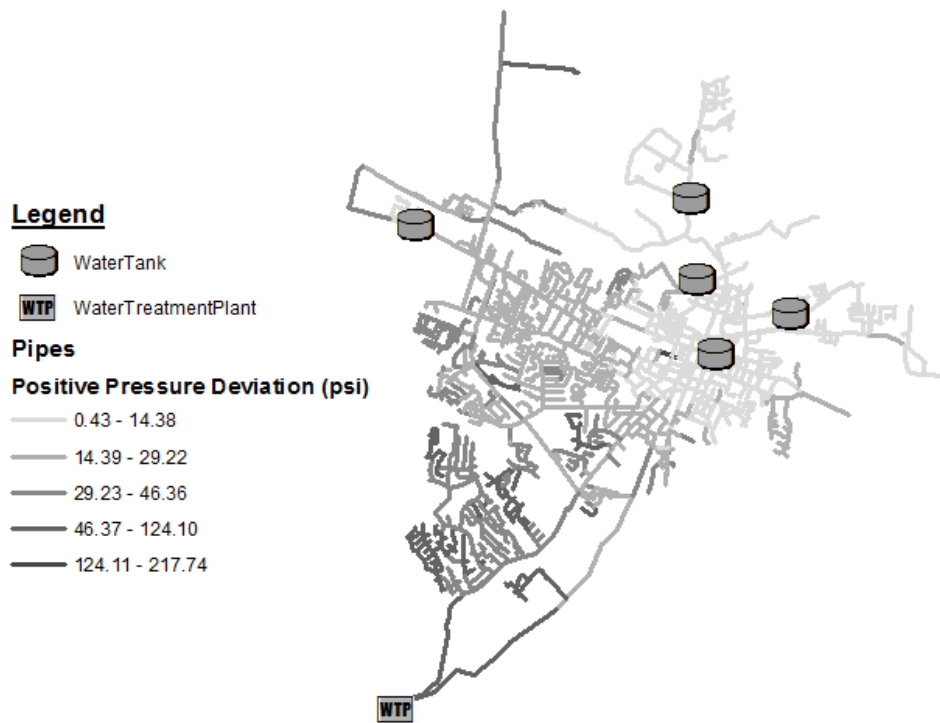
Figure C.54: Positive Pressure Deviation for KY8.

160
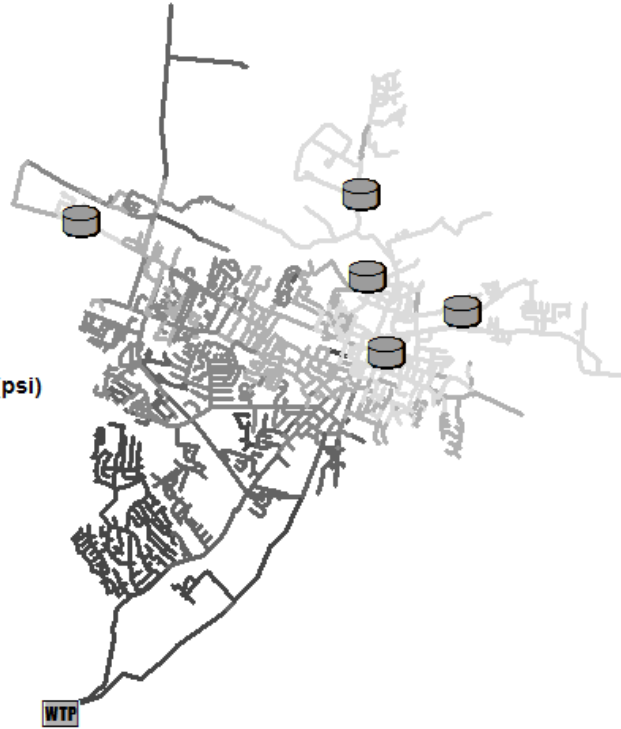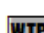
Figure C.55: Negative Pressure Deviation for KY8.

Figure C.56: Average Pipe Elevation for KY8.

161
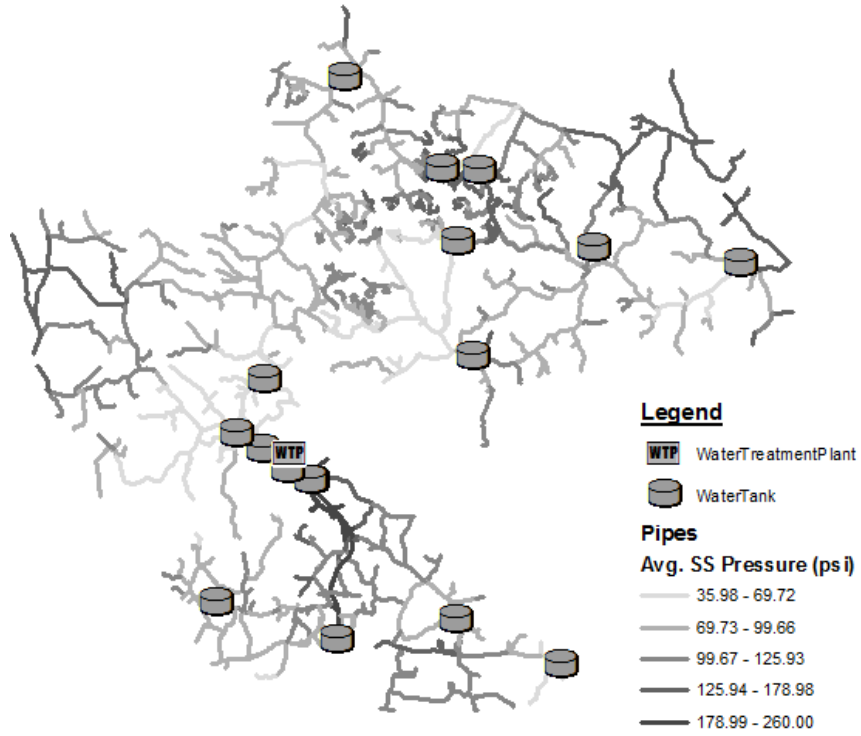
Figure C.57: Average Steady-State Pressure for KY9.
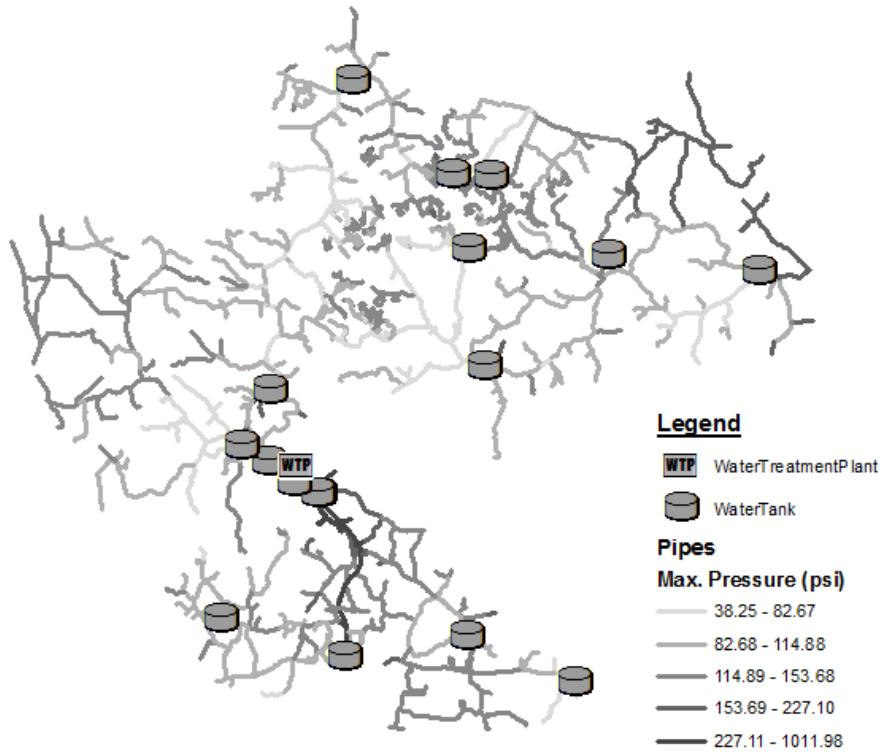
Figure C.58: Maximum Pressure for KY9.

162
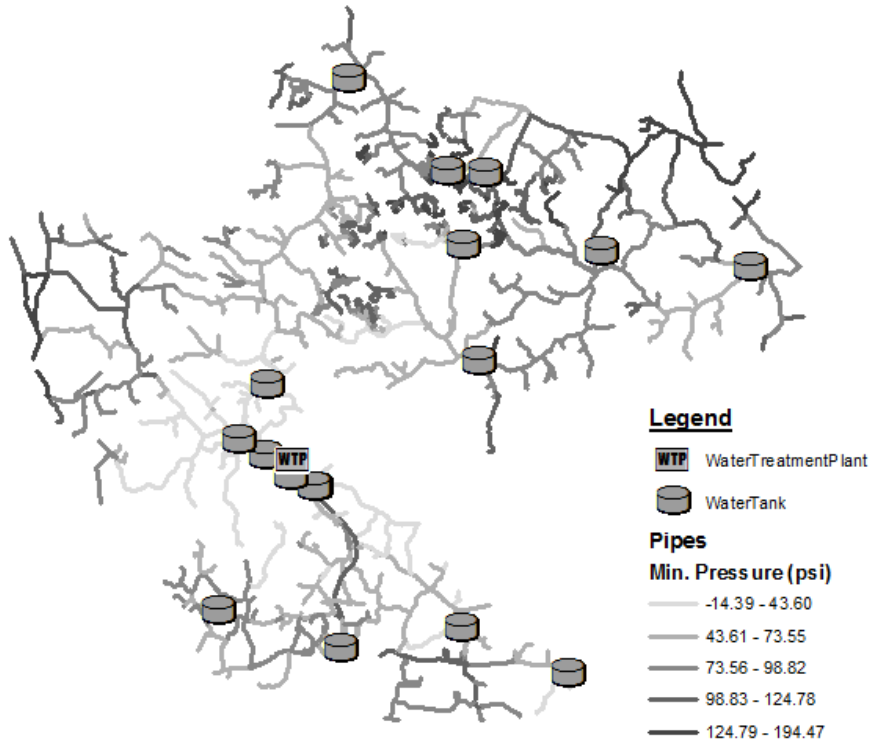
Figure C.59: Minimum Pressure for KY9.
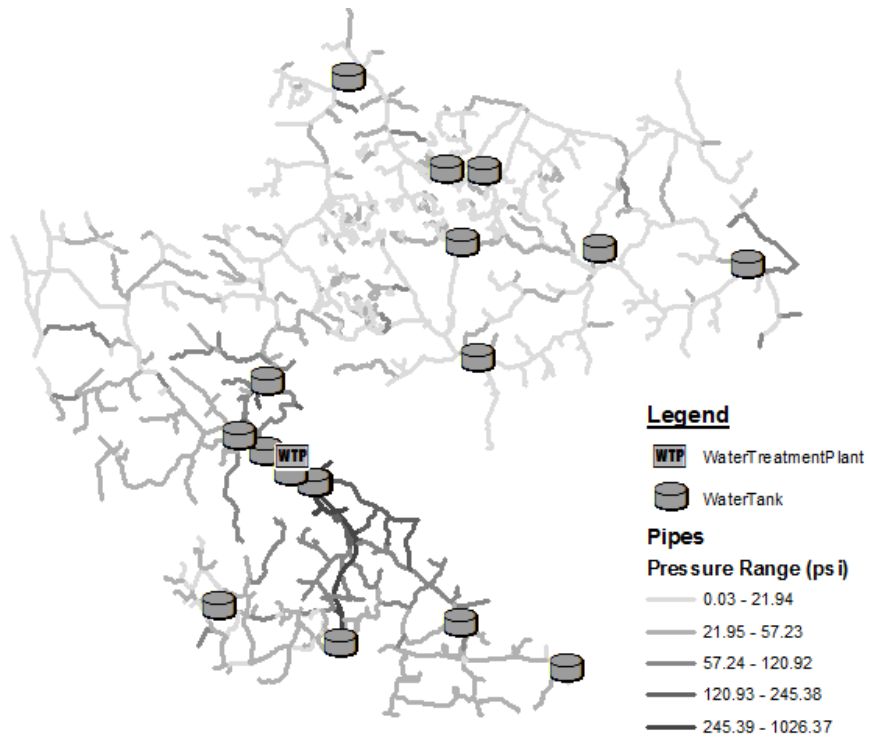
Figure C.60: Transient Pressure Range for KY9.
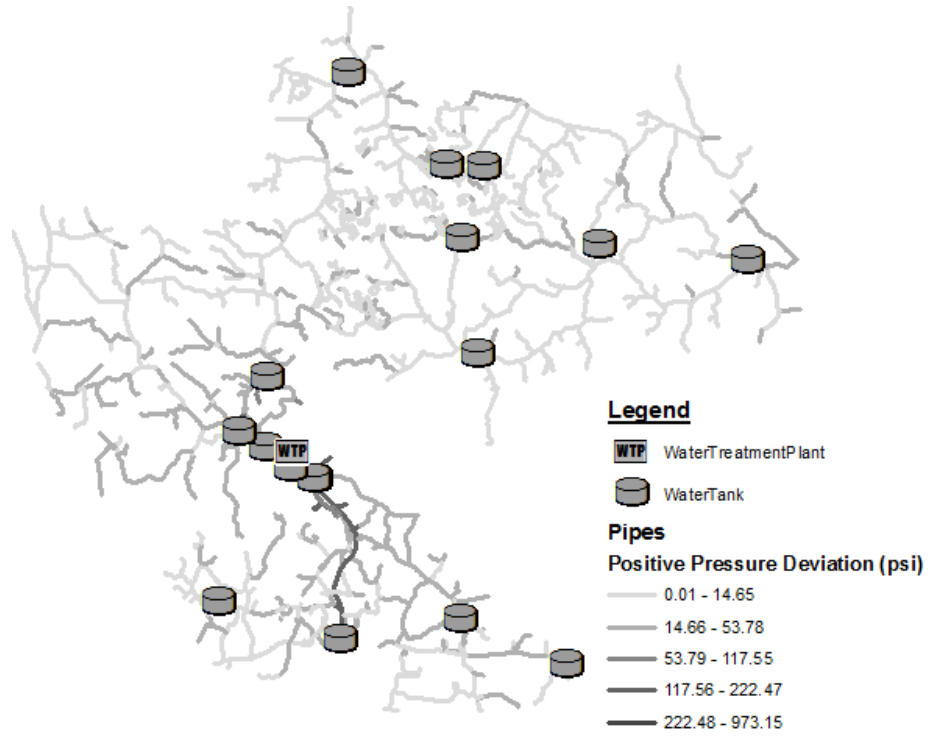
Figure C.61: Positive Pressure Deviation for KY9.
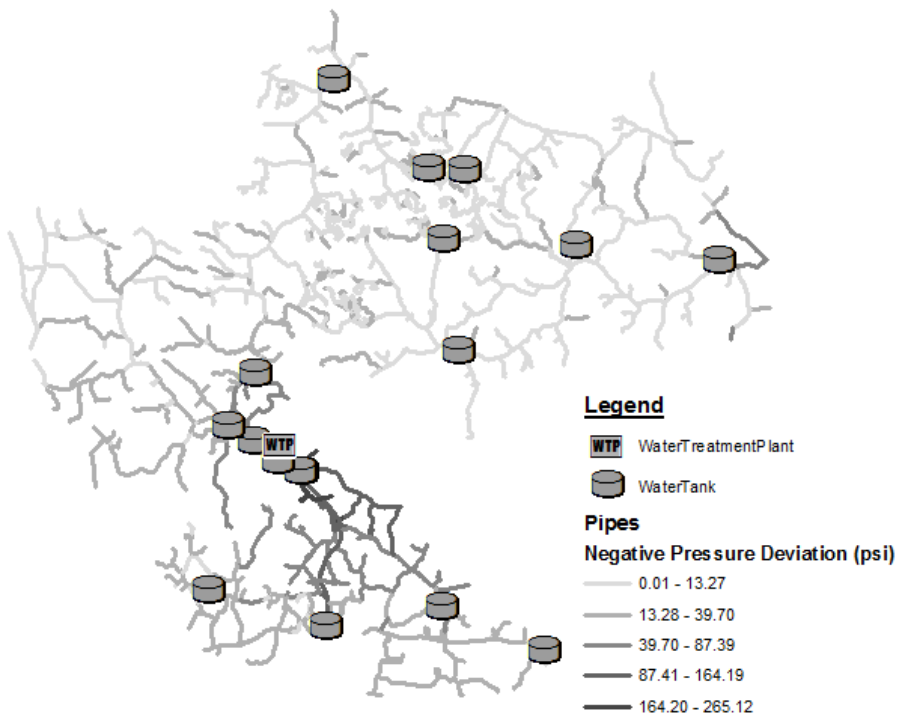
Figure C.62: Negative Pressure Deviation for KY9.

164
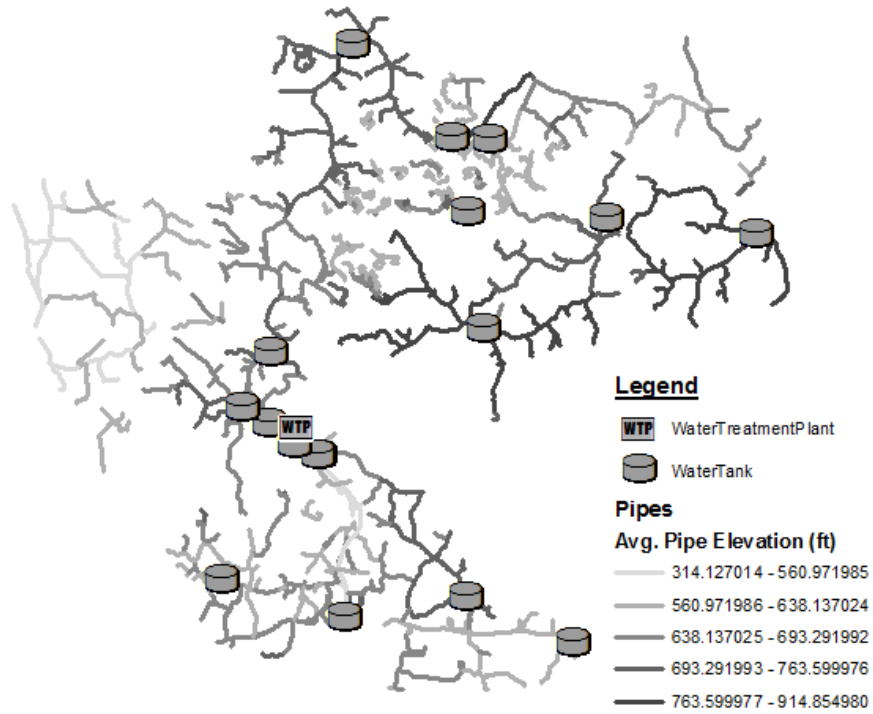
Figure C.63: Average Pipe Elevation for KY9.
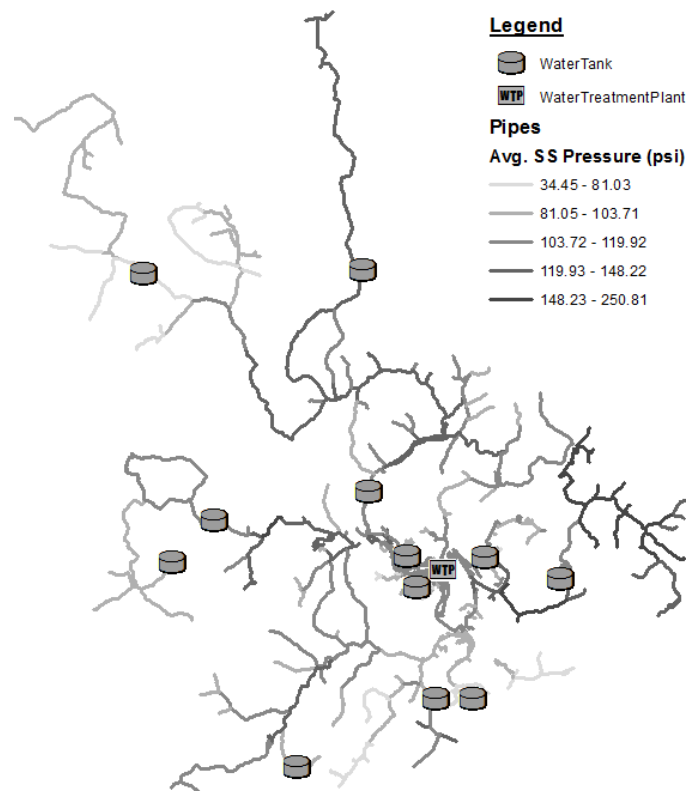
Figure C.64: Average Steady-State Pressure for KY10.
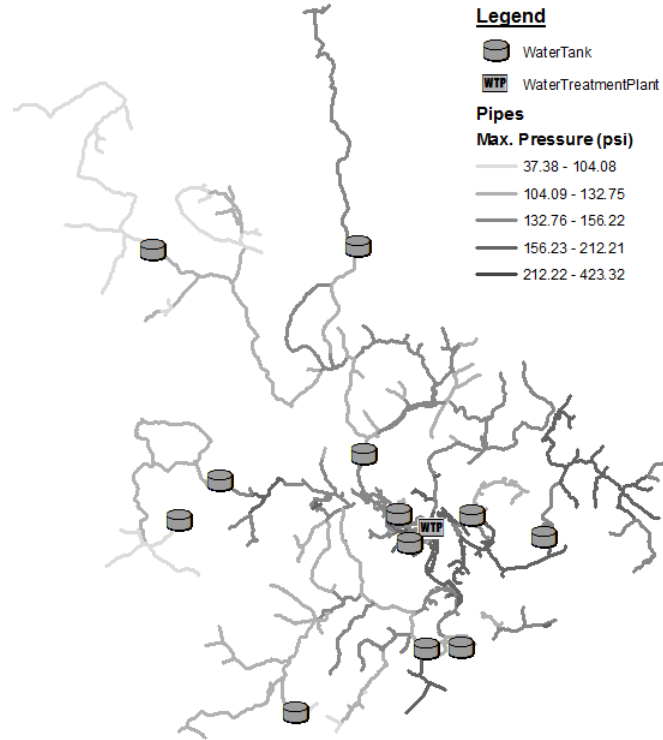
Figure C.65: Maximum Pressure for KY10.
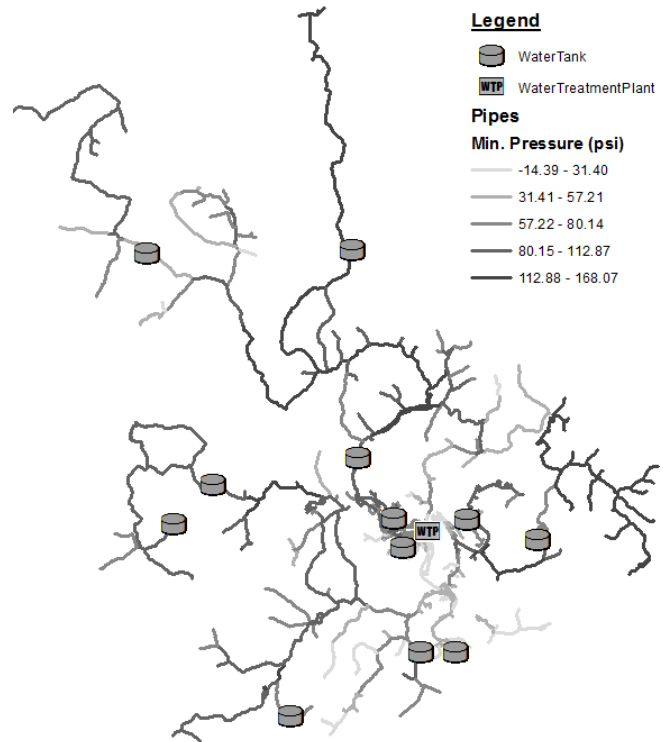
Figure C.66: Minimum Pressure for KY10.

166
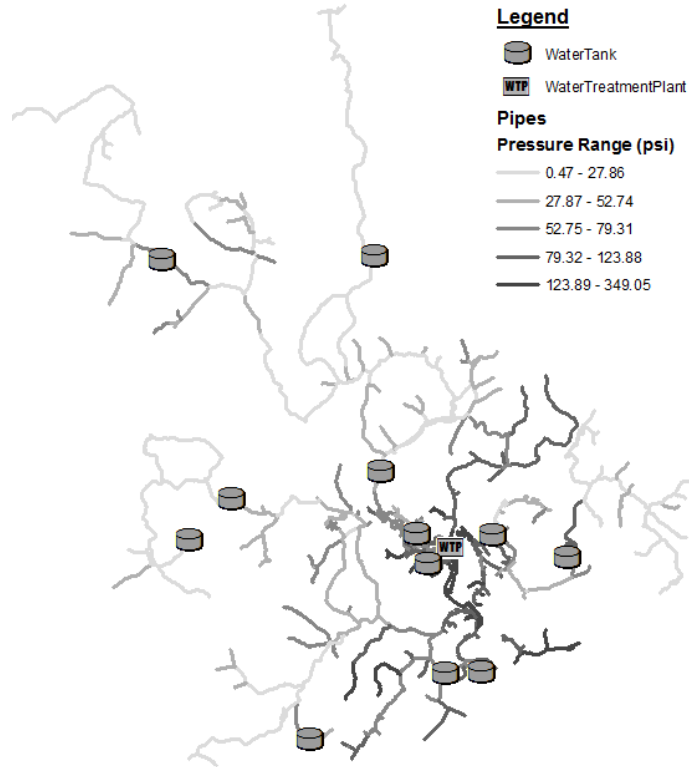
Figure C.67: Transient Pressure Range for KY10.
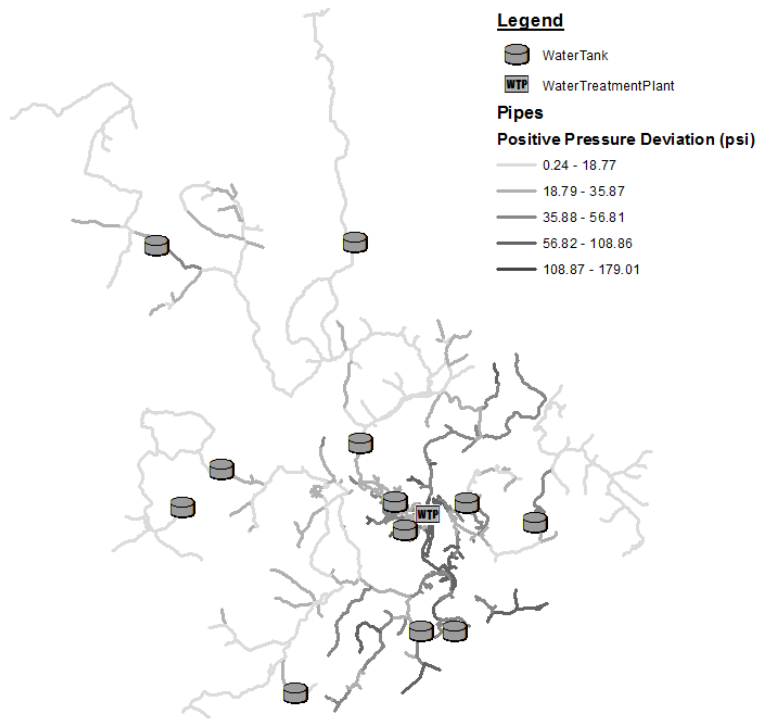
Figure C.68: Positive Pressure Deviation for KY10.
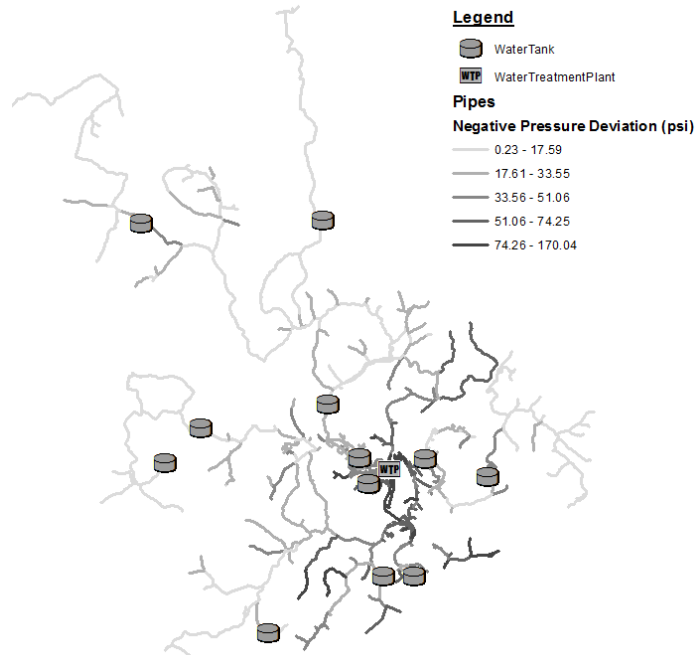
Figure C.69: Negative Pressure Deviation for KY10.
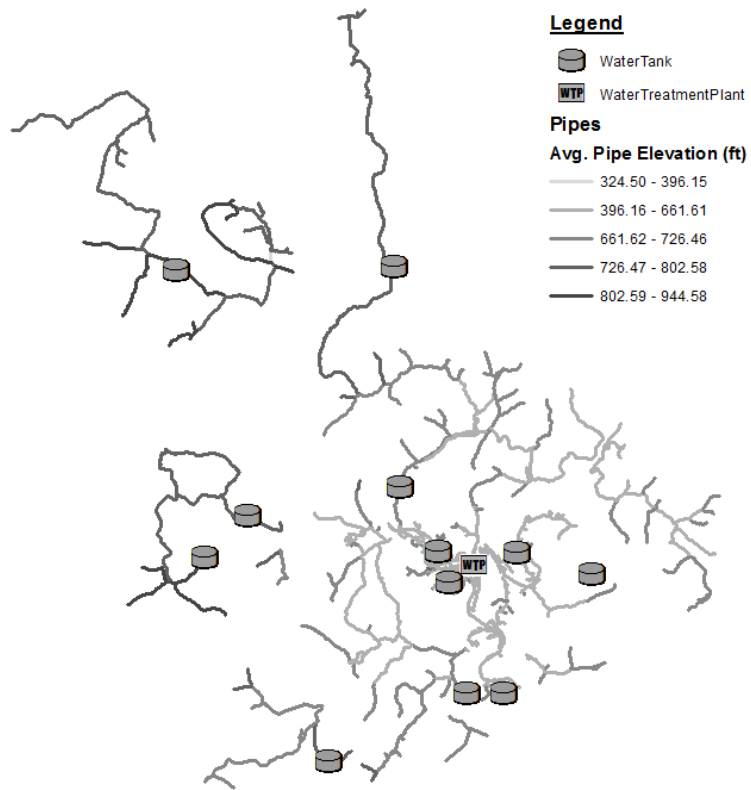
Figure C.70: Average Pipe Elevation for KY10.

168
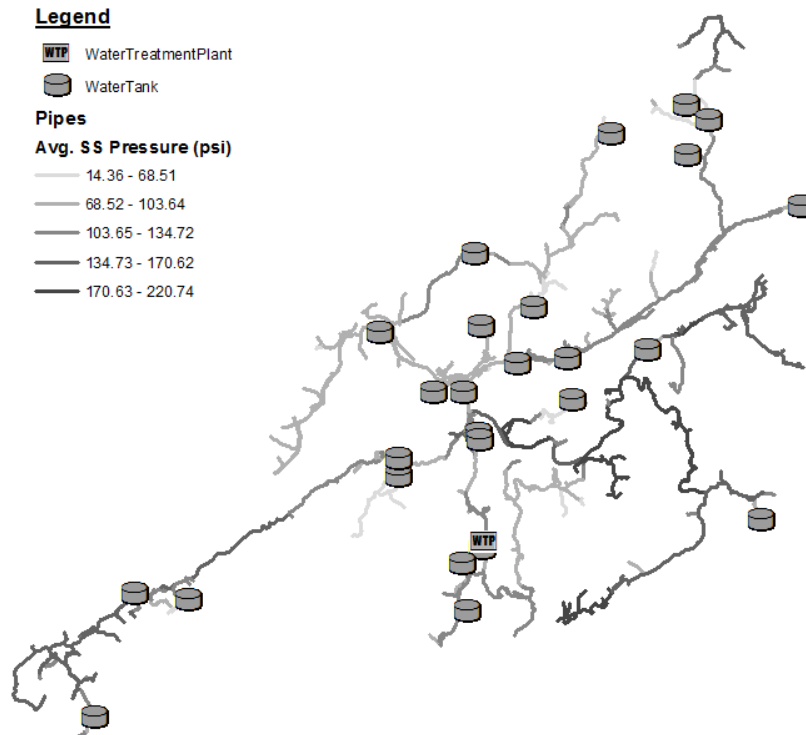
Figure C.71: Average Steady-State Pressure for KY11.
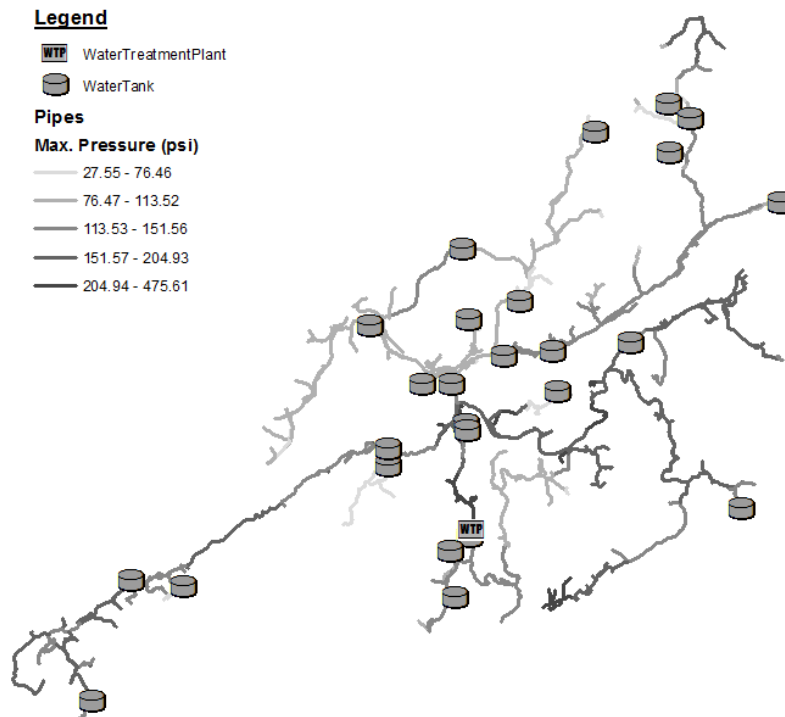
Figure C.72: Maximum Pressure for KY11.

169
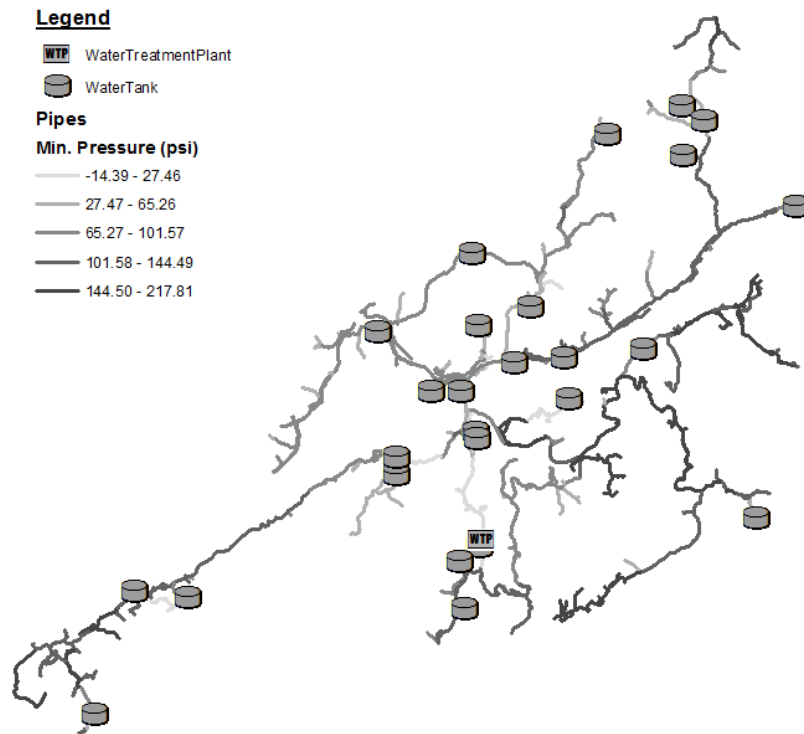
Figure C.73: Minimum Pressure for KY11.
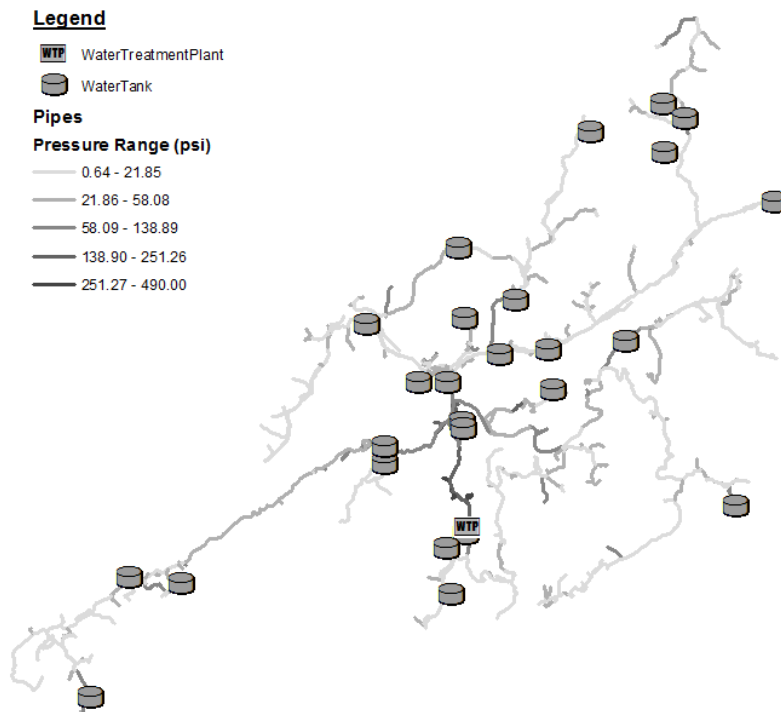
Figure C.74: Transient Pressure Range for KY11.
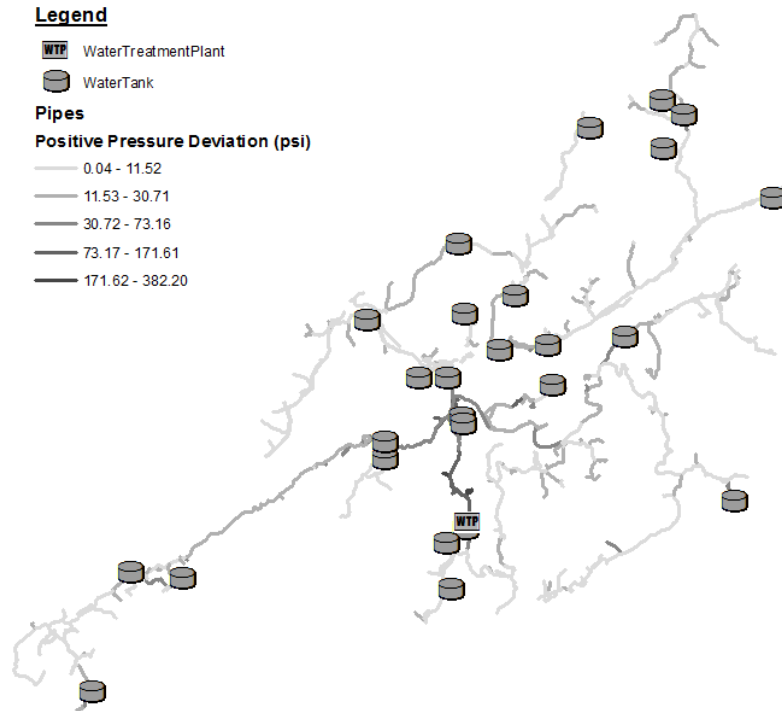
Figure C.75: Positive Pressure Deviation for KY11.
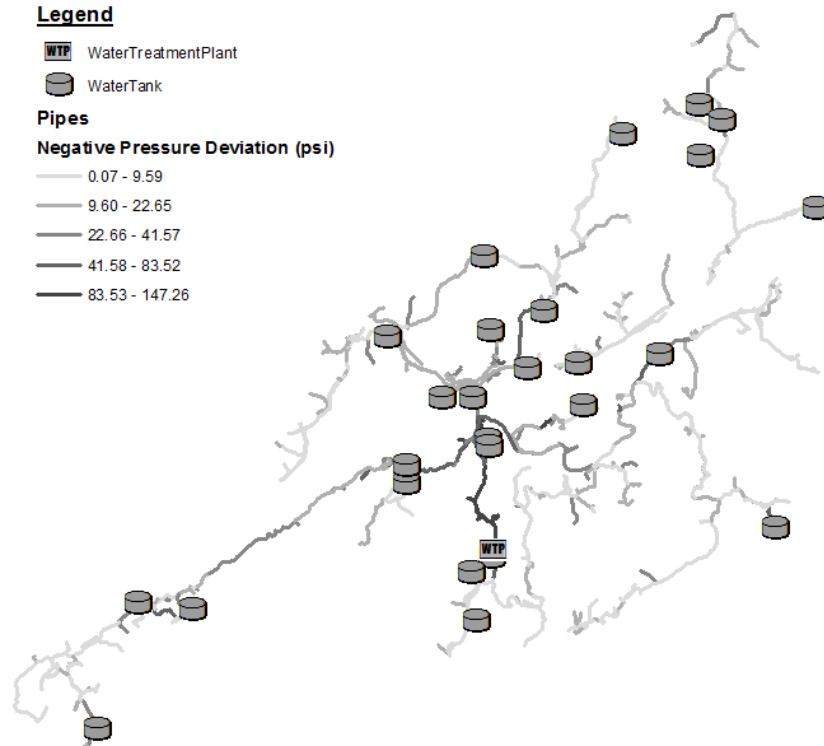
Figure C.76: Negative Pressure Deviation for KY11.
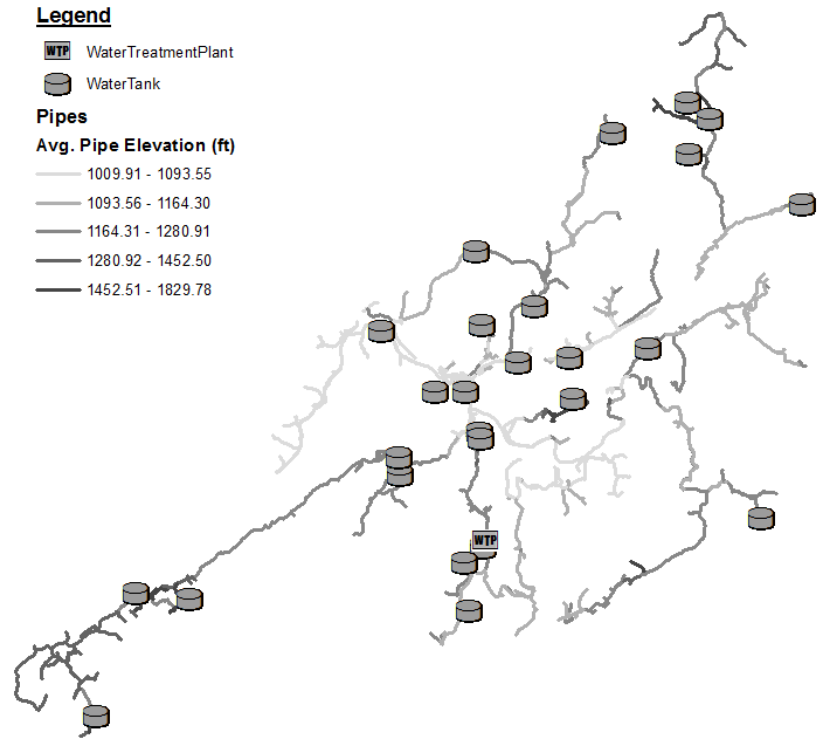
Figure C.77: Average Pipe Elevation for KY11.
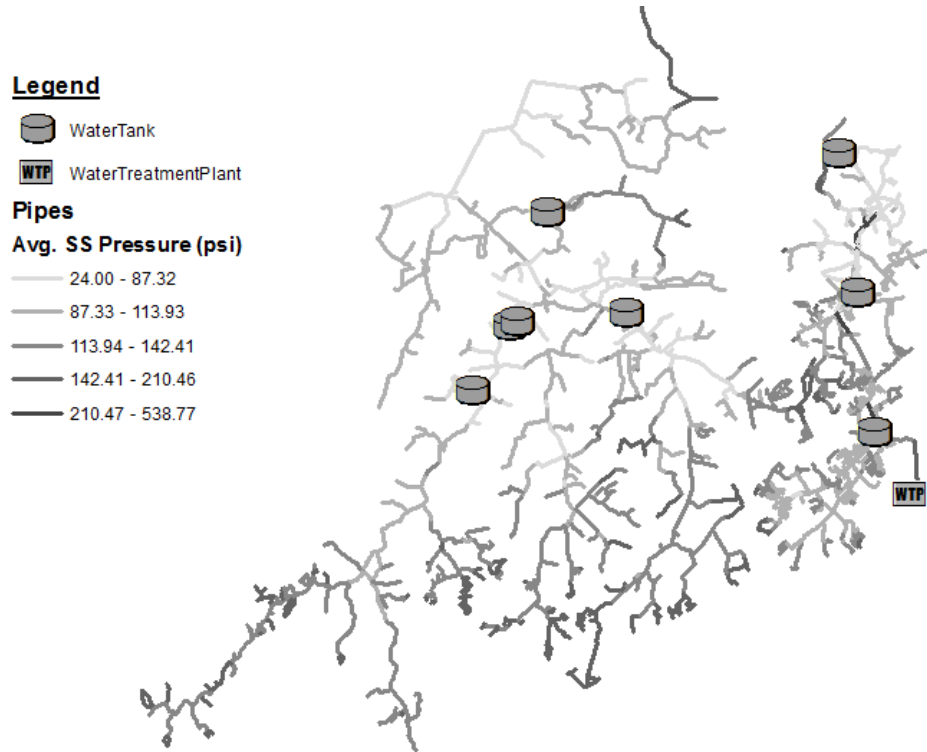
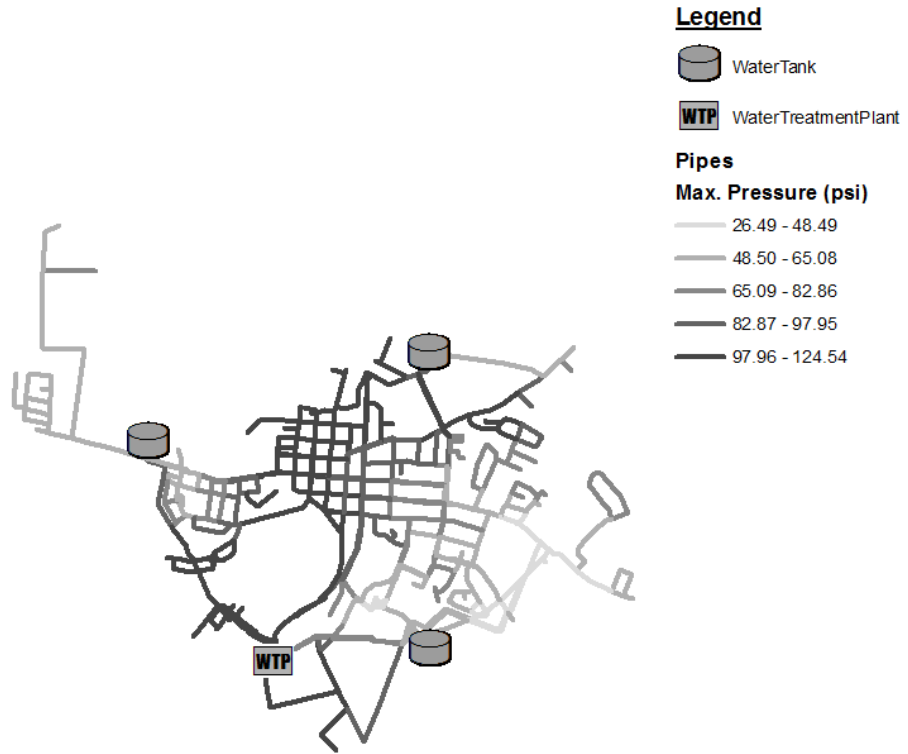Figure C.78: Average Steady-State Pressure for KY12.
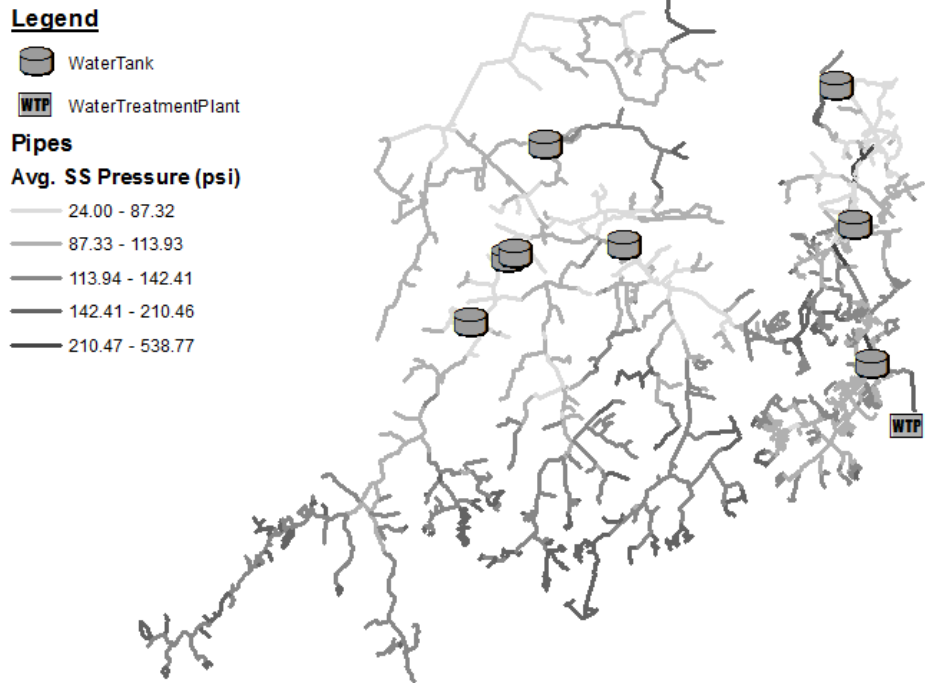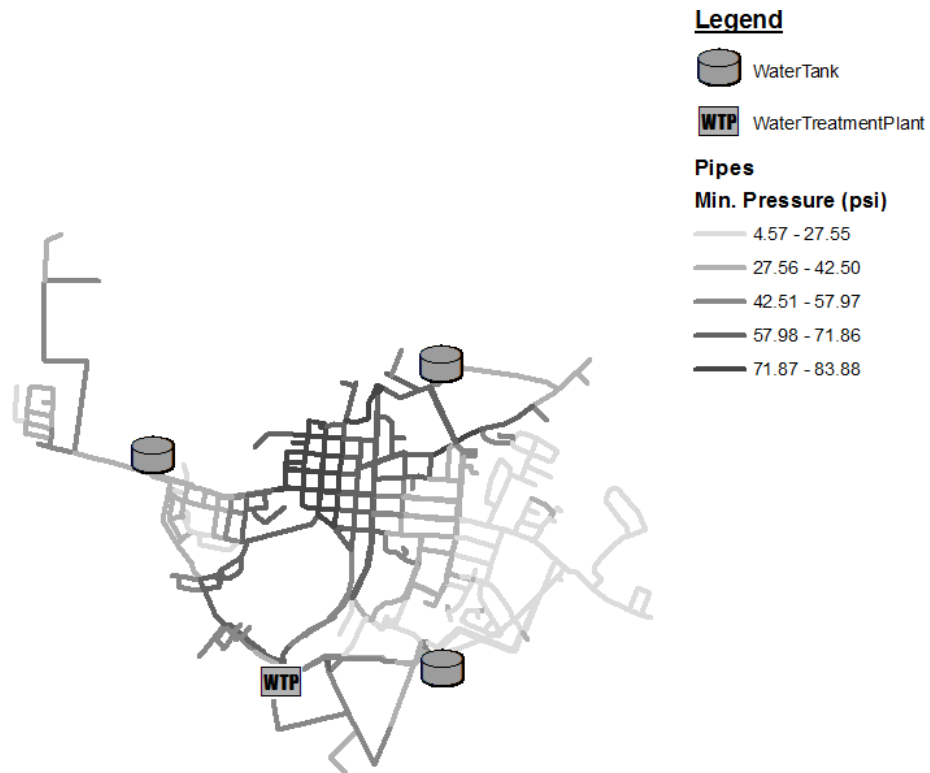
Figure C.79: Maximum Pressure for KY12.
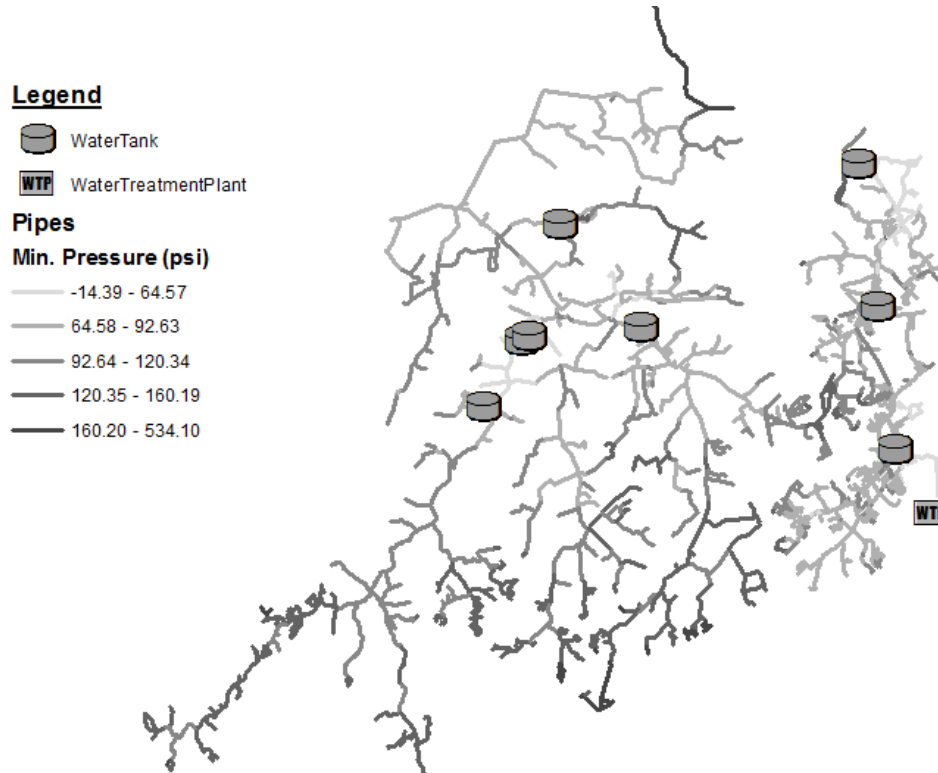
Figure C.80: Minimum Pressure for KY12.
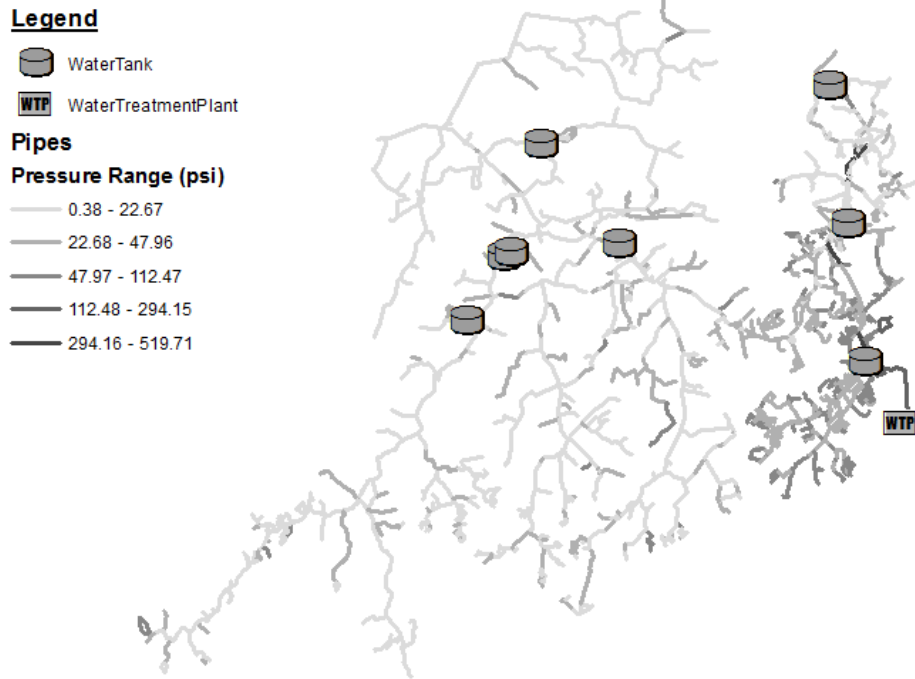
Figure C.81: Transient Pressure Range for KY12.
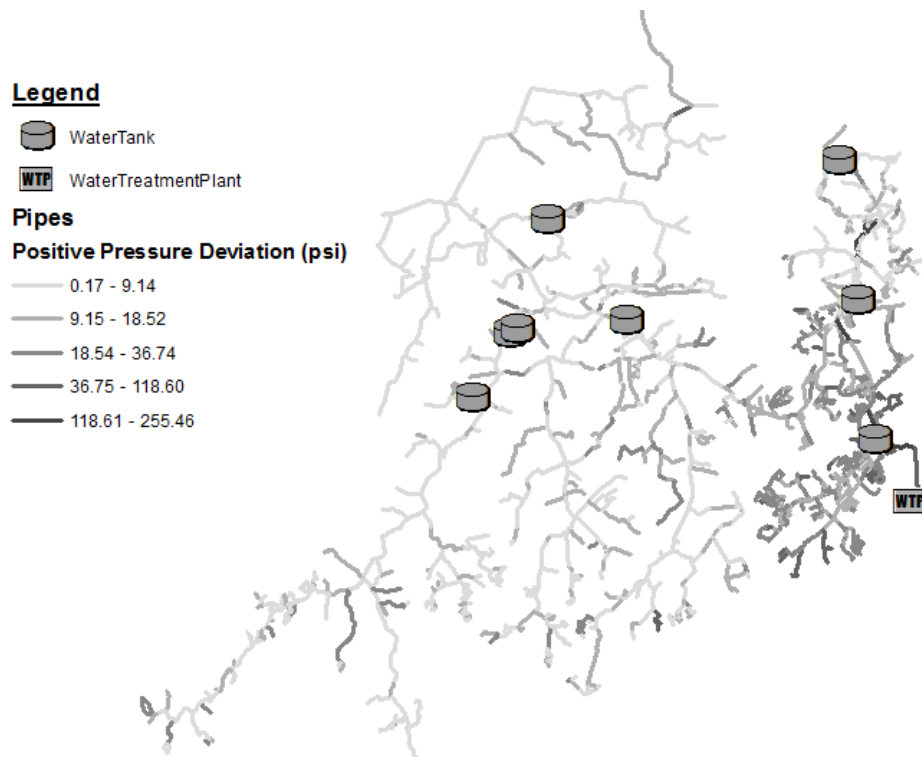
Figure C.82: Positive Pressure Deviation for KY12.

174
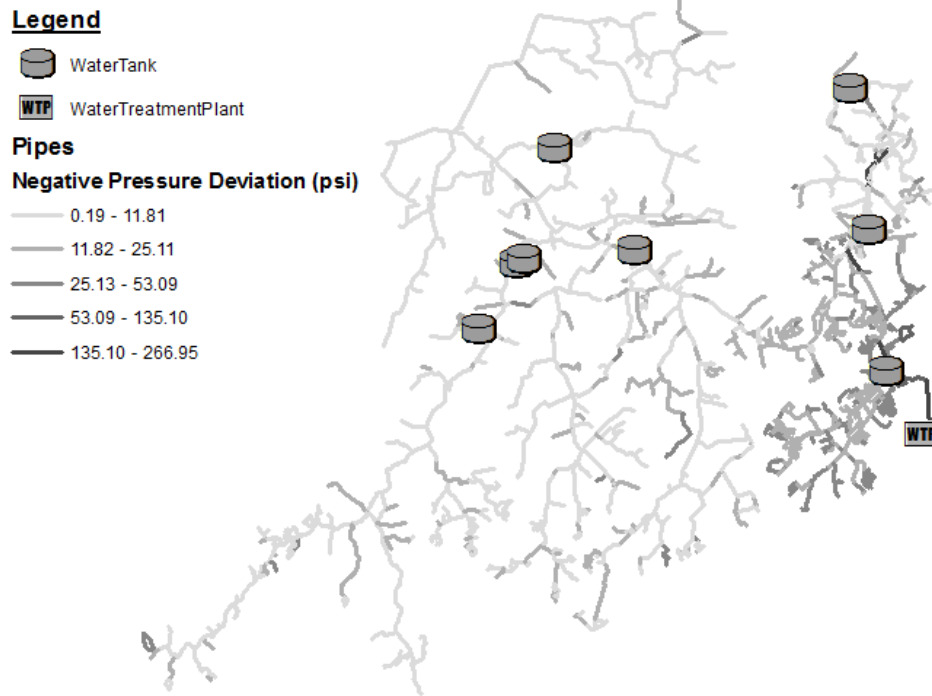
Figure C.83: Negative Pressure Deviation for KY12.
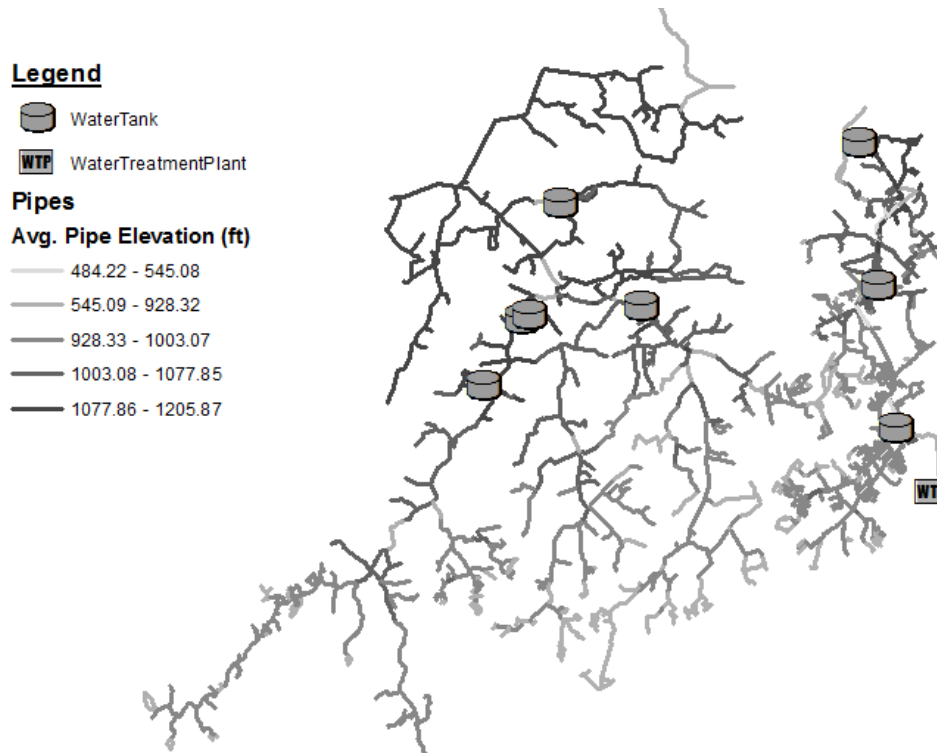
Figure C.84: Average Pipe Elevation for KY12.

Figure C.85: Average Steady-State Pressure for KY13.

Figure C.86: Maximum Pressure for KY13.

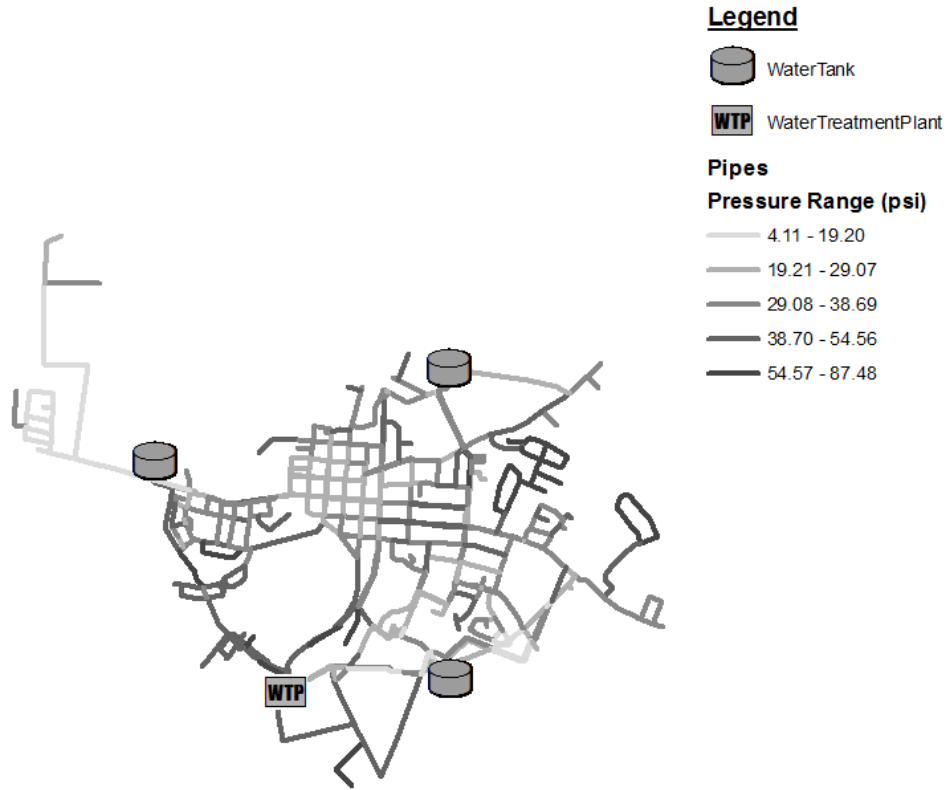Figure C.87: Minimum Pressure for KY13.

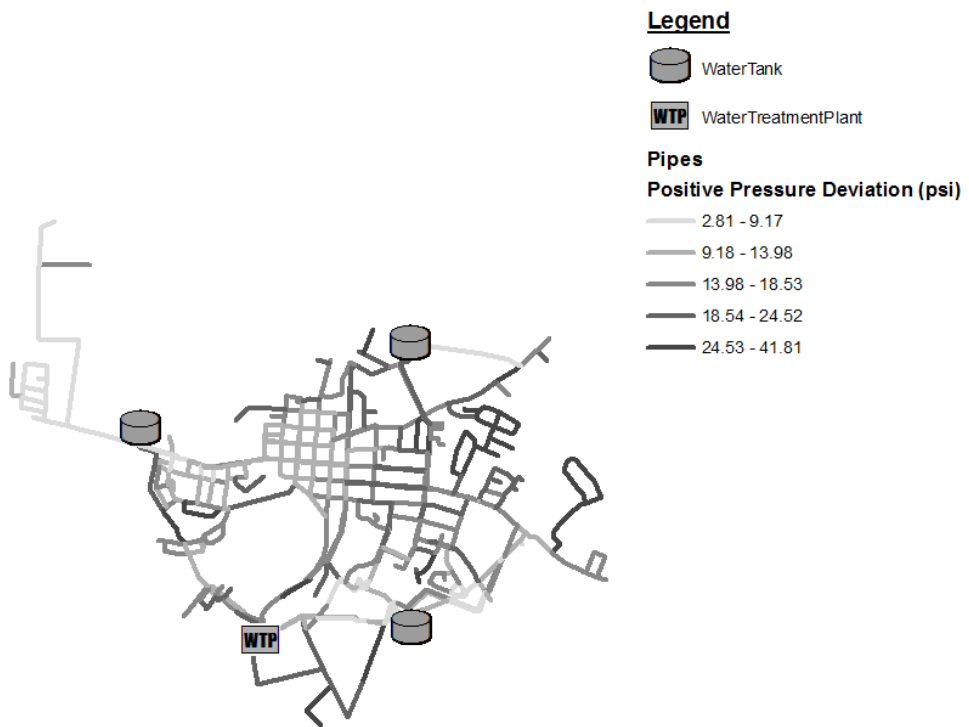Figure C.88: Transient Pressure Range for KY13.

Figure C.89: Positive Pressure Deviation for KY13.

Figure C.90: Negative Pressure Deviation for KY13.

Figure C.91: Average Pipe Elevation for KY13.

Figure C.92: Average Steady-State Pressure for KY14.

179

Figure C.93: Maximum Pressure for KY14.

Figure C.94: Minimum Pressure for KY14.

Figure C.95: Transient Pressure Range for KY14.

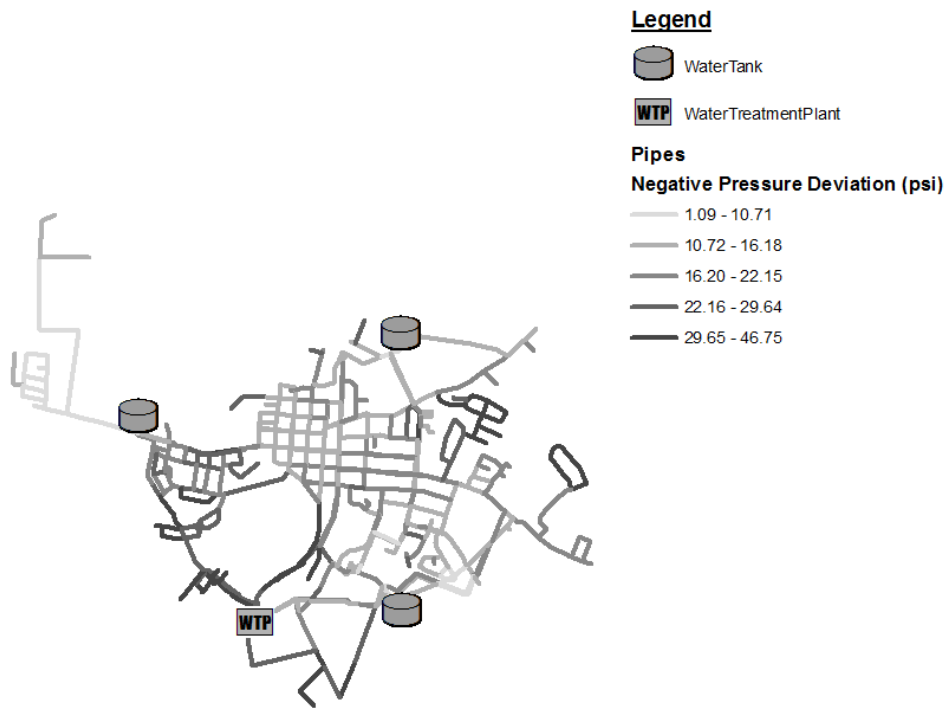Figure C.96: Positive Pressure Deviation for KY14.

Figure C.97: Negative Pressure Deviation for KY14.

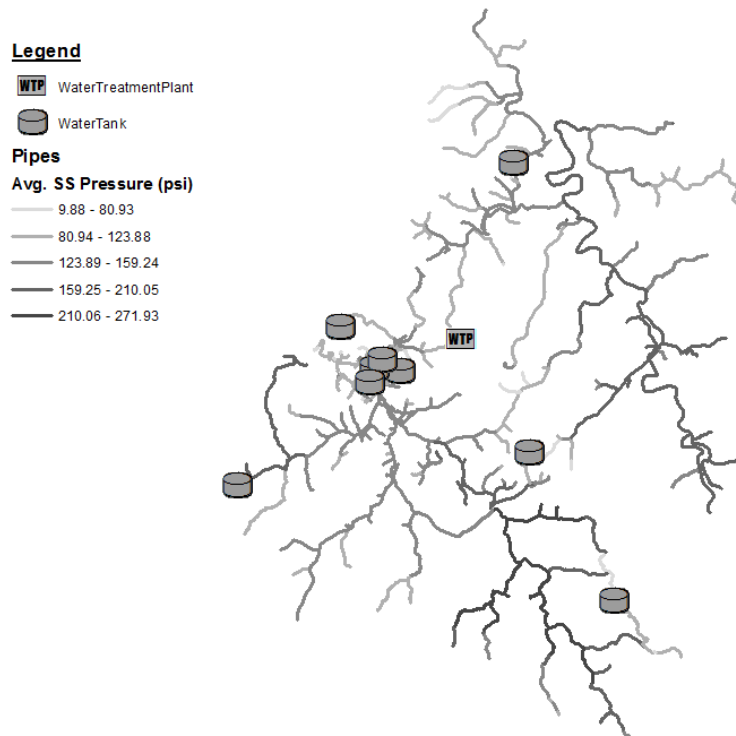Figure C.98: Average Pipe Elevation for KY14.

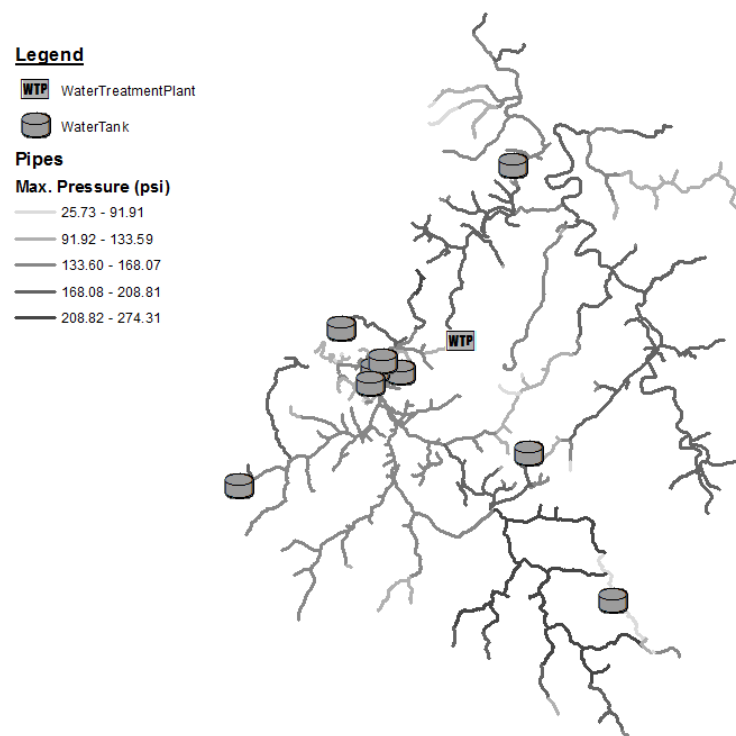Figure C.99: Average Steady-State Pressure for KY15.

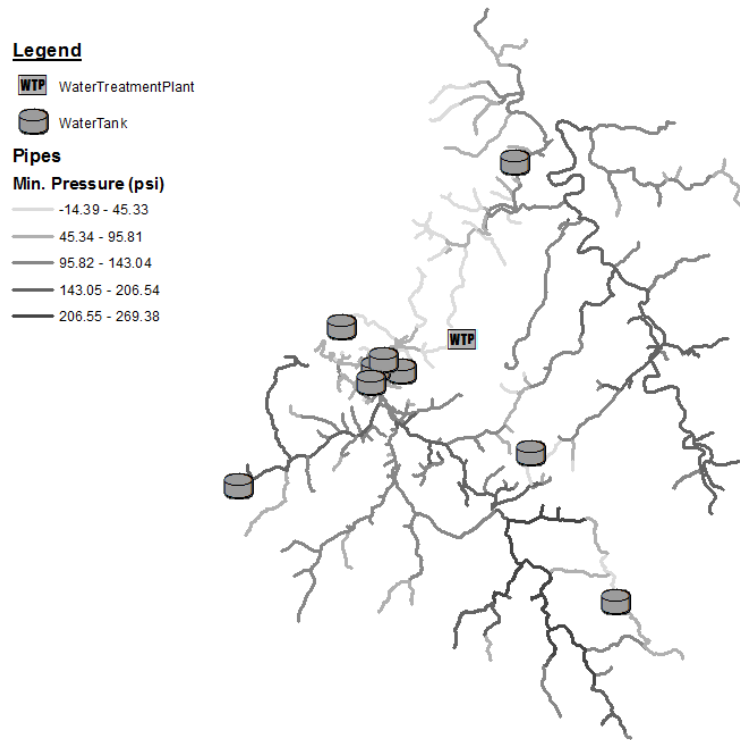Figure C.100: Maximum Pressure for KY15.

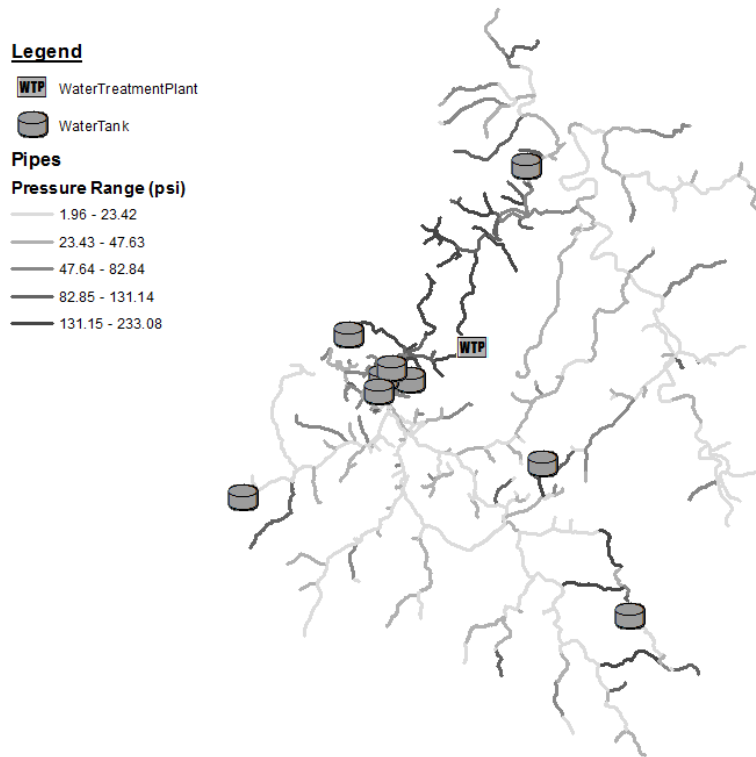Figure C.101: Minimum Pressure for KY15.
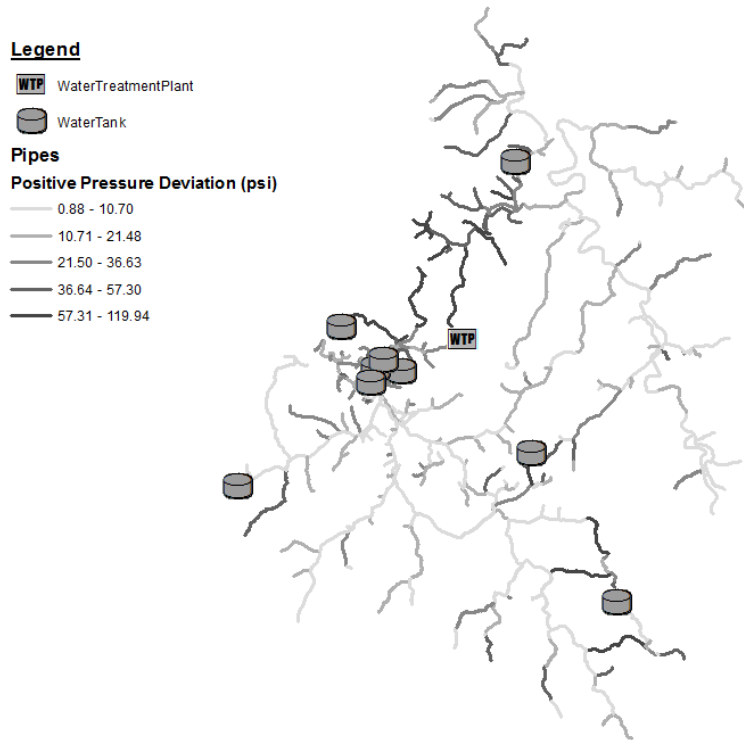

Figure C.102: Transient Pressure Range for KY15.
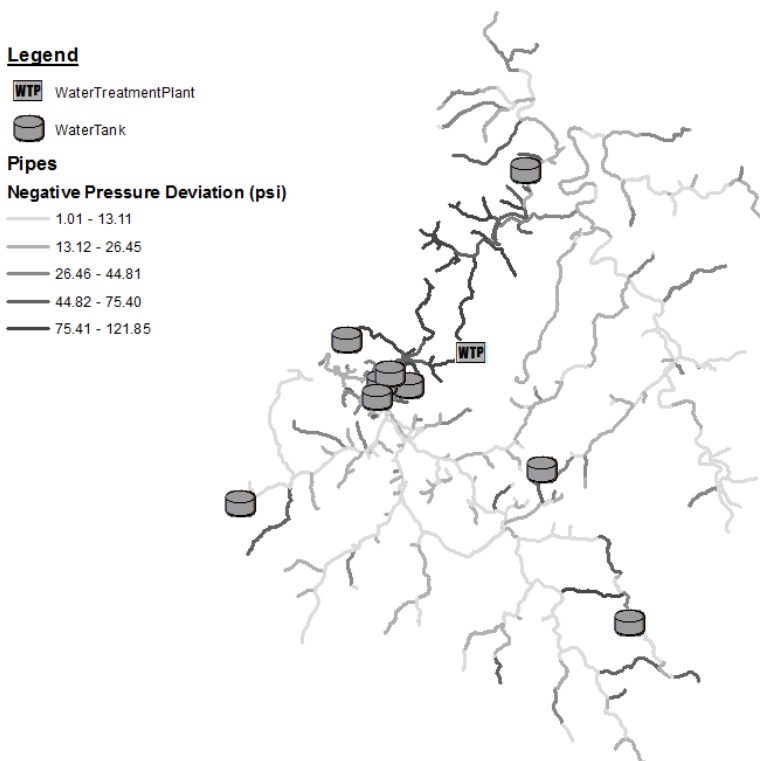
184

Figure C.103: Positive Pressure Deviation for KY15.

Figure C.104: Negative Pressure Deviation for KY15.

185
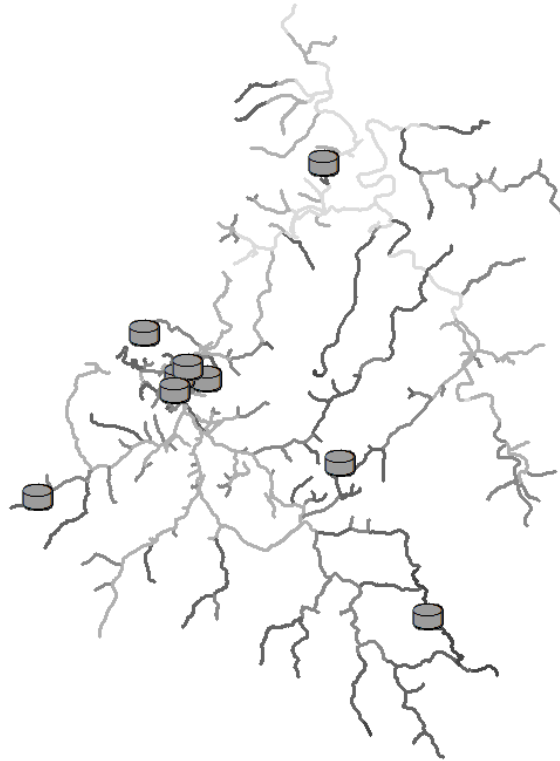
Figure C.105: Average Pipe Elevation for KY15.

REFERENCES

Achim, D., Ghotb, F., and McManus, K.J. (2007). "Prediction of Water Pipe Asset Life Using Artificial Neural Networks." J. Infrastructure Systems, March 2007.

Arulraj, G. P., and Suresh, H. R. (1995). "Concept of significance index for maintenance and design of pipe networks." J. Hydraul. Eng., 121 11, 833–837.

AWWA. (2012). Computer Modeling of Water Distribution Systems. Manual of Water Supply Practices- M32. Denver: American Water Works Association.

Boulos, P.F., Karney, B.W., Wood, D.J., and Lingireddy, S., (2005). Hydraulic Transient Guidelines for Protecting Water Distribution Systems. Journal AWWA, May 2005.

Boxall, J., O'Hagan, A., Pooladsaz, S., Saul, A., and Unwin, D. (2007). "Estimation of burst rates in water distribution mains." Proc. ICE Water Manage., 160(2), 73–82.

Brock (2014). Data: Explore 15 Years of Power Outages. http://insideenergy.org/2014/08/18/data-explore-15-years-of-power-outages/

Burn, L. S., Tucker, S. N., Rahilly, M., Davis, P., Jarrett, R., and Po, M. (2003). "Asset planning for water reticulation systems: The PARMS model." Water Sci. Technol., 3(1), 55–62.

Creaco, E., Franchini, M., and Walski, T. (2013). "Accounting for phasing of construction within the design of water distribution networks." J. Water Resour. Plann. Manage., 10.1061/(ASCE)WR.1943-5452. 0000358, in press.

Ellison, D., Bell, G., Reiber, S., Spencer, D., Romer, A., Matthews, J.C., Sterling, R. and Ariaratnam, S.T. (2014). Answers to Challenging Infrastructure Management Questions. WRF Project. Denver, Colorado.

Friedman, M. C. (2003). "Verification and control of low pressure transients in distribution systems," Proc., 18th Annual ASDWA Conf., Association of State Drinking Water Administrators, Boston.

Goulter. I. C., and A. Kazemi (1988). ""Spatial and Temporal Groupings of Water Main Pipe Breakage in Winnipeg."" Canadian Journal of Civil Eng., 15(1), pp. 91-97. 1988.

Halhal, D., Walters, G. A., Ouazar, D., and Savic, D. A. (1997). "Water network rehabilitation with structured messy genetic algorithm." J. Water Resour. Plann. Manage., 123(3), 137–146.

Harvey, R., McBean, E.A., and Gharabaghi, B. (2014). Predicting the Timing of Water Main Failure Using Artificial Neural Networks. J. Water Resour. Plann. Manage., 140(4), 425-434.

Hoagland, S., Schal, S., Ormsbee, L., and Bryson, S. (2015). Classification of Water Distribution Systems for Research Applications. Proc. EWRI Congress 2015.

Jolly, M. D., Lothes, A. D., Bryson, L. S., & Ormsbee, L. (2014). Research Database of Water Distribution System Models. Journal of Water Resources Planning and Management, 410-416.

Jung, B.S., Karney, B.W., Boulos, P.F., and Wood, D.J. (2007). "The need for comprehensive transient analysis of water distribution systems". J. AWWA, 98:1, 2007.

Kettler, A. J., and Goulter, C. (1985). "An analysis of pipe breakage in urban water distribution networks." Can. Geotech. J., 12(1982), 286–293.

Kirmeyer, G.J., Friedman, M., Martel, K., Howie, D., LeChevallier, M., Abbaszadegan, M., Karim, M., Funk, J., and Harbour, J. (2001). Pathogen Intrusion Into the distribution system. AwwaRF, Denver.

Kleiner, Y., and Rajani, B. B. (2001). "Comprehensive review of structural deterioration of water mains: Statistical models." Urban Water, 3(3), 131–150.

Kleiner, Y., and Rajani, B. (2002). Forecasting Variations and trends in Water-Main Breaks. Jour. Infrastructure Systems, 8(4), 122-131.

Kleiner, Y., Adams, B. J., and Rogers, J. S. (2001). "Water distribution network renewal planning." J. Comput. Civ. Eng., 15 1, 15–26.

Lansey, K., Basnet, C., Mays, L. W., and Woodburn, J. (1992). "Optimal maintenance scheduling for water distribution systems." Civ. Eng. Syst., 9(3), 211–226.

LeChevallier, M.W., Gullick, R.W., Karim, M.R., Friedman, M., and Funk, J.E. (2003). "The potential for health risks from intrusion of contaminants into the distribution system from pressure transients," J. Water, Health, 1, 3–14.

Malandain, J. (1999). "Modélisation de l'état de santé des réseaux de distribution d'eau pour l'organisation de la maintenance. Etude du patrimoine de l'agglomération de Lyon." Ph.D. thesis INSA, Lyon, URGC/Hydrologie Urbaine, France.

Male, J.W., Walski, T.M., and Slutsky, A.H. (1990). "Analyzing Water Main Replacement Policies." Journal Water Resources Planning & Management, 1990.

Mays, L.W. and Tung, Y. (1992). Hydrosystems Engineering and Management. McGraw-Hill Inc., New York, New York.

Moody, L. F. (1944). "Friction Factors for Pipe Flow." Transactions of the American Society of Mechanical Engineers, Vol. 66.

Munson, B.R., Young, D.F., Okiishi, T.H., and Huebsch, W.W. (2009). Fundamentals of Fluid Mechanics. John Wiley and Sons, Inc., Hoboken, New Jersey.

Nafi, A., and Kleiner, Y. (2010). "Scheduling renewal of water pipes while considering adjacency of infrastructure works and economies of scale. J. Water Resour. Plann. Manage., 10.1061/(ASCE)WR.1943-5452. 0000062, 519–530."

National Research Council. (2006). Drinking Water Distribution Systems: Assessing and Reducing Risks. Washington, DC: The National Academic Press.

Powers, David M.W. (2007). Evaluation: From Precision, Recall and F-Factor to ROC, Informedness, Markedness & Correlation. Technical Report SIE-07-001. December 2007.

Renaud, E., Demassiac, J. C., Bremond, B., and Laplaud, C. (2007). "SIROCO, a decision support system for rehabilitation adapted for small and medium size water distribution companies." IWA Conf. on Leading-Edge Asset Management, IWA, London, 15.

Rouse, H., and Ince, S., (1980). History of Hydraulics. Iowa Inst. of Hydraulic Res., Iowa City, Iowa.

Schal, S.L. (2013). Water Quality Sensor Placement Guidance for Small Water Distribution Systems. A thesis submitted in partial fulfillment of the requirements for the degree of M.S.CE. in the College of Engineering at the University of Kentucky.

Shamir, U., and Howard, C. D. D. (1979). "An analytic approach to scheduling pipe replacement." J. Am. Water Works Assoc., 71(5), 248–258.

Vanrenterghem-Raven, A. (2007). "Risk Factors of Structural Degradation of an Urban Water Distribution System." J. Infrastructure Systems, March 2007.

Von Huben, H. (2005). Water Distribution Operator Training Handbook. American Water Works Association. Denver, CO.

Walski, T. (1987). "Replacement rules for water mains." J. Am. Water Works Assoc., 79(11), 33–37.

Walski, T. M. (1984). Analysis of Water Distribution Systems. Van Nostrand Reinhold, New York, New York.

Walski, T., and Pelliccia, A. (1982). "Economic analysis of water main breaks." J. Am. Water Works Assoc., 74(3), 140–147.

Walski, T. M., Chase, D. V., Savic, D. A., Grayman, W., Beckwith, S., & Koelle, E. (2007). Advanced Water Distribution Modeling and Management. Bentley Institute Press.

Wang, R., Wang, Z., Wang, X., Yang, H., and Sun., J. (2014). "Pipe Burst Risk State Assessment and Classification Based on Water Hammer Analysis for Water Supply Networks." J. Water Resources Planning & Management, 2014.

Wood, Don J. (1981). Algorithms for Pipe Network Analysis and Their Reliability. Research Report No. 127 for University of Kentucky Water Resources Research Institute, March, 1981.

Wood, Don J. (2005). Waterhammer Analysis – Essential and Easy (and Efficient). J. Environmental Engineering, August, 2005.

Wood, D.J. and Charles, C.O.A. (1972). Hydraulic Network Analysis Using Linear Theory." Journal of Hydraulics Division, ASCE, 98(HY7): (115-1170).

Wood, D.J., Lingireddy, S., Boulos, P.F., Karney, B.W., and McPherson, D.L. (2005). Numerical Methods for Modeling Transient Flow in Pipe distribution Systems. Jour. AWWA, 97:7:104.

Wood, D.J., Lingireddy, S., and Boulos, P.F., (2005). Pressure Wave Analysis of Transient Flow in Pipe Distribution Systems. MWH Soft Inc. Publ., Pasadena Calif.

Wood, D. J., Dorsch, R. G., and Lightner, C. (1966). "Wave plan analysis of unsteady flow in closed conduits," J. Hydraul. Div., Am. Soc. Civ. Eng., 92(2), 83–110.

Woodburn, J., Lansey, K. E., and Mays, L. W. (1987). "Model for the optimal rehabilitation and replacement of water distribution system components." Proc., ASCE 1987 National Conf. on Hydraulic Engineering, ASCE, New York.

Wylie, E. B., and Streeter, V. L. (1978). Fluid Transients. McGraw-Hill, New York, New York.

VITA

Steven Hoagland, E.I.T., B.S.CE,

Department of Civil Engineering at the University of Kentucky

Place of Birth: Detroit, Michigan, USA

Education: University of Kentucky, Civil Engineering, B.S. 12/2014

Professional publications:

Hoagland, S., Schal, S., Ormsbee, L., and Bryson, S. (2015). Classification of Water Distribution Systems for Research Applications. Proc. EWRI Congress 2015.